

**ISTANBUL TECHNICAL UNIVERSITY ★ GRADUATE SCHOOL OF SCIENCE**  
**ENGINEERING AND TECHNOLOGY**

**FLUTTER ANALYSIS OF WING/STORE  
CONFIGURATIONS WITH APPLICATIONS TO  
ROBUST AEROELASTIC OPTIMIZATION**

**M.Sc. THESIS**

**Pınar ACAR**

**Department of Aeronautical and Astronautical Engineering**

**Aeronautical and Astronautical Engineering Programme**

**JANUARY 2012**



**ISTANBUL TECHNICAL UNIVERSITY ★ GRADUATE SCHOOL OF SCIENCE**  
**ENGINEERING AND TECHNOLOGY**

**FLUTTER ANALYSIS OF WING/STORE  
CONFIGURATIONS WITH APPLICATIONS TO  
ROBUST AEROELASTIC OPTIMIZATION**

**M.Sc. THESIS**

**Pınar ACAR  
(511101123)**

**Department of Aeronautical and Astronautical Engineering**

**Aeronautical and Astronautical Engineering Programme**

**Thesis Advisor: Assoc. Prof. Melike NİKBAY**

**JANUARY 2012**



**İSTANBUL TEKNİK ÜNİVERSİTESİ ★ FEN BİLİMLERİ ENSTİTÜSÜ**

**KANAT/DİŞ YÜK KONFIGÜRASYONLARININ  
KARARLI AEROELASTİK OPTİMİZASYON UYGULAMALARI İÇİN  
FLUTTER ANALİZİ**

**YÜKSEK LİSANS TEZİ**

**Pınar ACAR  
(511101123)**

**Uçak ve Uzay Mühendisliği Anabilim Dalı**

**Uçak ve Uzay Mühendisliği Programı**

**Tez Danışmanı: Doç. Dr. Melike NİKBAY**

**OCAK 2012**









## **FOREWORD**

I would firstly like to express my gratitude to my advisor, Assoc. Prof. Melike Nikbay for her continual support and guidance.

I specially thank to my parents and my sister for their never-ending support and patience since the day I was born. Furthermore, I am very grateful to my friends. Life is more simple, enjoyable and meaningful with them.

Finally, I also would like to thank to TÜBİTAK-BİDEB for providing me M.Sc. scholarship.

December 2011

Pınar ACAR  
Astronautical Engineer



## TABLE OF CONTENTS

	<u>Page</u>
<b>FOREWORD .....</b>	<b>vii</b>
<b>TABLE OF CONTENTS .....</b>	<b>ix</b>
<b>ABBREVIATIONS .....</b>	<b>xi</b>
<b>LIST OF TABLES .....</b>	<b>xiii</b>
<b>LIST OF FIGURES .....</b>	<b>xv</b>
<b>SUMMARY .....</b>	<b>xvii</b>
<b>ÖZET .....</b>	<b>xxi</b>
<b>1. INTRODUCTION .....</b>	<b>1</b>
1.1 Purpose of Thesis .....	3
1.2 Literature Review .....	4
<b>2. TWO DIMENSIONAL AEROELASTIC ANALYSIS .....</b>	<b>13</b>
2.1 Development of Aeroelastic Solution Methodology .....	13
2.2 Validation of 2D Aeroelastic Analysis .....	20
<b>3. THREE DIMENSIONAL FLUTTER ANALYSIS .....</b>	<b>23</b>
3.1 Flutter Solution Methodology .....	23
3.1.1 Determination of bending and torsional natural frequencies .....	31
3.1.2 Determination of final form of flutter solution .....	35
3.2 Validation of Flutter Analysis .....	38
3.3 Flutter Analysis of Goland Wing .....	39
3.4 Flutter Analysis of AGARD 445.6 Wing .....	41
<b>4. AEROELASTIC DESIGN OPTIMIZATION .....</b>	<b>45</b>
4.1 Multi-Objective Design Optimization of Two Dimensional Aeroelastic Systems .....	45
4.2 Flutter Based Aeroelastic Design Optimization of AGARD 445.6 .....	49
<b>5. UNCERTAINTY BASED AEROELASTIC ANALYSIS .....</b>	<b>53</b>
5.1 Uncertainty Based 2-Dimensional Aeroelastic Analysis .....	55
5.1.1 COV=1% case .....	55
5.1.2 COV=5% case .....	56
5.2 Uncertainty Based 3-Dimensional Flutter Analysis .....	58
5.2.1 COV=1% case .....	58
5.2.2 COV=5% case .....	58
<b>6. FLUTTER BASED OPTIMIZATION AND UNCERTAINTY BASED FLUTTER ANALYSIS OF WING/STORE CONFIGURATIONS .....</b>	<b>61</b>
6.1 Solution and Validation of Flutter Analysis of Wing/Store Configurations .....	62
6.2 Flutter Based Optimization of Initial AGARD 445.6 Wing/Store Configuration .....	66
6.2.1 Flutter based optimization for 3-stations case .....	67
6.2.2 Flutter based optimization for 4-stations case .....	68
6.2.3 Flutter based optimization for 5-stations case .....	70
6.2.4 Comparison of flutter results for different configurations of stations .....	72

6.3 Flutter Based Optimization of Optimum AGARD 445.6 Wing/Store Configuration.....	72
6.3.1 Flutter based optimization for 3-stations case .....	73
6.3.2 Flutter based optimization for 4-stations case .....	73
6.3.3 Flutter based optimization for 5-stations case .....	74
6.3.4 Comparison of flutter results for different configurations of stations .....	74
6.4 Comparison of Flutter Results for Initial and Optimum AGARD 445.6 Wing/Store Configuration .....	75
6.5 Uncertainty Based Flutter Analysis of AGARD 445.6 Wing/Store Configuration.....	76
6.5.1 $COV=1\%$ case .....	77
6.5.2 $COV=5\%$ case .....	77
<b>7. ROBUST AEROELASTIC DESIGN OPTIMIZATION OF WING/STORE CONFIGURATIONS BASED ON FLUTTER CRITERIA .....</b>	<b>81</b>
7.1 Robust Aeroelastic Optimization of 2-Dimensional Airfoil .....	83
7.2 Robust Optimization of AGARD 445.6 Clean Wing .....	87
7.3 Robust Optimization of AGARD 445.6 Wing/Store Configuration.....	89
<b>8. CONCLUSIONS AND RECOMMENDATIONS .....</b>	<b>95</b>
<b>REFERENCES .....</b>	<b>99</b>
<b>CURRICULUM VITAE.....</b>	<b>107</b>

## ABBREVIATIONS

<b>AGARD</b>	: Advisory Group for Aerospace Research and Development
<b>COV</b>	: Coefficient of Variation
<b>DoE</b>	: Design of Experiments
<b>LCO</b>	: Limit-Cycle Oscillation
<b>MC</b>	: Monte Carlo
<b>MCS</b>	: Monte Carlo Simulation
<b>MOGA</b>	: Multi-Objective Genetic Algorithm
<b>MORDO</b>	: Multi-Objective Robust Design Optimization
<b>NACA</b>	: National Advisory Committee for Aeronautics
<b>NSGA</b>	: Non-Dominated Sorting Genetic Algorithm
<b>PCE</b>	: Polynomial Chaos Expansion
<b>SESC</b>	: Simplex Elements Stochastic Collocation
<b>SISO</b>	: Single-Input Single-Output



## LIST OF TABLES

	<u>Page</u>
<b>Table 2.1</b> : Design parameters of 2D benchmark problem-I .....	20
<b>Table 2.2</b> : Validation of 2D aeroelastic solution-I .....	21
<b>Table 2.3</b> : Design parameters of 2D benchmark problem-II.....	21
<b>Table 2.4</b> : Validation of 2D aeroelastic solution-II .....	21
<b>Table 3.1</b> : Design parameters of benchmark wings.....	39
<b>Table 3.2</b> : Flutter speeds and relative errors of benchmark wings .....	39
<b>Table 3.3</b> : Design parameters of Goland wing .....	40
<b>Table 3.4</b> : Flutter solution results for Goland wing .....	40
<b>Table 3.5</b> : Design properties of AGARD 445.6 wing.....	43
<b>Table 3.6</b> : Natural frequency solution for AGARD 445.6 wing .....	43
<b>Table 3.7</b> : Flutter solution results for AGARD 445.6 wing .....	43
<b>Table 4.1</b> : Values of optimization variables in 2-dimensional case .....	46
<b>Table 4.2</b> : Optimum designs with MOGA-II algorithm .....	48
<b>Table 4.3</b> : Comparison of initial and optimum designs with MOGA-II algorithm..	48
<b>Table 4.4</b> : Comparison of initial and optimum designs with NSGA-II algorithm ...	49
<b>Table 4.5</b> : Comparison of MOGA-II and NSGA-II algorithms .....	49
<b>Table 4.6</b> : Design variables of 2-dimensional optimum model.....	49
<b>Table 4.7</b> : Design variables of initial and optimum AGARD 445.6 models .....	50
<b>Table 4.8</b> : Flutter results of initial and optimum AGARD 445.6 models.....	51
<b>Table 5.1</b> : Statistical information about 2-dimensional case with $COV=1\%$ .....	55
<b>Table 5.2</b> : Statistical information about 2-dimensional case with $COV=5\%$ .....	56
<b>Table 5.3</b> : Comparison of uncertainty based aeroelastic analyses.....	58
<b>Table 5.4</b> : Statistical information about AGARD 445.6 case with $COV=1\%$ .....	58
<b>Table 5.5</b> : Statistical information about AGARD 445.6 case with $COV=5\%$ .....	59
<b>Table 5.6</b> : Comparison of uncertainty based flutter analyses.....	59
<b>Table 6.1</b> : Reference values of example Goland wing/store model .....	64
<b>Table 6.2</b> : Flutter results for example wing/store configuration .....	66
<b>Table 6.3</b> : Optimum design parameters for 3-stations case .....	68
<b>Table 6.4</b> : Optimum design parameters for 4-stations case .....	70
<b>Table 6.5</b> : Optimum design parameters for 5-stations case .....	71
<b>Table 6.6</b> : Comparison of flutter speeds with respect to station numbers .....	72
<b>Table 6.7</b> : Optimum locations with respect to station numbers .....	72
<b>Table 6.8</b> : Initial design parameters of optimum AGARD 445.6.....	73
<b>Table 6.9</b> : Optimum design parameters for 3-stations case .....	73
<b>Table 6.10</b> : Optimum design parameters for 4-stations case .....	74
<b>Table 6.11</b> : Optimum design parameters for 5-stations case .....	74
<b>Table 6.12</b> : Comparison of flutter speeds with respect to station numbers .....	75
<b>Table 6.13</b> : Optimum locations with respect to station numbers .....	75
<b>Table 6.14</b> : Deterministic values of random variables in wing/store model.....	76
<b>Table 6.15</b> : Statistical results of 3-stations case with $COV=1\%$ .....	77

<b>Table 6.16</b> : Statistical results of 3-stations case with $COV=5\%$ .....	78
<b>Table 6.17</b> : Design properties and flutter results of optimum wing/store model.....	79
<b>Table 7.1</b> : Optimum robust design properties of 2-dimensional airfoil model.....	87
<b>Table 7.2</b> : Comparison of deterministic and robust design parameters.....	87
<b>Table 7.3</b> : Optimum robust design properties of AGARD 445.6 clean wing.....	89
<b>Table 7.4</b> : Comparison of deterministic and robust design parameters.....	89
<b>Table 7.5</b> : Optimum robust design of AGARD 445.6 wing/store model .....	92
<b>Table 7.6</b> : Comparison of deterministic and robust design parameters.....	92



## LIST OF FIGURES

	<u>Page</u>
<b>Figure 1.1</b> : General flowchart of MCS .....	11
<b>Figure 2.1</b> : Typical section geometry .....	14
<b>Figure 3.1</b> : General representation of 3D aeroelastic model.....	24
<b>Figure 3.2</b> : Geometry of Golang wing.....	40
<b>Figure 3.3</b> : Flutter frequency-damping term relation for Golang wing. ....	41
<b>Figure 3.4</b> : Geometry and solid model of AGARD 445.6. ....	42
<b>Figure 3.5</b> : Flutter frequency-damping term relation for AGARD 445.6.....	44
<b>Figure 4.1</b> : Workflow of 2-dimensional aeroelastic optimization problem.....	47
<b>Figure 4.2</b> : Optimization workflow for AGARD 445.6.....	51
<b>Figure 5.1</b> : Properties of Gaussian distribution .....	54
<b>Figure 5.2</b> : Flutter speed histograms with $COV=1\%$ and $COV=5\%$ .....	56
<b>Figure 5.3</b> : Divergence speed histograms with $COV=1\%$ and $COV=5\%$ .....	57
<b>Figure 5.4</b> : Control reversal speed histograms with $COV=1\%$ and $COV=5\%$ .....	57
<b>Figure 5.5</b> : AGARD 445.6 flutter speed histograms .....	59
<b>Figure 6.1</b> : General representation of a wing/store configuration.....	61
<b>Figure 6.2</b> : Flutter speed-damping term relation for $y_s=0.2794$ m .....	64
<b>Figure 6.3</b> : Flutter speed-damping term relation for $y_s=0.4318$ m .....	65
<b>Figure 6.4</b> : Flutter speed-damping term relation for $y_s=1.1684$ m .....	65
<b>Figure 6.5</b> : Flutter speed-damping term relation for $y_s=1.2192$ m .....	66
<b>Figure 6.6</b> : Optimization workflow for 3-stations case .....	68
<b>Figure 6.7</b> : Optimization workflow for 4-stations case .....	69
<b>Figure 6.8</b> : Optimization workflow for 5-stations case .....	71
<b>Figure 6.9</b> : Flutter speed variation with respect to station number .....	76
<b>Figure 6.10</b> : Flutter speed histograms for $COV=1\%$ and $COV=5\%$ .....	78
<b>Figure 7.1</b> : MORDO settings in modeFRONTIER .....	83
<b>Figure 7.2</b> : Workflow of 2-dimensional robust aeroelastic optimization .....	85
<b>Figure 7.3</b> : Probability density distribution of maximum flutter speed.....	86
<b>Figure 7.4</b> : Probability density distribution of maximum divergence speed .....	86
<b>Figure 7.5</b> : Probability density distribution of maximum control reversal speed ...	86
<b>Figure 7.6</b> : Robust optimization workflow of clean AGARD 445.6 wing .....	88
<b>Figure 7.7</b> : Probability density distribution of maximum flutter speed.....	89
<b>Figure 7.8</b> : Robust optimization workflow of AGARD 445.6 wing/store model ...	91
<b>Figure 7.9</b> : Probability density distribution of maximum flutter speed.....	92



# **FLUTTER ANALYSIS OF WING/STORE CONFIGURATIONS WITH APPLICATIONS TO ROBUST AEROELASTIC OPTIMIZATION**

## **SUMMARY**

The main scope and aim of the present work are to develop a parametric solution methodology to reach the best design for a wing/store configuration subjected to flutter phenomenon and form a basis for robust aeroelastic optimization. Proved solution is forced to be applicable for any wing/store configuration in accordance with requirements. The best design defines a configuration with store loads in optimum positions along wing span to provide maximum flutter speed however uncertainties can significantly affect the design and they have to be considered for a realistic application. Thus, the present work which deals with the problem in a highly broad sense involves deterministic and probabilistic flutter analyses and flutter based deterministic and robust aeroelastic optimization applications. The first part of the work involves flutter analysis of 2 and 3-dimensional wing models. Then, deterministic aeroelastic design optimization studies are carried out for these structures. After that, uncertainty based flutter analyses with structural and aerodynamic random parameters are applied to the wings of interest. Flutter analysis and flutter based design optimization of a 3-dimensional wing/store configuration form the next section. Uncertainty based flutter solution for the wing/store configuration is stated. Finally, robust optimization studies based on flutter criteria are carried out for 2 and 3-dimensional wing models and wing/store configuration.

Firstly, a simple aeroelastic system with 2-degrees of freedom is analyzed with respect to aeroelastic instability criteria via a developed MATLAB code. The aeroelastic instabilities consist of divergence, control reversal and flutter phenomena. A solution methodology based on stability analysis of a dynamic system in quasi-steady flow is proven. After that, 3-dimensional linear flutter analysis methodology with unsteady aerodynamic effects is developed, integrated in a computational code, validated and applied to Goland and AGARD (Advisory Group for Aerospace Research and Development) 445.6 wings.

As a second work, deterministic design optimization studies are accomplished for both 2 and 3-dimensional wing cases. 3-dimensional case involves flutter based optimization of AGARD 445.6 wing. Objectives are maximizing the speeds of aeroelastic instabilities in 2-dimensional case while maximizing flutter speed is the only objective in the design optimization of AGARD 445.6. Design variables in 2-dimensional case are static offset, linear and torsional spring coefficients, moment of inertia and mass of airfoil while constraints are specified for natural limits of radius of gyration and ratio of frequency terms and boundaries of aeroelastic instabilities. Optimization of AGARD 445.6 wing does not involve any constraints while defined design variables are taper ratio, sweep angle, elasticity and shear modulus along the spanwise direction. The developed MATLAB codes, which are coupled with the

optimization software, modeFRONTIER, are fully-parametric in terms of design variables. In both cases, Non-Dominated Sorting Genetic Algorithm (NSGA-II) is preferred as the optimization algorithm while Multi-Objective Genetic Algorithm (MOGA-II) is used as the second algorithm for 2-dimensional airfoil case.

Next, uncertainty based flutter analyses are applied to 2 and 3-dimensional wing models via extended computational codes. Random parameters are selected through structural, geometric and aerodynamic variables and modeled with Gaussian distribution. Monte Carlo Simulation (MCS) is employed to generate random samples. Each analysis involves the use of  $10^5$  samples so as to enhance the accuracy of MCS. The amount of uncertainties is determined by using Coefficient of Variation (*COV*) approach with  $COV = 1\%$  and  $COV = 5\%$  cases. Minimum available speeds are sought after for aeroelastic instabilities by considering reliability.

Flutter analysis methodology of a wing/store configuration is presented and validated with a benchmark problem involving Goland wing/store models. The solution, which is developed in a MATLAB code, contains the structural effects such as masses and inertias of store loads while flutter speed can be obtained for various positions of stores along the wing span. The presented methodology forms a basis for aeroelastic analysis of more complex wing/store configurations. The stores can be considered such as missiles, tanks, etc. in a more realistic manner. Structural and inertial effects of store loads are taken into account for Goland wing case however the stores are modeled as point masses for AGARD 445.6 wing application due to lack of information. The present study is the first attempt which develops an analytical flutter analysis methodology for AGARD 445.6 clean wing and wing/store configurations to the best of author's knowledge.

Aeroelastic optimization studies for AGARD 445.6 wing/store configurations are performed in order to determine the best locations for external stores to reach the maximum flutter speeds. The MATLAB code of previous section is coupled with the optimization software. NSGA-II is again preferred as the optimization algorithm. The configurations are divided into three categories involving 3-stations, 4-stations and 5-stations placements of stores along wing span. Total masses of store loads are the same for each configuration. By considering reality, constraints defining distances between successive two stations are specified even though the stores are modeled as point masses. Flutter based optimization studies are carried out and optimum positions are determined for each wing/store model. The aeroelastic optimization study does not involve the effects of uncertainties. After three optimization applications, the best configuration with maximum flutter speed is found as 3-stations case.

The next step is to apply uncertainty based flutter analysis to AGARD 445.6 wing/store configuration. The related computational code is extended to include uncertainties with  $COV = 1\%$  and  $COV = 5\%$  approaches however locations of store loads are modeled with respect to  $COV = 0.25\%$  approach due to physical limitations of their positions. The considered configuration is the 3-stations case of previous section as the best design. Random parameters are defined as the locations and masses of store loads and material properties as elasticity and shear modulus along spanwise direction. Uncertainties are modeled with Gaussian distribution by generating  $10^5$  samples with MCS. Minimum flutter speed is taken into for reliability.

Final step of the present work is robust aeroelastic optimization applications which combine the uncertainty based flutter analyses with aeroelastic design optimization. Robust optimization studies are performed in modeFRONTIER by coupling the deterministic flutter solution codes since random parameters can be defined and distributed via optimization software. 2-dimensional airfoil, AGARD 445.6 clean wing and the best wing/store configuration are considered. In all cases, NSGA-II is used as the optimization algorithm. In 2-dimensional case, deterministic design variables are selected as static offset term, linear and torsional spring coefficients while moment of inertia and mass of the airfoil are probabilistic optimization parameters. In AGARD 445.6 clean wing case, probabilistic variables are defined as elasticity and shear modulus while taper ratio and sweep angle are deterministic design parameters. For AGARD 445.6 wing/store configuration, taper ratio and sweep angle are defined as deterministic parameters while elasticity and shear modulus, locations of store loads are defined as probabilistic optimization variables. In all cases, random variables are distributed by using  $10^5$  samples with respect to MCS. 2<sup>nd</sup> order Polynomial Chaos Expansion (PCE) is used through MCS in order to reduce the computational time. The objective of the robust optimization process is to maximize the flutter speed while previously defined constraints of deterministic optimization applications are considered. Optimum robust flutter speed is the minimum flutter speed value of the optimum robust design. In other words, optimum robust flutter speed is the maximum of minimum flutter speeds in robust designs. Choice of minimum flutter speed guarantees withstanding of the worst case scenerio by force of robustness. Robust optimization study under the scope of the present work provides the most efficient and reliable aeroelastic design based on flutter criteria even in the presence of structural, geometric and aeodynamic uncertainties.

As a consequence, the present work proves deterministic and probabilistic flutter analysis methodologies for wing structures from simple designs to more complicated 3-dimensional models and wing/store configurations with applications to deterministic and robust aeroelastic optimization. The methodology forms a basis for flutter analysis and flutter based optimization of more complex wing structures and can be extended through the use of military and civilian purposes and requirements.



## KANAT/DIŞ YÜK KONFIGÜRASYONLARININ KARARLI AEROELASTİK OPTİMİZASYON UYGULAMALARI İÇİN FLUTTER ANALİZİ

### ÖZET

Bu çalışmanın temel amacı ve kapsamı, kanat/dış yük konfigürasyonları için flutter açısından en iyi tasarıma ulaşmayı sağlayacak analitik bir çözüm yöntemi geliştirmektir. Elde edilen çözüm yönteminin kararlı (robust) aeroelastik optimizasyon uygulaması için de temel oluşturması hedeflenmiştir. Ortaya konan çözüm adımlarının, herhangi bir kanat/dış yük konfigürasyonu ile uyumlu olacak şekilde genel bir parametrik çözümü içermesi sağlanmıştır. Bu doğrultuda, kanat/dış yük konfigürasyonları için en iyi tasarımın bulunması uygulamasına gidilmiştir. Sözü edilen en iyi tasarım, flutter hızının en yüksek değere ulaşmasını sağlayacak olan açıklık boyunca dış yüklerin optimum yerleşim pozisyonlarından oluşan yapıdır. Aeroelastik sistemlerde görülen belirsizlikler, hedeflenen flutter hızına ulaşılmasını engelleyebilirler. Bu nedenle, güvenilir bir tasarım elde edebilmek için belirsizliklerin uygun şekilde hesaba katılması gerekmektedir. Bu durum, yalnızca deterministik flutter analizi yapmanın yeterli olmayacağını göstermektedir. Bu nedenle, olasılıksal (probabilistik) flutter analizleri de gerçekleştirilmiştir. Bu çalışmanın temel konusu olan problem, çok geniş bir bakış açısıyla ele alınmış ve kolaydan zora uzanacak şekilde farklı model ve konfigürasyonlar üzerinde flutter çözüm yöntemi geliştirilmiş ve aeroelastik optimizasyon uygulamaları gerçekleştirilmiştir. Bu doğrultuda öncelikli olarak 2-boyutlu kanat modelleri için aeroelastik kararsızlıkların çözümüne yönelik bir yonteme yer verilmiş ve ardından 3-boyutlu gerçekçi kanat yapıları için flutter çözüm yöntemi geliştirilmiştir. Sözü edilen 2 ve 3-boyutlu modeller için deterministik aeroelastik optimizasyon çalışmaları uygulanarak en yüksek flutter hızını sağlayan en iyi tasarım parametrelerine ulaşılmıştır. Diğer bölümde, belirsizliklerin yer aldığı olasılıksal flutter analizleri gerçekleştirilmiş ve elde edilen en küçük flutter hızları, kararlı bir analizin gereği olarak belirsizliklerin varlığı durumundaki flutter hızı olarak dikkate alınmıştır. Ardından, gerçekleştirilen flutter çözümü, 3-boyutlu kanat/dış yük konfigürasyonlarının analizini de kapsayacak şekilde genişletilmiştir. Bu sayede flutter tabanlı aeroelastik optimizasyon yapılarak dış yüklerin kanat açıklığı boyunca yerleşmeleri gereken optimum pozisyonlar bulunmuştur. Son aşamada ise; flutter kriterine dayalı kararlı aeroelastik optimizasyon çalışması, 2 ve 3-boyutlu kanat modellerine ve 3-boyutlu kanat/dış yük konfigürasyonuna uygulanmıştır.

Çalışmanın ilk aşamasında; 2-serbestlik derecesine sahip olan, sanki-daimi akışa maruz basit bir kanat profili modeline aeroelastik analiz uygulanarak aeroelastik kararsızlıkların görüldüğü hızlar elde edilmiştir. Yapılan aeroelastik analiz, dinamik sistemler için uygulanan kararlılık analizi temeline dayanmaktadır. Kararlılığı ihlal eden noktalar, aeroelastik kararsızlıkların hızları olarak belirlenmiştir. Analizin kapsamındaki aeroelastik kararsızlıklar; flutter, diverjans ve kontrol tersliğidir. 2-boyutlu sistemlerde yapılan aeroelastik analizin ardından, 3-boyutlu sistemlerde

flutter hızı çözümünü sağlayacak olan bir yöntem geliştirilmiştir. Bu yöntem, enerji prensibine dayanmakla birlikte lineer flutter için çözüm geliştirmiştir. Aerodinamik modellemeye ise; daimi olmayan aerodinamik etkiler hesaba katılmış ve Theodorsen fonksiyonundan yararlanılmıştır. Geliştirilen 3-boyutlu lineer flutter çözümü, literatürden alınan örnek problemlere uygulanmış ve çözümler doğrulanmıştır. Aynı çözüm yönteminden yararlanılarak Golland ve AGARD 445.6 kanatlarının flutter hızları hesaplanmıştır. Gerek 2-boyutlu ve gerekse 3-boyutlu sistemlerin aeroelastik analizlerini içeren MATLAB kodları ile çözümler sağlanmıştır.

Çalışmanın bir sonraki bölümünde ise; 2 ve 3-boyutlu kanat modelleri için deterministik tasarım optimizasyonu uygulamaları gerçekleştirilmiştir. 2-boyutlu kanat profili için gerçekleştirilen optimizasyonda tasarım değişkenleri; statik denge terimi, lineer ve burulma yayları katsayıları, profilin atalet momenti ve kütlesi olarak tanımlanırken; kısıtlamalar ise; jirasyon yarıçapı ve doğal frekans oranı için gerekli olan doğal sınırlara ve aeroelastik kararsızlık hızlarının yükseltmek istendiği minimum mertebelere bağlı olarak belirlenmiştir. Amaç fonksiyonlarının flutter, diverjans ve kontrol tersliği hızlarının maksimize edilmesi olarak tanımlandığı optimizasyonda, yazılım olarak modeFRONTIER kullanılırken; ilgili kanat yapıları için geliştirilen MATLAB kodlarından parametrik bir çözümü ifade edecek şekilde yararlanılmıştır. 3-boyutlu model olarak AGARD 445.6 kanadının seçildiği optimizasyonun amacını flutter hızını maksimize etmek oluştururken; tasarım değişkenleri sivrilik oranı, ok açısı, açıklık doğrultusundaki elastisite ve kayma modülleri olarak belirlenmiştir, herhangi bir kısıtlama tanımlanmamıştır. AGARD 445.6 kanadı için uygulanan optimizasyonda da bu kanadın flutter çözümünü sağlayan hesaplamalı koddan ve modeFRONTIER yazılımından yararlanılmıştır. Gerek 2-boyutlu kanat profili ve gerekse AGARD 445.6 kanadı için yapılan tasarım optimizasyonu çalışmalarında NSGA-II optimizasyon algoritması olarak tercih edilmiştir. MOGA-II algoritması ise; 2-boyutlu çalışma için ikinci yöntem olarak kullanılmıştır.

Deterministik aeroelastik analizler için oluşturulan MATLAB kodlarının yapısal, geometrik ve aerodinamik parametrelerdeki belirsizlikleri içerecek şekilde genişletilmesi ile olasılıksal analizler gerçekleştirilmiştir. Tüm rastgele değişkenler, Gauss dağılımına uygun olacak şekilde Monte Carlo simülasyonu yöntemi ile  $10^5$  örnekleme kullanılarak modellenmiştir. Belirsizliklerin miktarları, varyans katsayısı yaklaşımı ile belirlenmiş olup varyans katsayısının 0.01 ve 0.05 değerleri için analizler gerçekleştirilmiştir. 2-boyutlu kanat profili için yapılan belirsizlik tabanlı aeroelastik kararsızlık analizinde; rastgele değişkenler, profilin atalet momenti ve kütlesi ile aerodinamik parametreler olarak tanımlanmıştır. 3-boyutlu flutter analizi, bu bölümde de AGARD 445.6 kanadına uygulanırken; belirsizlik içeren parametreler kanat açıklığı doğrultusundaki elastisite ve kayma modülleri olarak belirlenmiştir. Kararlı analizin gereği olarak elde edilen minimum hızlar dikkate alınmıştır.

Çalışmanın bir sonraki bölümünde, kanat/dış yük konfigürasyonlarında flutter çözümünü sağlayacak olan bir metodoloji geliştirilmiştir. 3-boyutlu kanat yapıları için flutter hızının bulunmasını sağlayan hesaplamalı kod, dış yüklerin yapısal ve ataletsel etkilerini içerecek şekilde genişletilmiş ve ardından oluşturulan çözüm yöntemi, literatürde Golland kanadı için uygulanan bir çalışma ile kıyaslanarak doğrulanmıştır. Kıyaslama probleminde açıklık boyunca farklı pozisyonlarda yer alan tek bir dış yükün kütsel ve ataletsel etkileri hesaba katılarak çözüm yapılmıştır. Geliştirilen çözüm yöntemi, daha gerçekçi kanat/dış yük konfigürasyonlarının aeroelastik açıdan analiz edilmesi konusunda bir temel



oluşturmaktadır. Bu konfigürasyonlarda yer alan dış yükler; mühimmat, tank, vs. olabilirler. Askeri ve sivil ihtiyaçları göz önünde bulundurarak daha karmaşık yapılı ve daha gerçekçi konfigürasyonların flutter analizlerinin yapılması, bu çalışmada ortaya konulan flutter çözüm yöntemi temeline dayandırabilir. Geliştirilen çözüm yöntemi, deterministik flutter çözümünü sağlayan MATLAB kodunun revize edilmesi ile AGARD 445.6 kanat/dış yük konfigürasyonuna da uygulanmıştır. AGARD 445.6 kanat/dış yük konfigürasyonu için varsayılan dış yüklerin geometri ve ataletine dair herhangi bir veri bulunmaması nedeniyle, bu yükler birer noktasal kütle olarak modellenmişlerdir. Bu çalışma, 3-boyutlu AGARD 445.6 kanadı ve kanat/dış yük konfigürasyonu için analitik bir flutter çözümü sunan literatürdeki ilk ve tek girişimdir.

AGARD 445.6 kanat/dış yük konfigürasyonu için gerçekleştirilen aeroelastik optimizasyon ile dış yüklerin ayrı ayrı 3, 4 ve 5 istasyonda konumlandırıldığı modeller için flutter hızını maksimize eden tasarımların bulunması amaçlanmıştır. Böylece dış yüklerin kanat açıklığı boyunca hangi pozisyona yerleştirilmeleri ile flutter hızının maksimize edilebileceği bulunmuştur. Dış yükler noktasal kütleler olarak modellenmelerine rağmen; aeroelastik optimizasyon uygulamasında, gerçekçi bir tasarım varsayılarak bu kütlelerin pozisyonları arasında aynı noktada konumlanmayı önleyecek küçük mesafeler kısıtlama olarak tanımlanmıştır. İstasyon sayıları birbirinden farklı olmasına rağmen, dış yüklerin toplam kütlesi tüm durumlarda birbirine eşittir. Böylece seçilen istasyon sayıları arasında en iyi tasarıma ulaşmayı sağlayan istasyon sayısı da elde edilmiştir. 3, 4 ve 5 istasyon halleri için ayrı olarak gerçekleştirilen optimizasyonlar sonunda, flutter açısından en verimli tasarımın dış kütlelerin kanat açıklığı boyunca 3 istasyona konumlandırıldığı durum olduğuna ulaşılmıştır.

Çalışmanın bir diğer aşamasında; AGARD 445.6 kanat/dış yük konfigürasyonuna belirsizlik tabanlı flutter analizi uygulanmıştır. Bu amaçla, aynı konfigürasyonun deterministik flutter çözümünü sağlayan MATLAB kodu, yapısal ve geometrik parametrelerdeki belirsizlikleri kapsayacak şekilde genişletilmiştir. Geometrik rastgele değişkenler, dış yüklerin pozisyonları olarak belirlenirken; dış yüklerin kütleleri ile kanadın elastisite ve kayma modülleri yapısal belirsizlikleri oluşturmuştur. Belirsizlikler, temel olarak varyans katsayısının 0.01 ve 0.05 değerlerine eşit olduğu iki durum için gerçekleştirilirken; dış yüklerin pozisyonlarına ilişkin belirsizliklerde, yükler arası mesafelerin getirdiği fiziksel kısıtlamalar nedeniyle varyans katsayısı 0.0025 olarak alınmıştır. Tüm rastgele değişkenler, Gauss dağılımına uygun olacak şekilde modellenmiştir. Her bir değişken için Monte Carlo yöntemine uygun  $10^5$  örnekleme kullanılarak modelleme yapılmıştır. AGARD 445.6 kanat/dış yük konfigürasyonu için yapılan flutter analizlerinde güvenilirlik göz önüne alınarak en küçük flutter hızları dikkate alınmıştır.

Çalışmanın son aşamasını, belirsizlik tabanlı flutter analizi ile aeroelastik optimizasyon uygulamalarının birleşimi olarak değerlendirilebilecek kararlı aeroelastik optimizasyon oluşturmaktadır. Kararlı optimizasyon, 2-boyutlu kanat profili modeline, AGARD 445.6 kanat ve 3 istasyona sahip kanat/dış yük modellerine uygulanmıştır. Temel olarak, deterministik flutter çözümlerinde kullanılan hesaplamalı kodlar modeFRONTIER optimizasyon yazılımı ile birleştirilmiştir. Kararlı optimizasyon uygulamalarında, önceki bölümlerde belirsizlik içerdiği varsayılan parametreler bir kez daha rastgele değişken olarak tanımlanmış, kalan deterministik optimizasyon değişkenleri de yine deterministik olarak atanmıştır. Belirsizlikler, optimizasyon yazılımı yardımıyla Gauss dağılımına uygun

olacak şekilde Monte Carlo örnekleme kullanılarak modellenmiştir. Hesaplama zamanını azaltmak amacıyla 2. mertebeden PCE yönteminden yararlanılmıştır. 2-boyutlu kanat profili için yapılan kararlı optimizasyon uygulamasında; profilin atalet momenti ve kütlesi olasılıksal optimizasyon değişkeni olarak atanırken; deterministik değişken olarak statik offset terimi, lineer ve burulma yay katsayılarına yer verilmiştir. Optimizasyonun amaç ve kısıtlamaları, aynı model için yapılan deterministik optimizasyon uygulaması ile aynıdır. AGARD 445.6 kanadının flutter hızını maksimize etmek için gerçekleştirilen kararlı optimizasyonda; elastisite ve kayma modülleri olasılıksal değişken olarak alınırken sivrilik oranı ve ok açısı deterministik parametreler olmuştur. AGARD 445.6 kanat/dış yük konfigürasyonuna uygulanan kararlı optimizasyon uygulamasında; dış yüklerin kütleleri ve pozisyonları, elastisite ve kayma modüllerinin belirsizlik içerdiği varsayılırken; sivrilik oranı ve ok açısı bir kez daha deterministik optimizasyon değişkenleri olarak atanmıştır. Optimizasyonun kısıtlamalarını, dış yükler arasında olması gereken minimum açıklık boyu uzaklıklar oluşturmaktadır. Sözü edilen optimizasyon uygulamalarında elde edilen kararlı tasarımlardan, en yüksek minimum flutter hızı değerine sahip olan tasarım göz önüne alınmıştır. Minimum flutter hızına bağlı bir seçimin yapılması, ilgili aeroelastik sistemde görülebilecek en kötü senaryonun bile kabul edilebilir olmasını garanti ederek kararlı bir tasarım elde edilmesini sağlamaktadır. Kararlı optimizasyon çalışması ile flutter kriteri göz önünde bulundurularak; yapısal, geometrik ve aerodinamik belirsizliklerin görülmesi halinde dahi en etkin ve güvenilir aeroelastik tasarımların elde edilmesi sağlanmıştır.

Bu çalışma, basit tasarımlardan 3-boyutlu kanat ve kanat/dış yük modelleri gibi daha karmaşık kanat yapılarına kadar giden tasarımlar için deterministik ve olasılıksal yöntemlerle flutter analizi yapılmasını sağladığı gibi deterministik ve kararlı aeroelastik optimizasyon uygulamalarına da yer vermektedir. 3-boyutlu AGARD 445.6 kanat modeli için ortaya konulan flutter analizi metodolojisi ve flutter tabanlı optimizasyon uygulamaları, daha karmaşık yapılara sahip kanat modelleri için yapılabilecek çalışmalara bir temel oluşturmaktadır. Geliştirilen 3-boyutlu flutter çözümü yöntemi, parametrik olarak ifade edildiğinden başka modellere de uygulanmaya açıktır. Örneğin bu çalışma içerisinde de hem Goland hem de AGARD 445.6 kanatlarına uygulanmıştır. Benzeri şekilde, dış yüklerin yapısal etkisini göz önünde bulundurarak genişletilen flutter çözüm yöntemi ile daha karmaşık kanat/dış yük konfigürasyonları için de temel olacak bir çözüm ortaya konmuştur. Askeri ve sivil ihtiyaç ve talepler doğrultusunda ortaya çıkabilecek karmaşık konfigürasyonların flutter analizi için temel bir yöntem ifade edilmekle birlikte, bu yapılar için aeroelastik anlamda daha kararlı ve güvenilir tasarımların geliştirilmesi için de yol gösterilmiştir.

## 1. INTRODUCTION

The scope of the present work involves a parametric solution methodology to reach the optimum design for a wing/store configuration subjected to flutter phenomenon with application to robust aeroelastic optimization. Firstly, deterministic flutter analyses and aeroelastic design optimization are performed. Next, probabilistic flutter analyses are applied to 2 and 3-dimensional wing structures. Then, 3-dimensional aeroelastic analysis is extended to flutter determination of wing/store configurations and flutter based optimization of store locations by changing number of stations. Uncertainty based flutter analysis is applied to optimum design of wing/store configuration. Finally, robust optimization studies are carried out for 2 and 3-dimensional clean wing cases and wing/store configuration of the previous step.

2-dimensional aeroelastic analysis constitutes the basis of realistic flutter calculations. In this work, a 2-dimensional stability analysis is performed via a MATLAB code to compute the speeds of aeroelastic instabilities in a quasi-steady, incompressible flow. The stability analysis determines the critical points where an aeroelastic instability can occur. By considering the geometrical features of the airfoil of interest, it is possible to find the speeds at which flutter, control reversal and divergence can be seen.

The methods in 2-dimensional analysis are not totally compatible with 3-dimensional flutter analysis since the wing span effects have to be considered in 3-dimensional modeling. An analytical solution based on assumed mode technique is developed by using energy principle of Lagrange equations in 3-dimensional linear flutter analysis. Aerodynamic modeling involves the use of Theodorsen Function. Sweep angle effects in aerodynamic forces are considered in order to represent an accurate aerodynamic model. A methodology for determination of bending and torsional natural frequencies is also presented. Three dimensional flutter analysis is implemented in a computational code, then validated by benchmark problems from literature and finally applied to Goland and AGARD 445.6 wings.

The next step of the present work includes design optimization studies based on aeroelastic instability criteria for 2 and 3-dimensional wing models. Firstly, the 2-dimensional solution code is implemented into the optimization software, modeFRONTIER, for the multi-objective aeroelastic optimization in order to provide an automatic solution in terms of input variables. The objectives of the optimization problem are maximizing the speeds of aeroelastic instabilities as flutter, divergence and control reversal while the optimization variables are linear and torsional spring coefficients, mass of the airfoil, moment of inertia and static offset term. Constraints are defined for natural boundaries of reduced coefficients and specified minimum boundaries of aeroelastic instabilities. Optimum solutions are obtained with MOGA-II and NSGA-II algorithms. As a second application, the MATLAB code developed for the flutter solution of AGARD 445.6 is coupled with the optimization software. The developed code for the calculation of flutter speed is employed as a tool in deterministic optimization loop while modeFRONTIER is used as optimization software. The objective in this optimization problem is maximizing flutter speed while the optimization variables are taper ratio, sweep angle, elasticity and shear modulus. NSGA-II is preferred as the optimization algorithm.

In the next step of the present work, uncertainty based flutter analyses are applied to 2 and 3-dimensional wing structures. 3-dimensional case involves probabilistic flutter analysis of AGARD 445.6 wing. Random parameters are defined as moment of inertia and mass of the airfoil and aerodynamic parameters in 2-dimensional case while elasticity and shear modulus along spanwise direction in 3-dimensional analysis. The computational codes are extended to contain uncertainty effects in aeroelastic analyses. The uncertainties are included with MCS method by distributing the variables randomly with Gaussian distribution. By considering reliability, minimum available instability speeds are taken into account.

The following steps of the present work concentrate on the flutter analysis and flutter based design optimization of AGARD 445.6 wing/store configurations. Firstly, a flutter analysis in the presence of external masses is performed in Goland wing/store configurations example from literature for validation purpose with a revised computational code and then applied to AGARD 445.6 wing/store configurations whose stores are placed in 3, 4 and 5 stations respectively along the wing span. The total masses of store loads are the same for each case. The code which includes the

structural effects of store loads is then implemented into the optimization software with the objective as maximization of flutter speed. The optimization variables in this case are defined as locations of stations for 3, 4 and 5-stations cases respectively while NSGA-II is again preferred as optimization algorithm. The constraints define minimum distances between locations of successive stations for enabling a realistic wing configuration in the presence of store loads. The optimum design with maximum flutter speed value is found as 3-stations model.

The next section involves flutter analysis of optimum AGARD 445.6 wing/store configuration of previous section by considering the effects of structural and geometric uncertainties. The computational code involving deterministic flutter analysis of a wing/store configuration is extended by the way of including uncertainty effects while again MCS is used to generate random samples. The structural uncertainties involve masses of store loads and material properties while the station locations are defined as geometric uncertainties. Minimum flutter speed is taken into account as the worst case scenerio.

Finally, flutter based robust optimization is accomplished for 2 and 3-dimensional clean wing models and optimum wing/store configuration of the previous sections. Robust optimization involves the use of deterministic and probabilistic variables of previous sections all together. Constraints remain the same with the previous deterministic optimization studies. MCS provides random distributions of probabilistic variables while 2<sup>nd</sup> order PCE is used through MCS to reduce the computational time. Optimum wing designs are obtained through minimum flutter speeds based on robustness criterion. Optimum robust flutter speed is the maximum of minimum flutter speeds in robust designs. Choice of minimum flutter speed guarantees withstanding of the worst case scenerio by force of robustness. Robust optimization study under the scope of the present work provides the most efficient and reliable aeroelastic design based on flutter criteria even in the presence of structural, geometric and aerodynamic uncertainties.

## **1.1 Purpose of Thesis**

The main purpose of the present work is to represent an efficient parametric solution methodology for uncertainty based flutter analysis and flutter based deterministic and robust aeroelastic optimization of realistic wing structures. The parametric solution is

expected to provide a guideline for analysis and optimization of various types of clean wings and wing/store configurations from the simplest models to designs with high complexity levels. Flutter analysis and design optimization studies under the scope of the present work are vital in order to attain robust structures. Wing/store configurations with efficient aeroelastic designs can fulfill the needs of military and civilian purposes which forms one of the basic expectations from the present work. The present work provides robust aeroelastic design by considering the placement of external stores and structural properties of wing/store configurations. A mathematical model to the solution of both deterministic and probabilistic flutter analysis is developed and applied successfully. Moreover, the solution methods form a basis for the optimization applications leading to designs with further aeroelastic capabilities. Since, to the best of author's knowledge, this study is the first attempt for analytical deterministic and probabilistic flutter solutions of AGARD 445.6 clean wing and wing/store configurations and robust aeroelastic design application, it has a leading role for the further aeroelastic analyses and optimization studies in various complex geometries due to its innovational approach. The stated robust optimization study in the present work provides the most efficient and reliable aeroelastic designs based on flutter criteria.

## **1.2 Literature Review**

Aeroelasticity, as a multidisciplinary research field, investigates the behavior of an elastic structure in airstream and interaction of inertial, aerodynamic and structural forces. Aeroelastic effects must be considered in the design of aircrafts, helicopters, bridges, etc. Although elastic structures in aviation sector are useful since they provide comfortable flights for passengers even in the existence of gust loads, application of these structures is limited due to aeroelastic phenomena.

Aeroelasticity deals with the effects of aerodynamic forces that can cause harmful oscillations with increasing magnitudes. Aeroelasticity is basically interested in stability and control, static and dynamic phenomena, structural loadings with respect to atmospheric turbulence and maneuvers.

The most dramatic physical phenomenon in the field of aeroelasticity is flutter, a dynamic instability which often leads to catastrophic structural failure [1]. It happens when the structure extracts energy from the air stream. Flutter can affect an aircraft

in various ways so that it must be taken into account in order to prevent possible harms. Therefore, determination of flutter speed according to related flight conditions is an indispensable process for aeroelasticians.

Researches in the topic of flutter are extensive including various mathematical models and physical knowledge. Calculation of flutter region includes several methods under the topics of analytical, experimental and numerical approaches.

Analytical solutions are the bases of modern numerical calculations and they help to understand the physical background of a dynamic aeroelastic system. Shubov [2] states that the physical meaning of flutter cannot be completely understood unless an analytical solution procedure is applied. Both experimental and numerical studies do not provide sufficient knowledge to understand the full physical meaning. An aircraft wing can be modeled by considering 2 or 3-dimensional cases in order to calculate the flutter boundaries while different fidelity levels of aerodynamic solutions can be applied to flow regimes.

Flutter speed can be calculated by considering subsonic, supersonic and transonic flight regimes. In transonic solution, nonlinear aerodynamic expressions are used and can be linearized to represent the general characteristics of transonic regime. Although aerodynamic expressions are different for each of various flight regimes, transonic regime is considered as the most critical case for flutter due to its nonlinear features.

Analytical solutions produced for transonic regime should be verified by experiments in order to prove accuracy and validity of nonlinear models. Matsushita [3] used nonlinear mathematical model including all features of transonic regime and presented this type of an experimental work.

Analytical flutter solution is basically based on three approaches.

- Frequency Based Flutter Calculations
- Time Based Flutter Calculations
- Laplace Domain Based Flutter Calculations

These methods employ different solution steps and approaches, however frequency based calculations are traditionally preferred. Time based approaches are known as "Time Marching Methods" and based on a coupled analysis including correct estimations in both aerodynamics and structural displacements [4]. These methods

are based on a coupled approach since they provide the correct estimations for aerodynamics of rigid wing geometries compatible with computational fluid dynamics and convenient finite element models with structural deformations [4].

Frequency based approaches contain methods as well-known p-k and V-g solutions. A flutter problem with the characteristics of decreasing speed is solved in transonic regime with p-k and V-g methods [5]. A more reliable flutter solution is applied and Laplace transformation feature is used in the aeroelastic method called as “The New g-Method” [6].

$\mu$ -method is a frequently preferred solution method for robust flutter analysis. A match-point solution based on  $\mu$ -method is constructed with uncertainties and noises affecting the equations of motion for the worst flight conditions [7].

Another flutter solution method contains low pressure values and determination of coefficients of equations of motion related to these pressure values [8].

Robust  $\mu$ -k method is generalized based on Laplace domain and the new solution model is called as robust  $\mu$ -p method (p shows Laplace variable in this work) [9]. The method obtained after generalization provides the distinction of valid eigenvalues in imaginary plane which is the flutter solution area. The objective is to find the eigenvalues at tip points since these eigenvalues construct the boundaries of flutter area and provide initial estimation for flutter speed.

Solution method for a flutter problem contains an iterative process based on an eigenvalue problem. A method called “Complex Velocity Solution” for the determination of flutter speed in 2-dimensional and incompressible flow employs the solution of imaginary component of the speed for the eigenvalue set corresponding to each reduced flutter frequency values [10]. Since the eigenvalues are imaginary numbers, the corresponding speeds are imaginary, too.

Laplace domain based studies provide a solution independent from time terms such that algebraic equations are adequate to find flutter speed [11]. Laplace transformation method employs an initial value problem starting from present time to positive infinity compatible with flutter motion in aircraft wings. An aeroelastic system can be modeled and solved without an iterative process by using the algebraic methods and control approaches that can be provided by Laplace transformation [12]. Algebraic approaches based on Laplace domain can produce an eigenvalue



problem similar to frequency based solutions. A nonlinear flutter problem based on Laplace variable for NACA64A006 airfoil is solved as an eigenvalue problem and validated [13]. Eller [14] employs a flutter analysis methodology based on linearization of nonlinear terms and use of aerodynamic expressions in terms of Laplace variable.

Use of control approach for the stability of a system in flutter condition is another research topic as an extension of Laplace domain based calculations [12, 15, 16]. Routh-Hurwitz Control Criterion can be used to determine the stability of an aeroelastic system composed of coupled form of fluid and structure [15]. Another method for stability analysis is root locus method which is a graphical technique and provides correct expressions for system roots in terms of varying parameters in  $s$ -plane and contains an approximate plot for system stability [15].

Root locus method has another application area based on equations of motion in 2-dimensional flow case and starts from matrix equations in terms of Laplace variable. Variation of flutter speed values of an aeroelastic system with respect to variation of system roots can be observed graphically. Thus, root locus method is direct solution among analytical flutter calculation approaches [12].

Flutter analysis in 3-dimensional cases involves use of energy principle and assumed mode technique in addition to the explained methods above. Assumed mode technique, which contains the use of shape functions and time dependent generalized coordinates, is also compatible with aeroservoelastic analyses. Heeg [17] uses assumed mode technique for aeroservoelastic modeling in a flutter suppression problem.

Aerodynamic force and moment terms need to be approximated for 2 and 3-dimensional wing cases by using several approaches. These approaches should adapt to the solution method (frequency based, time based, Laplace domain based) and flight regime (steady flow, unsteady flow). A realistic flutter solution method must contain unsteady aerodynamics effects. Aerodynamic models used in unsteady flight regime solutions can be categorized as below.

- Aerodynamic Model with Theodorsen Function
- Aerodynamic Model with Wagner Function
- Rational Function Approximation

- Indicial Function Approach

Theodorsen Function, which is derived for thin airfoil in oscillations with small amplitudes in unsteady and incompressible flight regime, is frequently used in frequency based flutter calculations [18].

Wagner Function is used to determine magnitude of lift and circulation around a wing with constant small angle of attack value and a speed value increasing impulsively from the beginning [19]. Aerodynamic lift and moment expressions in equations of motion for 2 and 3-dimensional wing cases can be defined in terms of Wagner Function [20] for both open and close loop aeroelastic systems [21]. Moreover, aerodynamic expressions in terms of Wagner Function can be derived in supersonic regimes [21]. Wagner Function has two approaches depending on the principle that instantaneous lift at the beginning is the half of steady lift value. Although mathematical expressions are different from each other, both of them accept that instantaneous lift value is theoretically equal to steady lift value at infinity. These approaches are known as Garrick and Jones Approximations. Jones Approximation provides more efficient aerodynamic models and more accurate results for aeroelastic response and flutter problems since the mathematical formulation is more complex with higher order terms [22].

Rational Function Approximation represents generalized aerodynamic forces by using undetermined coefficients with mathematical series approach and mathematical expressions in terms of Laplace variable [23]. Parameter optimization method which is frequently used in the solution of aeroelastic systems is based on optimization of undetermined coefficients in order to employ the most efficient aerodynamic model [16].

Marzocca [24] calculated flutter for incompressible, subsonic and incompressible, supersonic flight regimes by using Indicial Function Approach with both computational fluid dynamics analysis and analytical modeling [24]. Indicial Function Approach can involve both a linear expression in terms of downwash speed and a mathematical formulation depending on nonlinear characteristics of transonic regime.

Uncertainties are unpreventable randomness in systems and their models. The parameters including uncertainties can be distributed by using the information

coming from the manufacturer. Uncertainties in modeling can be divided into two categories as dynamic and parametric uncertainties. Dynamic uncertainties are arisen from nonlinearities and unmodeled features while the sources of parametric uncertainties are related to mass, damping and aerodynamics [25].

The sources of uncertainties can be various while the most common ones seen in aeroelastic systems are in structural and aerodynamic models [25]. Uncertainties such as in structural damping, mass distribution, flow boundary conditions, geometry and material properties and flight conditions have been studied in prior works in literature [26]. The appropriate definitions of aerodynamic uncertainties are stated in [27] and [28]. As stated by Danowski [26], further investigations of uncertainty analysis with respect to flutter problems are desired. The uncertainty in flutter speed is also rather sensitive to structural dynamics [29]. As an example, in the work of Poirion [30], uncertainties in stiffness matrix elements are included.

Traditional flutter analysis methods are based on deterministic aeroelastic simulation models but nothing is exactly as designed [26]. Robust flutter analysis is based on calculation of flutter speed in both cases with uncertainties and large variations [31]. Critical flutter speed is the available lowest flutter speed. Flutter speed also becomes a random variable when random parameters are defined and have properties such as mean value and standard deviation [32]. Robust flutter analysis has great importance in terms of flight safety [29]. Therefore, robustness analyses with respect to uncertainties form a research topic with growing interest. Flutter speed can be obtained with a linear stability analysis for an accurate model of vehicle dynamics. It is also severe to determine the distributions of parameters with uncertainties [29].

A linear flutter analysis by considering the uncertainties in various parameters is performed by Potter [29] and the worst case flutter speed is taken into account within the context of robust analysis while parameters including uncertainties are selected as natural frequencies and modal parameters of damping terms.

Borglund [33] performs a robust flutter analysis by considering the uncertainties in aerodynamics and mass properties. The analysis makes use of p-k method eigenvalues sets.  $\mu$ -p analysis is used to directly calculate the boundaries of the same eigenvalues sets.  $\mu$ -p and p-k methods produce similar results in the presence of various uncertainties.

The new development in the aeroelastic analysis considering model uncertainty is stated  $\mu$ -p method. The basic principle of this method is to obtain the uncertainties with a singular value ( $\mu$ ) if flutter determinant for any flutter eigenvalue  $p$  can be zero in the presence of these uncertainties. Therefore, the eigenvalue in complex plane and the boundaries of damping can be computed to perform a robust flutter analysis. This method makes use of a standard linear flutter analysis in order to obtain deterministic values and variations. Perturbations in only complex valued aerodynamics are included in [27, 34, 35]. Both real and complex uncertainties in structural and aerodynamic properties are included in the work of Borglund [33].

$\mu$ -method in the work of Lind [25] provides accurate information about robustness as long as an appropriate mathematical model can be set up. The difficulty in this method is to determine the uncertainty operators. An approach to overcome this difficulty is to validate the model by using transfer function data in frequency domain.  $\mu$ -method holds importance for both control and aeroelasticity. It is a severe tool for flutter analysis since it provides the determination of flutter margins similar with p-k method and definitions of robust flutter margins in the presence of modeling errors. The margins calculated for flutter are the worst case scenerios.

Prazenica [36] gives information about flutterometer which is a tool used during flight tests. It is based on linear flutter analysis procedure by using a model with uncertainty definitions. Uncertainty information is useful since it comes from flight tests.

Flutterometer contributes to the test by obtaining flutter speed [25]. Methods using analytical predictions try to form a computational model without flight data.

Analytical prediction methods can be summarized as following.

- 1) 1<sup>st</sup> order perturbation analysis
- 2) Stochastic robustness

Monte Carlo (MC) methods from stochastic robustness class make use of repeated random sampling for random variables to reach the results. They basically contain simulation of a physical system while randomly changing the parameters [26].

MCS provides the most inexpensive solution to obtain the probabilistic flutter speed [30]. MCS is the most reliable method in stochastic analysis. It provides accurate

solution for a system with a deterministic solution. MCS is rather a lot appropriate for modeling random uncertain parameters [30]. MCS can include many types of random variations. The general flowchart for MCS [37] is shown in Figure 1.1.

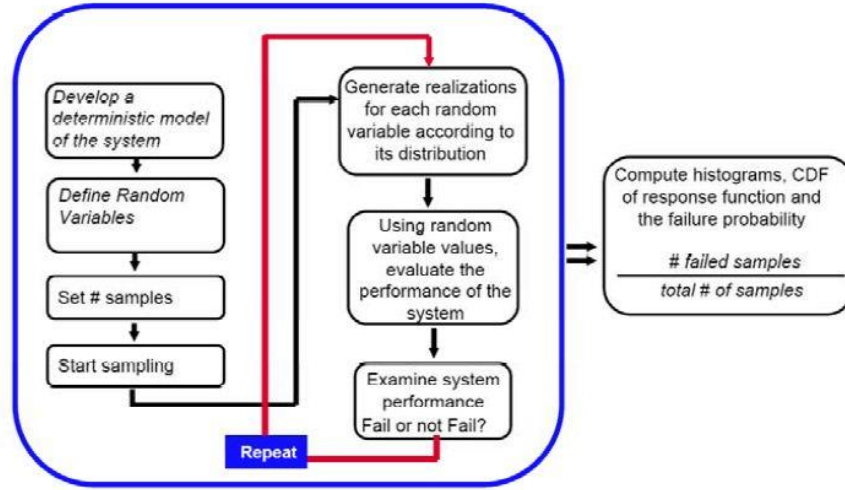


**Figure 1.1 :** General flowchart of MCS

Results obtained from MC methods can be analyzed statistically. Danowski [26] states that “The optimal number of runs is that which is a minimum number but produces relatively identical statistical results if more runs are made”. Statistical results of MCS are used when deterministic solution is impossible or infeasible [26].

MCS is a frequently used method in uncertainty quantification in a stochastic framework however it becomes nonconvergent in computationally expensive problems. Polynomial Chaos Expansion (PCE) is preferred or reduced order models can be used in more complex systems [30]. PCE defines the uncertainties as orthogonal polynomials while giving optimal exponential convergence for Gaussian inputs [38]. The resulting deterministic systems are solved with known methods. [32] As an example, Poirion [30] states a work based on MCS by making use of chaos expansion of random matrices.

Marques [39] considers MCS, perturbation and interval analyses in stability calculation of Golland wing based on eigenvalues containing Euler aerodynamics effects. Kurdi [40] determines flutter boundaries of heavy version of Golland<sup>+</sup> wing and wing/store configuration with uncertainties in structural dimensions. Random variables are distributed with MCS while flutter speed is calculated by using the linear aerodynamic theory of ZONA6 code.

In recent years, extensive research has been done in the robust analysis of aeroelastic systems. Limit Cycle Oscillation (LCO) and flutter characteristics of a wing modeled as a cantilever beam are investigated in transonic regime with time domain simulations and bifurcation analysis for various positions and numbers of store loads [41]. Robust LCO and flutter analyses are also accomplished with computational codes such as MSC/NASTRAN, ANSYS, ZONA Software, etc. [42, 43, 44, 45, 46, 47, 48]. Graham [49] determines flutter boundaries of an aeroservoelastic system with robust analyses based on  $\mu$ -method.

Robust design optimization in aeroelastic systems is an ongoing research topic in the field of aeroelasticity and robust optimization. There are several considerable works in robust aeroelastic design optimization [50, 51, 52, 53, 54], however structural uncertainties are not considered in many of the works. A robust design optimization of a backswept wing considering structural uncertainties such as the thicknesses of upper and lower skins, trailing edge, lugs, stringers and webs so as to minimize the structural weight is represented by Wan [55].

The main principle of a robust analysis is to determine the worst condition for the current design. Kim [56] performs a gradient-based robust nonlinear aeroelastic optimization for NACA0012 airfoil in order to investigate the system performance in the worst-case scenario. Witteveen [57] performs a robust design optimization by using Simplex Elements Stochastic Collocation (SESC) method matching with MC sampling in order to distribute the uncertainties.

The present work involves robust optimization of 2 and 3-dimensional structures by employing MCS. Three dimensional clean wing and wing/store configurations consist of AGARD 445.6 model. This work is the first attempt for robust aeroelastic design optimization of AGARD 445.6 wing to the best of author's knowledge.

## 2. TWO DIMENSIONAL AEROELASTIC ANALYSIS

This section involves development of an aeroelastic analysis methodology for a 2-dimensional airfoil to obtain the boundaries of static and dynamic instabilities. The considered instabilities are flutter, divergence and control reversal. The solution procedure is based on a primary approach since it makes use of simple aerodynamic theory in quasi-steady, incompressible and inviscid flow. The main purpose is to form an aeroelastic solution which can be extended to use in more realistic wing structures and flow conditions. Proposed solution method is implemented into a computational code and validated with benchmark problems from literature.

### 2.1 Development of Aeroelastic Solution Methodology

Formulation of an aeroelastic problem in 2-dimensional case requires convenient use of Lagrange and energy equations in order to obtain equations of motion. The basic approach involves the use of open loop dynamics and stability analysis procedure. The derived formulation can be used for divergence, control reversal and flutter instabilities since it is based on control theory. A suppressing control approach for aeroelastic effects contains two main phases as determination of open loop dynamic characteristics and design of compensator. Determination of open loop dynamic characteristics step is based on obtaining the region or speed in which an instability happens and it is compatible with the content of the present work since it can provide a solution for divergence, control reversal and flutter as aeroelastic instabilities.

The airfoil is modeled by using linear and torsional springs as shown in Figure 2.1. Equations of motion which describe both plunging and pitching motions are derived from Lagrange equations. Lagrange equations can be written in a form as shown in (2.1) where  $t$  is time variable,  $T$  and  $V$  are kinetic and potential energies respectively.  $Q$  and  $q$  show generalized forces and coordinates.

$$\frac{d}{dt} \left( \frac{\partial T}{\partial \dot{q}_i} \right) - \left( \frac{\partial T}{\partial q_i} \right) + \left( \frac{\partial V}{\partial q_i} \right) = Q_i \quad (2.1)$$

Kinetic and potential energy equations can be written for the reference geometry.

$$V = \frac{1}{2}k_h h^2 + \frac{1}{2}k_\alpha \alpha^2 \quad (2.3)$$

Convenient energy terms for Lagrange equations can be extended by using geometrical relations and a matrix system that describes the reference model. The equations of motion for a reference aeroelastic system are defined as in (2.4) and (2.5). In (2.4) and (2.5),  $h$  and  $\alpha$  define plunging and pitching motions respectively while  $b$  is half chord distance,  $x_\alpha = (S_\alpha / mb)$  is static offset term,  $S_\alpha$  is static moment and  $I_\alpha$  is moment of inertia.  $L$  and  $M_y$  show aerodynamic lift force and pitching moment.

14



$$mbx_\alpha \ddot{h} + I_\alpha \ddot{\alpha} + k_\alpha \alpha = M_y(t) \quad (2.5)$$

This section is based on open loop characteristics of 2-dimensional dynamic systems. Therefore, it will be more practical to define the system of equations with Laplace variable,  $s$ . Time related terms can be transformed into Laplace domain to obtain algebraic equations. Equations of motion in time domain can be constituted in matrix form.

$$\begin{pmatrix} \frac{1}{r_\alpha^2} & \frac{x_\alpha}{r_\alpha^2} \\ \frac{x_\alpha}{r_\alpha^2} & 1 \end{pmatrix} \begin{Bmatrix} \ddot{h}(t) \\ \ddot{\alpha}(t) \end{Bmatrix} + \begin{pmatrix} \bar{\omega} & \bar{q}C_{L\alpha} \\ 0 & 1 - \bar{q}C_{M\alpha} \end{pmatrix} \begin{Bmatrix} h(t) \\ \alpha(t) \end{Bmatrix} = \begin{Bmatrix} L(t) \\ M_y(t) \end{Bmatrix} \quad (2.6)$$

where  $r_\alpha$  is radius of gyration and  $\bar{\omega}$  is the ratio of natural frequencies.  $C_{L\alpha}$  and  $C_{M\alpha}$  are aerodynamic lift and moment coefficients for pitching deflection while  $\bar{q}$  is normalized dynamic pressure. Definitions of reduced coefficients are given in (2.7), (2.8), (2.9) and (2.10).

$$r_\alpha = \sqrt{\frac{I_\alpha}{mb^2}} \quad (2.7)$$

$$\bar{\omega} = \frac{\omega_h}{\omega_\alpha} \quad (2.8)$$

$$\omega_h = \sqrt{\frac{k_h}{m}} \quad (2.9)$$

$$\omega_\alpha = \sqrt{\frac{k_\alpha}{I_\alpha}} \quad (2.10)$$

Time dependent matrix equations are transformed into Laplace domain so that necessary algebraic equations can be constructed for an aeroelastic system. Application of Laplace transformation includes the use of displacement terms  $h$  and  $\alpha$  in Laplace domain. By using Laplace transformation procedure, related equations for time dependent terms can be obtained.

$$h(t) \rightarrow h(s) \quad (2.11)$$

$$\alpha(t) \rightarrow \alpha(s) \quad (2.12)$$

$$\ddot{h}(t) \rightarrow s^2 h(s) - sh(0) - \dot{h}(0) \quad (2.13)$$

$$\ddot{\alpha}(t) \rightarrow s^2 \alpha(s) - s\alpha(0) - \dot{\alpha}(0) \quad (2.14)$$

By assuming that all displacements and their derivatives in initial case are zero, the following definitions must be used.

$$\ddot{h}(t) \rightarrow s^2 h(s) \quad (2.15)$$

$$\ddot{\alpha}(t) \rightarrow s^2 \alpha(s) \quad (2.16)$$

Then, the equations of motion in Laplace domain can be defined.

$$\begin{pmatrix} \frac{1}{r_\alpha^2} & \frac{x_\alpha}{r_\alpha^2} \\ \frac{x_\alpha}{r_\alpha^2} & 1 \end{pmatrix} \begin{Bmatrix} s^2 h(s) \\ s^2 \alpha(s) \end{Bmatrix} + \begin{pmatrix} \bar{\omega} & \bar{q}C_{L\alpha} \\ \frac{\bar{\omega}}{r_\alpha^2} & 1 - \bar{q}C_{M\alpha} \end{pmatrix} \begin{Bmatrix} h(s) \\ \alpha(s) \end{Bmatrix} = \begin{Bmatrix} L(s) \\ M_y(s) \end{Bmatrix} \quad (2.17)$$

where reduced dynamic pressure, reduced speed and airfoil mass ratio can be defined as follows. In (2.20),  $\rho$  is density of airfoil.

$$\bar{q} = \frac{U_\alpha^2}{\pi \mu r_\alpha^2} \quad (2.18)$$

$$U_\alpha = \frac{U}{\omega_\alpha b} \quad (2.19)$$

$$\mu = \frac{m}{\pi \rho b^2} \quad (2.20)$$

In the presence of control surfaces in both trailing and leading edge of the airfoil, the aerodynamic terms must be obtained by considering their effects. In (2.21) and (2.22),  $C_{L\beta}$  and  $C_{L\xi}$  are aerodynamic lift coefficients and,  $C_{M\beta}$  and  $C_{M\xi}$  are aerodynamic moment coefficients for the control surfaces in trailing and leading edges respectively.  $\beta$  and  $\xi$  define the deflections of control surfaces in trailing and leading edges while  $\alpha_0$  shows the initial pitch deflection.

$$L = -\rho U^2 b C_{L_\beta} \beta - \rho U^2 b C_{L_\xi} \xi - \rho U^2 b C_{L_\alpha} (\alpha + \alpha_0) \quad (2.21)$$

$$M_y = \rho U^2 b^2 C_{M_\beta} \beta + \rho U^2 b^2 C_{M_\xi} \xi + \rho U^2 b^2 C_{M_\alpha} (\alpha + \alpha_0) \quad (2.22)$$

Obtaining control reversal speed value requires the use of control surfaces actively. Thus, the effects of control surfaces in both trailing and leading edges must be considered. General definition for the aeroelastic system is given in (2.23).

$$\begin{pmatrix} \frac{1}{r_\alpha^2} & \frac{x_\alpha}{r_\alpha^2} \\ \frac{x_\alpha}{r_\alpha^2} & 1 \end{pmatrix} \begin{Bmatrix} s^2 \bar{h} \\ s^2 \alpha \end{Bmatrix} + \begin{pmatrix} \bar{\omega} & \bar{q} C_{L_\alpha} \\ 0 & 1 - \bar{q} C_{M_\alpha} \end{pmatrix} \begin{Bmatrix} \bar{h} \\ \alpha \end{Bmatrix} = \begin{pmatrix} 1 & 0 & -\bar{q} C_{L_\beta} & -\bar{q} C_{L_\xi} \\ 0 & 1 & \bar{q} C_{M_\beta} & \bar{q} C_{M_\xi} \end{pmatrix} \begin{Bmatrix} \bar{h} \\ \alpha \\ \beta \\ \xi \end{Bmatrix} + \begin{pmatrix} -\bar{q} C_{L_\alpha} \\ \bar{q} C_{M_\alpha} \end{pmatrix} \alpha_0 \quad (2.23)$$

Such control approach requires a state-space representation of the system of equations. General form of a state-space representation is given in (2.24).

$$\dot{y} = a_1 y + b_1 x \quad (2.24)$$

If the following equality is assumed:

$$y_1 = y \quad (2.25)$$

Then:

$$y_2 = \dot{y}_1 = \dot{y} \quad (2.26)$$

Another type of state-space form is:

$$\dot{y}_2 = a_2 y + b_2 x \quad (2.27)$$

General system can be derived by using the following equation.

$$\ddot{y}_2 = a_1 y + b_1 x \quad (2.28)$$

System of equations for the airfoil model can be re-written in terms of second derivatives after obtaining the equations in a simplified form in time domain by making use of some matrix operations and mathematical calculations.

$$\begin{Bmatrix} \ddot{h} \\ \ddot{\alpha} \end{Bmatrix} = [A]_{2 \times 2} \begin{Bmatrix} \bar{h} \\ \alpha \end{Bmatrix} + [B]_{2 \times 4} \begin{Bmatrix} h \\ \alpha \\ \beta \\ \xi \end{Bmatrix} \quad (2.29)$$

2-degrees of freedom are used in flutter and divergence calculations for simplicity, however control reversal analysis has to include 4-degrees of freedom. Displacements of control surfaces do not have a considerable effect on both flutter and divergence speed although control reversal is directly related to control surfaces of an airfoil.

System of equations in Laplace domain can be determined for flutter and divergence as follows:

$$\begin{pmatrix} \frac{1}{r_\alpha^2}(s^2 + \bar{\omega}^2) & \frac{x_\alpha}{r_\alpha^2}s^2 + \bar{q}C_{L_\alpha} \\ \frac{x_\alpha}{r_\alpha^2}s^2 & s^2 + (1 - \bar{q}C_{M_\alpha}) \end{pmatrix} \begin{Bmatrix} h(s) \\ \alpha(s) \end{Bmatrix} = \begin{Bmatrix} 0 \\ 0 \end{Bmatrix} \quad (2.30)$$

The stability analysis can be applied for flutter and divergence cases by obtaining the characteristic equation of the system. Characteristic equation of the system is determined in (2.31).

$$C(s) = \left[1 - \frac{x_\alpha^2}{r_\alpha^2}\right]s^4 + \left[(\bar{\omega}^2 + 1) - \bar{q}(C_{L_\alpha}x_\alpha + C_{M_\alpha})\right]s^2 + \bar{\omega}^2(1 - \bar{q}C_{M_\alpha}) = 0 \quad (2.31)$$

Roots of a characteristic equation are known as system poles in stability analysis. The case which roots place in imaginary axis is the critical transition between stable and unstable states. In aeroelastic stability analysis, the point that indicates this transition is known as critical speed value. Critical flutter and divergence speeds can be obtained via the roots of related characteristic equation. The imaginary components of the roots give the critical speeds. Flutter and divergence speed values differ from each other due to the geometrical features of the airfoil. Flutter is seen before divergence in most cases but this is not necessary.

In order to find the value of control reversal speed, the system can be written in state-space form by using the characteristic equation with the effects of control surfaces.

$$\begin{Bmatrix} s^2 \bar{h} \\ s^2 \alpha \end{Bmatrix} = \frac{r_\alpha^2}{C(s)} \begin{pmatrix} T_{11} & T_{12} & T_{13} & T_{14} \\ T_{21} & T_{22} & T_{23} & T_{24} \end{pmatrix} \begin{Bmatrix} \bar{h} \\ \alpha \\ \beta \\ \xi \end{Bmatrix} \quad (2.32)$$

where  $T_{ij}$  ( $i=1$  to 2 and  $j=1$  to 4) shows the transfer functions related to aeroelastic phenomena.  $T_{ij}$  is a transfer function including effects of  $i$ th terms as output and  $j$ th terms as input.

By considering the stability of each transfer function, both divergence and control reversal speeds can be obtained via root locus plots. The root locus plots are compatible with stability analysis of the dynamic systems since a pole in the imaginary axis shows the critical point between stable and unstable plants.

Transfer functions which can be obtained from the system of equations for aeroelastic instabilities are known as transfer functions of SISO (Single-Input Single-Output) systems and can be used for further applications of control analysis in the field of aeroelastic control. The transfer functions are listed as below [58].

1.  $T_{11} = T_{hh} = s^2 + 1 - \bar{q}C_{M_\alpha}$
2.  $T_{12} = T_{h\alpha} = -\frac{x_\alpha s^2}{r_\alpha^2} - \bar{q}C_{L_\alpha}$
3.  $T_{13} = T_{h\beta} = \bar{q}C_{L_\beta} \left( \bar{q}C_{M_\alpha} \left( 1 - \frac{C_{L_\alpha} C_{M_\beta}}{C_{M_\alpha} C_{L_\beta}} \right) - 1 - s^2 \left( 1 + \frac{C_{M_\beta} x_\alpha}{C_{L_\beta} r_\alpha^2} \right) \right)$
4.  $T_{14} = T_{h\xi} = \bar{q}C_{L_\xi} \left( \bar{q}C_{M_\alpha} \left( 1 - \frac{C_{L_\alpha} C_{M_\xi}}{C_{M_\alpha} C_{L_\xi}} \right) - 1 - s^2 \left( 1 + \frac{C_{M_\xi} x_\alpha}{C_{L_\xi} r_\alpha^2} \right) \right)$
5.  $T_{21} = T_{\alpha h} = -\frac{x_\alpha s^2}{r_\alpha^2}$
6.  $T_{22} = T_{\alpha\alpha} = \frac{s^2}{r_\alpha^2} + \frac{\omega_h^2}{r_\alpha^2}$
7.  $T_{23} = T_{\alpha\beta} = \frac{1}{r_\alpha^2} \bar{q}C_{M_\beta} \left( s^2 \left( 1 + \frac{C_{L_\beta} x_\alpha}{C_{M_\beta}} \right) + \bar{\omega}^2 \right)$
8.  $T_{24} = T_{\alpha\xi} = \frac{1}{r_\alpha^2} \bar{q}C_{M_\xi} \left( s^2 \left( 1 + \frac{C_{L_\xi} x_\alpha}{C_{M_\xi}} \right) + \bar{\omega}^2 \right)$

The reduced speed value can be obtained by using  $T_{h\beta}$  for control reversal since  $T_{h\beta}$  indicates the stability of  $h$  displacement that is related to lift force effected by control

surface displacement in trailing edge,  $\beta$ . Control reversal speed can be determined by solving for the roots of this transfer function.

## 2.2 Validation of 2D Aeroelastic Analysis

The presented 2D aeroelastic solution technique is implemented in a in-house MATLAB code and applied to benchmark problems chosen from literature as follows.

Parameters of the 1<sup>st</sup> benchmark problem are given by Dowell et al. [58] in Table 2.1. Here,  $a$  shows the distance between center of gravity and elastic axis of the airfoil.

**Table 2.1 :** Design parameters of 2D benchmark problem-I.

Parameter	Value
$a$	-0.2
$x_a$	0.2
$r_a^2$	0.25
$\mu$	20
$\bar{\omega}$	0.2
$t / 2b$	0.51%
$I / b$	3.92
$C_{L_\alpha}$	$2\pi$
$C_{M_\alpha}$	1.885
$C_{L_\beta}$	2.487
$C_{M_\beta}$	-0.334
$C_{L_\xi}$	-0.087
$C_{M_\xi}$	-0.146

The wing mass is assumed to be evenly distributed so that the center of mass lies at the midchord. In order to assure that flutter occurs before divergence, the elastic axis location is shifted ten percent forward of the midchord, which is representative of a 4.5 degree forward fiber sweep if constructed of common graphite epoxy materials in a unidirectional laminate. The flaps are both 10% of the chord [58].

The reduced speeds of flutter, divergence and control reversal are calculated by using the developed in-house code and are presented in Table 2.2.

**Table 2.2 :** Validation of 2D aeroelastic solution-I.

	Flutter	Divergence	Control Reversal
Reference Speed <sup>[58]</sup>	1.90	2.47	2.40
Calculated Speed	1.9638	2.4779	2.3992
Relative Error	3.36%	0.32%	0.03%

The problem in the work of Munteanu [59] is used as the 2<sup>nd</sup> benchmark problem for 2-dimensional aeroelastic analyses. The design parameters are defined in Table 2.3:

**Table 2.3 :** Design parameters of 2D benchmark problem-II.

Parameter	Value
$a$	-0.6
$x_\alpha$	0.2466
$k_h$	2844.4 N/m
$k_\alpha$	3.525 Nm/rad
$m$	12.3870
$I_\alpha$	0.065
$b$	0.135 m
$C_{L_\alpha}$	6.28
$C_{M_\alpha}$	-0.635
$C_{L_\beta}$	3.358
$C_{M_\beta}$	12.39

By using the same Matlab code, the speed values of aeroelastic instabilities can be calculated as shown in Table 2.4. Calculations for 2 benchmark problems give satisfactory results with small relative errors for static and dynamic aeroelastic instabilities, then the presented methodology for a 2-dimensional model is validated.

**Table 2.4 :** Validation of 2D aeroelastic solution-II.

	Flutter	Divergence	Control Reversal
Reference Speed <sup>[59]</sup>	11.243 m/s	-	-
Calculated Speed	11.3612 m/s	57.6617 m/s	-
Relative Error	1.0513%	-	-





### **3. THREE DIMENSIONAL FLUTTER ANALYSIS**

This section presents development and validation of a methodology for flutter solution of 3-dimensional wing structures. The methodology basically incorporates effects of wing span and variations in design parameters such as taper ratio and sweep angle of the wing. The solution methodology also includes determination of bending and torsional natural frequencies since they are dependent on the variations of wing parameters. Finally, a solution procedure to obtain natural frequencies and flutter speeds of 3-dimensional wings is developed, then validated by using two examples from literature and finally applied to well-known aeroelastic benchmark configurations, Goland and AGARD 445.6 wings so as to further carry out a realistic flutter analysis.

#### **3.1 Flutter Solution Methodology**

An analytical solution based on assumed mode technique for determination of flutter speed of a 3-dimensional wing is presented in the current work. Assumed mode technique basically involves the correct representation for replacing displacements with mode shapes and generalized coordinates. Equations of motion can be derived with Lagrange equations including energy equalities and convenient aerodynamic expressions for the flight regime. Flutter boundary is calculated by introducing V-g solution based on artificial damping term. Displacement of a wing is expressed by product of assumed modes and generalized coordinates. Convenient equations for bending and torsional displacements can be obtained in series forms. General representation of a 3-dimensional aeroelastic model is shown in Figure 3.1 [60].

Several assumptions are made to construct a 3-dimensional linear flutter analysis by considering sweep angle effects and their details are given as follows.

1) The first bending and the first torsional modes are assumed for flutter calculations since they have the major effects on flutter boundary. Their effects will also be

examined in Goland and AGARD 445.6 wing applications. Existence of flutter motion due to the first modes will be justified.

2) The design parameters which depend on cross-sectional geometry are assumed to be constant in order to prevent to solve nonlinear differential equations. Average values are used for all of them in calculations.

3) Euler-Bernoulli beam equations are used to calculate natural frequencies. Their feasibility in AGARD 445.6 will be justified by the example studies from literature and calculated results of the present work.

4) Theodorsen aerodynamics is considered for aerodynamic load calculation since both Goland and AGARD 445.6 wings are sufficiently thin.

5) One pole approach is used for Theodorsen function since it gives accurate results between a specific reduced frequency range where flutter typically occurs.

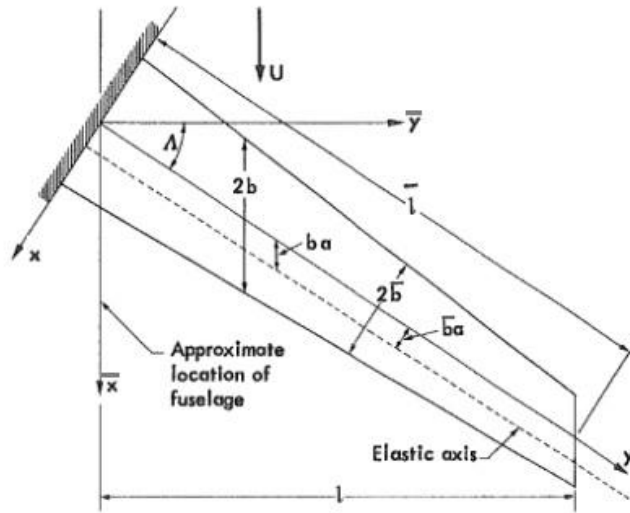


**Figure 3.1 :** General representation of 3D aeroelastic model.

Equations of motion in assumed mode flutter analysis are given in (3.1) and (3.2).

$$m\ddot{w}(y,t) - S_y\ddot{\theta}(y,t) + EI \frac{\partial^4 w(y,t)}{\partial y^4} = L(y,t) \quad (3.1)$$

$$I_y\ddot{\theta}(y,t) - S_y\ddot{w}(y,t) - GJ \frac{\partial^2 \theta(y,t)}{\partial y^2} = M_y(y,t) \quad (3.2)$$

where  $S_y$  is static moment and  $I_y$  is moment of inertia of the wing structure while  $EI$  and  $GJ$  define bending and torsional rigidities.

The displacement terms can be treated as separable variables where  $F(x, y) = f(x) \cdot g(y)$  is general definition for a separable variable which is only function of  $x$  and  $y$ . Similarly, the displacements of a cantilever beam can be defined as follows.

$$\bar{w}(x, y, t) = w_R(t) \cdot \phi(x, y) \quad (3.5)$$

$$\bar{\theta}(x, y, t) = \theta_R(t) \cdot \varphi(x, y) \quad (3.6)$$

where  $\phi(x, y)$  and  $\varphi(x, y)$  are mode shapes for bending and torsional motions respectively while  $\bar{w}$  and  $\bar{\theta}$  show bending and torsional deflections depending on  $x$  and  $y$ -coordinates and time. These displacement terms can be obtained by using series approach. The design parameters which are depending on cross-sectional geometry are assumed to have constant values. Average values are calculated and used in flutter equations. Thus, variations of bending and torsional deflections with respect to time and distance along spanwise direction are only investigated.

$$\tilde{w}(y, t) = \sum_{i=1}^m \phi_i(y) \cdot w_i(t) \quad (3.7)$$

$$\tilde{\theta}(y, t) = \sum_{i=1}^{n-m} \varphi_i(y) \cdot \theta_i(t) \quad (3.8)$$

$$w = \tilde{w} - x\tilde{\theta} \quad (3.9)$$

$$w(y, t) = \sum_{i=1}^m \phi_i(y) \cdot w_i(t) - \sum_{i=1}^{n-m} x\varphi_i(y) \cdot \theta_i(t) \quad (3.10)$$

where  $w$  and  $\theta$  indicate bending and torsional displacements respectively while  $m$  and  $n-m$  total number of assumed modes for bending and torsional modes. The first bending and the first torsional modes are assumed in the present work since the major effects on flutter boundary come from the first modes. This case will be justified by Goland and AGARD 445.6 wings flutter problems.

Three dimensional aeroelastic modeling requires the use of Lagrange equations. Kinetic and potential energy equations must be defined by considering 3-dimensional effects. Kinetic energy can be written as in (3.11).

$$T = \frac{1}{2} m V^2 = \frac{1}{2} m \dot{w}^2 \quad (3.11)$$

For a 3-dimensional structure, kinetic energy equation becomes:

$$T = \frac{1}{2} \iiint (\dot{w}(x, y, t))^2 dm \quad (3.12)$$

Differential mass elements can be defined as follows:

$$dm = \rho dA \quad (3.13)$$

$$dA = dx dy \quad (3.14)$$

$$dm = \rho dx dy \quad (3.15)$$

Kinetic energy equation can now be defined with a more simplified form.

$$T = \frac{1}{2} \int_0^l \int_0^c [\dot{w}(x, y, t)]^2 \rho(x, y) dx dy \quad (3.16)$$

Same assumption involving the use of average values is considered.

$$T = \frac{1}{2} \int_0^l \left( \frac{1}{2} \rho dx \dot{w}^2 - \rho x dx \dot{w} \dot{\theta} + \frac{1}{2} x^2 \rho dx \dot{\theta}^2 \right) dy \quad (3.17)$$

By using the definitions along the span of the wing and about the elastic axis of the profile, the energy equation can be simplified by using below definitions:

- Mass:  $m = \rho dx$
- Static unbalance:  $S_y = \rho x dx$
- Moment of inertia:  $I_y = \rho x^2 dx$

Now, the obtained 3 equations become:

$$\bar{w}(y, t) = \sum_{i=1}^m \phi_i(y) \cdot w_i(t) \quad (3.18)$$

$$\bar{\theta}(y, t) = \sum_{i=1}^{n-m} \varphi_i(y) \cdot \theta_i(t) \quad (3.19)$$

$$T = \frac{1}{2} \int_0^l \left( \frac{1}{2} m \dot{w}^2 - S_y \dot{w} \dot{\theta} + \frac{1}{2} I_y \dot{\theta}^2 \right) dy \quad (3.20)$$

Related terms placed in kinetic energy equation can be shown as follows:

- i.  $\dot{w}(y, t) = \sum_{i=1}^m \phi(y) \dot{w}_i(t)$
- ii.  $\dot{\theta}(y, t) = \sum_{i=1}^{n-m} \varphi(y) \dot{\theta}_i(t)$
- iii.  $\dot{w}^2(y, t) = \sum_{i=1}^m \sum_{j=1}^m \phi_i(y) \phi_j(y) \dot{w}_i(t) \dot{w}_j(t)$
- iv.  $\dot{\theta}^2(y, t) = \sum_{i=1}^{n-m} \sum_{j=1}^{n-m} \varphi_i(y) \varphi_j(y) \dot{\theta}_i(t) \dot{\theta}_j(t)$

If these terms are used in kinetic energy equation, then (3.21) can be obtained.

$$T = \frac{1}{2} \sum_{i=1}^m \sum_{j=1}^m \dot{w}_i(t) \dot{w}_j(t) \int_0^l \int_0^c m \phi_i(y) \phi_j(y) dy - \sum_{i=1}^m \sum_{j=1}^{n-m} \dot{w}_i(t) \dot{\theta}_j(t) \int_0^l \int_0^c S_y \phi_i(y) \varphi_j(y) dy + \frac{1}{2} \sum_{i=1}^{n-m} \sum_{j=1}^{n-m} \dot{\theta}_i(t) \dot{\theta}_j(t) \int_0^l \int_0^c I_y \varphi_i(y) \varphi_j(y) dy \quad (3.21)$$

This energy equation can now be used for a reference station of the wing. Reference station involves the cross-section whose properties are considered to determine flutter speed. Reference station provides minimum flutter speed among all stations along wing span and it is 75% of span distance away from the wing root [58, 60]. The computational code of the present work involves a station-based flutter analysis. The analysis contains flutter calculations in  $10^5$  stations along wing span while the station with minimum flutter speed is selected as reference station. The addressed reference station is the same place stated by Dowell et. al [58] and Bisplinghoff et. al [60]. Thus, the reference station will be considered to be 75% span distance away from wing span for flutter calculations of wing/store configurations to reduce the computational time instead of using a station-based analysis. The definitions below show the transformations of general displacement expressions to displacements in reference station.

- $w \rightarrow w_R$  : Bending displacement with respect to reference station
- $\theta \rightarrow \theta_R$  : Torsion displacement with respect to reference station

In terms of the displacements of reference station and by using orthogonality, kinetic energy equation can be finally written as in (3.22).

$$T = \frac{1}{2} \dot{w}_R^2 \int_0^l m \phi^2(y) dy - \dot{w}_R \dot{\theta}_R \int_0^l S_y \phi(y) \varphi(y) dy + \frac{1}{2} \dot{\theta}_R^2 \int_0^l I_y \varphi^2(y) dy \quad (3.22)$$

General formulation of strain (potential) energy along wing span is defined in (3.23).

$$U = \frac{1}{2} \int_0^l \left( EI \left( \frac{\partial^2 \bar{w}(y,t)}{\partial y^2} \right)^2 + GJ \left( \frac{\partial \bar{\theta}(y,t)}{\partial y} \right)^2 \right) dy \quad (3.23)$$

In (3.23), the related derivations can be written as:

$$\frac{\partial^2 \bar{w}(y,t)}{\partial y^2} = \frac{\partial^2}{\partial y^2} [\phi(y) \bar{w}(t)] = \bar{w}(t) \frac{d^2 \phi(y)}{dy^2} \quad (3.24)$$

$$\frac{\partial \bar{\theta}(y,t)}{\partial y} = \frac{\partial}{\partial y} [\varphi(y) \bar{\theta}(t)] = \bar{\theta}(t) \frac{d\varphi(y)}{dy} \quad (3.25)$$

For the reference station of the wing:

- $w \rightarrow w_R$
- $\theta \rightarrow \theta_R$

The new form of the strain energy becomes:

$$U = \frac{1}{2} w_R^2 \int_0^l EI \left( \frac{d^2 \phi(y)}{dy^2} \right)^2 dy + \frac{1}{2} \theta_R^2 \int_0^l GJ \left( \frac{d\varphi(y)}{dy} \right)^2 dy \quad (3.26)$$

By using the definitions of free vibration frequencies for bending and torsional modes, final form of the strain energy equation can be obtained by using below definitions [60]:

- i.  $\frac{1}{2} \int_0^l EI \left( \frac{d^2 \phi(y)}{dy^2} \right)^2 dy \rightarrow \frac{1}{2} \omega_{w_1}^2 \int_0^l m \phi^2 dy$
- ii.  $\frac{1}{2} \int_0^l GJ \left( \frac{d\varphi(y)}{dy} \right)^2 dy \rightarrow \frac{1}{2} \omega_{\theta_1}^2 \int_0^l I_y \varphi^2 dy$

$$U = \frac{1}{2} \omega_{w_1}^2 w_R^2 \int_0^l m \phi^2(y) dy + \frac{1}{2} \omega_{\theta_1}^2 \theta_R^2 \int_0^l I_y \varphi^2(y) dy \quad (3.27)$$

where  $\omega_{w_1}$  and  $\omega_{\theta_1}$  are the first bending and torsional natural frequencies.

General form of Lagrange equation is summarized again in (3.28).

$$\frac{d}{dt} \left( \frac{\partial T}{\partial \dot{q}_i} \right) - \frac{\partial T}{\partial q_i} + \frac{\partial U}{\partial q_i} = Q_i \quad (3.28)$$

The generalized coordinates and forces can be classified as follows:

- 1) Bending Motion:  $q_1 = w_R$  and  $Q_1 = Q_w$
- 2) Torsion Motion:  $q_2 = \theta_R$  and  $Q_2 = Q_\theta$

Final form of kinetic energy equation is again given in (3.29).

$$T = \frac{1}{2} \dot{w}_R^2 \int_0^l m \phi^2(y) dy - \dot{w}_R \dot{\theta}_R \int_0^l S_y \phi(y) \varphi(y) dy + \frac{1}{2} \dot{\theta}_R^2 \int_0^l I_y \varphi^2(y) dy \quad (3.29)$$

Then, the necessary derivative terms for Lagrange equation are determined by using the final kinetic energy definition:

- i.  $\frac{\partial T}{\partial q_1} = \frac{\partial T}{\partial w_R} = 0$
- ii.  $\frac{\partial T}{\partial q_2} = \frac{\partial T}{\partial \theta_R} = 0$
- iii.  $\frac{\partial T}{\partial \dot{q}_1} = \frac{\partial T}{\partial \dot{w}_R} = \dot{w}_R \int_0^l m \phi^2(y) dy - \dot{\theta}_R \int_0^l S_y \phi(y) \varphi(y) dy$
- iv.  $\frac{\partial T}{\partial \dot{q}_2} = \frac{\partial T}{\partial \dot{\theta}_R} = -\dot{w}_R \int_0^l S_y \phi(y) \varphi(y) dy + \dot{\theta}_R \int_0^l I_y \varphi^2(y) dy$

Final form of strain energy equation is again given in (3.30).

$$U = \frac{1}{2} \omega_{w_1}^2 w_R^2 \int_0^l m \phi^2(y) dy + \frac{1}{2} \omega_{\theta_1}^2 \theta_R^2 \int_0^l I_y \varphi^2(y) dy \quad (3.30)$$

where:

- i.  $\frac{\partial U}{\partial q_1} = \frac{\partial U}{\partial w_R} = \omega_{w_1}^2 w_R \int_0^l m \phi^2(y) dy$
- ii.  $\frac{\partial U}{\partial q_2} = \frac{\partial U}{\partial \theta_R} = \omega_{\theta_1}^2 \theta_R \int_0^l I_y \varphi^2(y) dy$

Now, Lagrange equations can be applied for bending and torsional motions.

$$\begin{aligned}
1) \quad & \frac{d}{dt} \left( \dot{w}_R \int_0^l m \phi^2(y) dy - \dot{\theta}_R \int_0^l S_y \phi(y) \phi(y) dy \right) + \omega_{w_1}^2 w_R \int_0^l m \phi^2(y) dy = Q_w \\
& \ddot{w}_R \int_0^l m \phi^2(y) dy - \ddot{\theta}_R \int_0^l S_y \phi(y) \phi(y) dy + \omega_{w_1}^2 w_R \int_0^l m \phi^2(y) dy = Q_w \\
2) \quad & \frac{d}{dt} \left( -\dot{w}_R \int_0^l S_y \phi(y) \phi(y) dy + \dot{\theta}_R \int_0^l I_y \phi^2(y) dy \right) + \omega_{\theta_1}^2 \theta_R \int_0^l I_y \phi^2(y) dy = Q_\theta \\
& -\ddot{w}_R \int_0^l S_y \phi(y) \phi(y) dy + \ddot{\theta}_R \int_0^l I_y \phi^2(y) dy + \omega_{\theta_1}^2 \theta_R \int_0^l I_y \phi^2(y) dy = Q_\theta
\end{aligned}$$

The equations of motion for the wing model are described in (3.31) and (3.32).

$$\ddot{w}_R \int_0^l m \phi^2(y) dy - \ddot{\theta}_R \int_0^l S_y \phi(y) \phi(y) dy + \omega_{w_1}^2 w_R \int_0^l m \phi^2(y) dy = Q_w \quad (3.31)$$

$$-\ddot{w}_R \int_0^l S_y \phi(y) \phi(y) dy + \ddot{\theta}_R \int_0^l I_y \phi^2(y) dy + \omega_{\theta_1}^2 \theta_R \int_0^l I_y \phi^2(y) dy = Q_\theta \quad (3.32)$$

Generalized aerodynamic forces are defined in (3.33) and (3.34).

$$Q_w = \int_0^l L(y, t) \phi(y) dy \quad (3.33)$$

$$Q_\theta = \int_0^l M(y, t) \phi(y) dy \quad (3.34)$$

Generalized aerodynamic forces are related to aerodynamic lift and pitching moment. Theodorsen aerodynamics is considered in the present work for unsteady flow regime. Definitions presented by Theodorsen for lift and pitching moment terms are given in (3.35) and (3.36) [60] while final lift and moment equations are obtained as in (3.37) and (3.38).  $L_w$ ,  $L_\theta$ ,  $M_w$  and  $M_\theta$  are aerodynamic functions and can be defined in terms of reduced frequency,  $k$ , and Theodorsen function,  $C(k)$  where  $i$  indicates the complex variable.

$$L(y, t) = \pi \rho b^2 \left[ -\omega^2 \bar{w}_R + U i \omega \bar{\theta}_R - \omega^2 b a \bar{\theta}_R \right] + 2 \pi \rho U b C(k) \left[ i \omega \bar{w}_R + U \bar{\theta}_R + i \omega b \left( \frac{1}{2} - a \right) \bar{\theta}_R \right] \quad (3.35)$$



$$M(y,t) = \pi \rho b^2 \left[ -\omega^2 b a \bar{w}_R - i \omega U b \left( \frac{1}{2} - a \right) \bar{\theta}_R + \omega^2 b^2 \left( \frac{1}{8} + a^2 \right) \bar{\theta}_R \right] + 2 \pi \rho U b C(k) \left( \frac{1}{2} + a \right) \left[ i \omega \bar{w}_R + U \bar{\theta}_R + i \omega b \left( \frac{1}{2} - a \right) \bar{\theta}_R \right] \quad (3.36)$$

$$L(y,t) = \pi \rho b^3 \omega^2 \left[ \frac{w_R(t)}{b} \phi(y) L_h - \theta_R(t) \phi(y) \left( L_\theta - L_h \left( \frac{1}{2} + a \right) \right) \right] \quad (3.37)$$

$$M(y,t) = \pi \rho b^4 \omega^2 \left[ -\frac{w_R(t)}{b} \phi(y) \left( M_h - L_h \left( \frac{1}{2} + a \right) \right) \right] + \pi \rho b^4 \omega^2 \left[ \theta_R(t) \phi(y) \left[ M_\theta - (M_h + L_h) \left( \frac{1}{2} + a \right) + L_h \left( \frac{1}{2} + a \right)^2 \right] \right] \quad (3.38)$$

$$L_w = 1 - \frac{2i}{k} C(k) \quad (3.39)$$

$$L_\theta = \frac{1}{2} - \frac{i}{k} - \frac{2i}{k} C(k) - \frac{2}{k^2} C(k) \quad (3.40)$$

$$M_w = \frac{1}{2} \text{ (for subsonic cases)} \quad (3.41)$$

$$M_\theta = \frac{3}{8} - \frac{i}{k} \quad (3.42)$$

$C(k)$  can approximately be taken as in (3.43) with one pole approach [58]. This approach gives accurate results between  $k=0$  and  $k=0.5$  which defines the range flutter typically occurs [61].

$$C(k) = 1 + \frac{-0.4544ik}{ik + 0.1902} \quad (3.43)$$

### 3.1.1 Determination of bending and torsional natural frequencies

System of flutter equations requires use of the first bending and torsional natural frequencies since the first bending and the first torsional modes are assumed for flutter calculation. Natural frequencies in bending and torsional motions have to be solved distinctly since the related equations have different physical meanings and

mathematical expressions. In the present work, a methodology based on Euler-Bernoulli beam equations are presented and considered for AGARD 445.6 wing since next sections involve deterministic and robust aeroelastic design optimization applications. Any variation in design parameters can severely affect natural frequencies as well as flutter boundary. The natural frequency calculations involve the effects of design variables.

Bending and torsional natural frequencies can be obtained by using bending and torsional motion equations for a cantilever beam. The considered equations are Euler-Bernoulli beam formulas.

Use of Euler-Bernoulli beam equations define a general case for the present work, however feasibility of beam formulas is examined for Goland and AGARD 445.6 wing applications since they involve calculation of natural frequencies as well as flutter boundaries.

Equation of motion for bending is defined in (3.44).

$$\rho A \frac{\partial^2 w}{\partial t^2} + \frac{\partial^2}{\partial y^2} \left( EI \frac{\partial^2 w}{\partial y^2} \right) = q(y, t) \quad (3.44)$$

where  $A$  is cross-sectional area of the beam while  $q$  shows the external force.

In free vibration case, external forces must be equal to zero, then:  $q(y, t) = 0$

$$\rho A \frac{\partial^2 w}{\partial t^2} + \frac{\partial^2}{\partial y^2} \left( EI \frac{\partial^2 w}{\partial y^2} \right) = 0 \quad (3.45)$$

By using separation of variables approach in partial differential equations, the bending displacement term can be divided into two discrete functions.

$$w(y, t) = Y(y) \cdot Z(t) \quad (3.46)$$

These function can be used in equation of bending motion.

$$\rho A Y(y) \ddot{Z}(t) + EI Y''''(y) Z(t) = 0 \quad (3.47)$$

If a variable is defined for simplicity as:  $\alpha^4 = \frac{EI}{\rho A}$

Then, the equation becomes:

$$\alpha^4 Y''''(y)Z(t) + Y(y)\ddot{Z}(t) = 0 \quad (3.48)$$

$$\alpha^4 \frac{Y''''(y)}{Y(y)} = \frac{\ddot{Z}(t)}{Z(t)} = -\beta^2 \quad (3.49)$$

where  $\beta$  is an arbitrary constant, the use of  $-\beta^2$  is because of satisfying the related boundary conditions.

$$1) \quad \alpha^4 \frac{Y''''(y)}{Y(y)} = -\beta^2$$

$$Y(y) = A_1 \sin(\lambda y) + A_2 \cos(\lambda y) + A_3 \sinh(\lambda y) + A_4 \cosh(\lambda y) \quad (3.50)$$

where:

$$\lambda^4 = \frac{\beta^2}{\alpha^4} \quad (3.51)$$

$$2) \quad \frac{\ddot{T}(t)}{T(t)} = -\beta^2$$

$$T(t) = B_1 \sin(\beta t) + B_2 \cos(\beta t) \quad (3.52)$$

Boundary conditions in bending motion for a cantilever beam which has its clamped end at  $y = 0$ :

- i.  $w(0, t) = 0 \Rightarrow$  (Deflection)
- ii.  $w_y(0, t) = 0 \Rightarrow$  (Slope)
- iii.  $w_{yy}(L, t) = 0 \Rightarrow$  (Bending moment)
- iv.  $w_{yyy}(L, t) = 0 \Rightarrow$  (Shear)

where  $L$  indicates total span distance of the wing.

After applying the boundary conditions and solving the characteristic equation for  $\lambda$  constant, the definition of the first bending natural frequency can be shown as in (3.53).

$$\omega_{w_1} = 1.875^2 \sqrt{\frac{EI}{\rho AL^4}} \quad (3.53)$$

Equation of motion for torsion is defined in (3.54).

$$\frac{\partial T}{\partial y} = \rho I_p \frac{\partial^2 \theta}{\partial t^2} \quad (3.54)$$

In (3.54),  $T$  indicates torsion while  $I_p$  is polar moment of inertia.

Equation of torsion is given in (3.55).

$$T = GJ \frac{\partial \theta}{\partial y} \quad (3.55)$$

If we combine above equations:

$$\frac{\partial^2 \theta(y,t)}{\partial y^2} = \frac{\rho I_p}{GJ} \frac{\partial^2 \theta(y,t)}{\partial t^2} \quad (3.56)$$

$$\frac{1}{\gamma^2} = \frac{\rho I_p}{GJ} \quad (3.57)$$

Under these definitions, the new equation of torsional motion becomes:

$$\gamma^2 Y''(y) T(t) = Y(y) \ddot{T}(t) \quad (3.58)$$

$$\gamma^2 \frac{Y''(y)}{Y(y)} = \frac{\ddot{T}(t)}{T(t)} = -\tau^2 \quad (3.59)$$

where  $\tau$  is an arbitrary constant similar with bending solution.

$$1) \quad \gamma^2 \frac{Y''(y)}{Y(y)} = -\tau^2$$

$$Y(y) = C_1 \sin\left(\frac{\tau}{\gamma} y\right) + C_2 \cos\left(\frac{\tau}{\gamma} y\right) \quad (3.60)$$

$$2) \quad \frac{\ddot{T}(t)}{T(t)} = -\tau^2$$

$$T(t) = D_1 \sin(\tau t) + D_2 \cos(\tau t) \quad (3.61)$$

Boundary conditions in torsion for a cantilever beam which has its clamped end at  $y = 0$ :

$$1) \quad \theta(0,t) = 0 \Rightarrow (\text{Twist Angle})$$

$$2) \quad T(L, t) = 0 \Rightarrow (\text{Torsion})$$

After applying the boundary conditions and solving the characteristic equation, the definition of the first torsional natural frequency is determined in (3.62).

$$\omega_{\theta_1} = \frac{\pi}{L} \sqrt{\frac{GJ}{\rho I_p}} \quad (3.62)$$

### 3.1.2 Determination of final form of flutter solution

After obtaining aerodynamic and structural terms, they can be combined in order to construct a set of equations to calculate flutter speed.

The solution procedure is based on damping term effect for various reduced frequencies. In flutter analysis, an artificial damping term can be added to the natural frequencies so that the flutter speed in related reduced frequency value can be determined. While iterating the solution for various reduced frequency values, there is a region that we have zero damping which indicates the flutter motion. The region where we obtain no damping determines flutter velocity. Bending and torsional natural frequencies have to be re-written with respect to artificial damping terms.

$$\omega_{w_1}^2 \rightarrow \omega_{w_1}^2 (1 + i g_w) \quad (3.63)$$

$$\omega_{\theta_1}^2 \rightarrow \omega_{\theta_1}^2 (1 + g_\theta) \quad (3.64)$$

where  $g_w$  and  $g_\theta$  indicate artificial damping terms for bending and torsional motions respectively.

For simplicity, the following assumption for artificial damping term,  $g$ , can be used.

$$g_w = g_\theta = g \quad (3.65)$$

Now, a variable,  $Z$ , whose complex component is composed of damping term can be defined for the solution of the system.

$$Z = \left( \frac{\omega_{\theta_1}}{\omega} \right)^2 (1 + i g) \quad (3.66)$$

$$g = \frac{\text{Im}(Z)}{\text{Re}(Z)} \quad (3.67)$$

In flutter condition, the system frequency is equal to flutter frequency:

$$\omega = \omega_f \quad (3.68)$$

$$g = 0 \quad (3.69)$$

In order to obtain the final flutter equations, the displacement terms have to be defined by using harmonic motion assumption which is the boundary of flutter region:

$$w_R(t) = \tilde{w}_R e^{i\omega t} \quad (3.70)$$

$$\tilde{\theta}_R(t) = \tilde{\theta}_R e^{i\omega t} \quad (3.71)$$

Then, the new form of the flutter equations is given in (3.73) and (3.74) by defining a reduced parameter for the distance along wing span. In (3.74) and (3.75),  $b_R$  defines semi chord distance of reference station.

$$\tilde{y} = \frac{y}{L} \quad (3.72)$$

$$\begin{aligned} & \frac{\tilde{w}_R}{b_R} \left[ \frac{1}{\pi \rho_\infty b_R^2} \left( 1 - (1 + ig) \left( \frac{\omega_{w_1}}{\omega} \right)^2 \right) \int_0^1 m \phi^2 d\tilde{y} + \int_0^1 \left( \frac{b}{b_R} \right)^2 L_h \phi^2 d\tilde{y} \right] \\ & - \tilde{\theta}_R \left[ \frac{1}{\pi \rho_\infty b_R^3} \int_0^1 S_y \phi \phi d\tilde{y} + \int_0^1 \left( \frac{b}{b_R} \right)^3 \left( L_\theta - L_h \left( \frac{1}{2} + a \right) \right) \phi \phi d\tilde{y} \right] = 0 \end{aligned} \quad (3.73)$$

$$\begin{aligned} & - \frac{\tilde{w}_R}{b_R} \left[ \frac{1}{\pi \rho_\infty b_R^3} \int_0^1 S_y \phi \phi d\tilde{y} + \int_0^1 \left( \frac{b}{b_R} \right)^3 \left( M_h - L_h \left( \frac{1}{2} + a \right) \right) \phi \phi d\tilde{y} \right] \\ & + \tilde{\theta}_R \left[ \frac{1}{\pi \rho_\infty b_R^4} \left( 1 - (1 + ig) \left( \frac{\omega_{\theta_1}}{\omega} \right)^2 \right) \int_0^1 I_y \phi^2 d\tilde{y} \right] \\ & + \tilde{\theta}_R \left[ + \int_0^1 \left( \frac{b}{b_R} \right)^4 \left( M_\theta - (M_h + L_\theta) \left( \frac{1}{2} + a \right) + L_h \left( \frac{1}{2} + a \right)^2 \right) \phi^2 d\tilde{y} \right] = 0 \end{aligned} \quad (3.74)$$

There can be some simplifications in natural frequency terms.

$$(1+ig)\left(\frac{\omega_{w_1}}{\omega}\right)^2 = (1+ig)\left(\frac{\omega_{w_1}}{\omega_{\theta_1}}\right)^2 \left(\frac{\omega_{\theta_1}}{\omega}\right)^2 = \omega^2 Z \quad (3.75)$$

$$(1+ig)\left(\frac{\omega_{\theta_1}}{\omega}\right)^2 = Z \quad (3.76)$$

New system of equations becomes:

$$\begin{aligned} & \frac{\tilde{w}_R}{b_R} \left[ \frac{1}{\pi \rho_\infty b_R^2} (1 - \omega^2 Z) \int_0^1 m \phi^2 d\tilde{y} + \int_0^1 \left( \frac{b}{b_R} \right)^2 L_h \phi^2 d\tilde{y} \right] \\ & - \tilde{\theta}_R \left[ \frac{1}{\pi \rho_\infty b_R^3} \int_0^1 S_y \phi \phi d\tilde{y} + \int_0^1 \left( \frac{b}{b_R} \right)^3 \left( L_\theta - L_h \left( \frac{1}{2} + a \right) \right) \phi \phi d\tilde{y} \right] = 0 \end{aligned} \quad (3.77)$$

$$\begin{aligned} & - \frac{\tilde{w}_R}{b_R} \left[ \frac{1}{\pi \rho_\infty b_R^3} \int_0^1 S_y \phi \phi d\tilde{y} + \int_0^1 \left( \frac{b}{b_R} \right)^3 \left( M_h - L_h \left( \frac{1}{2} + a \right) \right) \phi \phi d\tilde{y} \right] \\ & + \tilde{\theta}_R \left[ \frac{1}{\pi \rho_\infty b_R^4} (1 - Z) \int_0^1 I_y \phi^2 d\tilde{y} \right] \\ & + \tilde{\theta}_R \left[ \int_0^1 \left( \frac{b}{b_R} \right)^4 \left( M_\theta - (M_h + L_\theta) \left( \frac{1}{2} + a \right) + L_h \left( \frac{1}{2} + a \right)^2 \right) \phi^2 d\tilde{y} \right] = 0 \end{aligned} \quad (3.78)$$

Sweep angle,  $\Lambda$ , basically affects the aerodynamic loads. Aerodynamic terms under sweep angle effect can be defined as in (3.79) and (3.80).

$$L(y, t) = \pi \rho b^3 \omega^2 \cos \Lambda \left[ \frac{w_R(t)}{b} \phi(y) L_h - \theta_R(t) \phi(y) \left( L_\theta - L_h \left( \frac{1}{2} + a \right) \right) \right] \quad (3.79)$$

$$\begin{aligned} M(y, t) = & \pi \rho b^4 \omega^2 \cos \Lambda \left[ - \frac{w_R(t)}{b} \phi(y) \left( M_h - L_h \left( \frac{1}{2} + a \right) \right) \right] \\ & + \pi \rho b^4 \omega^2 \cos \Lambda \left\{ \theta_R(t) \phi(y) \left[ M_\theta - (M_h + L_\theta) \left( \frac{1}{2} + a \right) + L_h \left( \frac{1}{2} + a \right)^2 \right] \right\} \end{aligned} \quad (3.80)$$

Then, by using the definitions above, a final system of equations for flutter motion can be determined.

$$\begin{bmatrix} A & B \\ C & D \end{bmatrix} \begin{Bmatrix} \frac{w_R}{b} \\ \theta \end{Bmatrix} = \begin{Bmatrix} 0 \\ 0 \end{Bmatrix} \quad (3.81)$$

Flutter determinant is given in (3.82).

$$\begin{vmatrix} A & B \\ C & D \end{vmatrix} = 0 \quad (3.82)$$

where:

$$A = \frac{1}{\pi \rho_\infty b_R^2} (1 - \omega^2 Z) \int_0^1 m \phi^2 d\tilde{y} + \cos \Lambda \int_0^1 \left( \frac{b}{b_R} \right)^2 L_h \phi^2 d\tilde{y} \quad (3.83)$$

$$B = -\frac{1}{\pi \rho_\infty b_R^3} \int_0^1 S_y \phi \phi d\tilde{y} + \cos \Lambda \int_0^1 \left( \frac{b}{b_R} \right)^3 \left( L_\theta - L_h \left( \frac{1}{2} + a \right) \right) \phi \phi d\tilde{y} \quad (3.84)$$

$$C = -\frac{1}{\pi \rho_\infty b_R^3} \int_0^1 S_y \phi \phi d\tilde{y} + \cos \Lambda \int_0^1 \left( \frac{b}{b_R} \right)^3 \left( M_h - L_h \left( \frac{1}{2} + a \right) \right) \phi \phi d\tilde{y} \quad (3.85)$$

$$D = \frac{1}{\pi \rho_\infty b_R^4} (1 - Z) \int_0^1 I_y \phi^2 d\tilde{y} + \cos \Lambda \int_0^1 \left( \frac{b}{b_R} \right)^4 \left( M_\theta - (M_h + L_\theta) \left( \frac{1}{2} + a \right) + L_h \left( \frac{1}{2} + a \right)^2 \right) \phi^2 d\tilde{y} \quad (3.86)$$

### 3.2 Validation of Flutter Analysis

The derived flutter solution methodology is validated by using two benchmark problems from literature [60].

The design parameters of two wings are given as in Table 3.1 [60].

The given properties are used in flutter equations in order to calculate the flutter boundary. By using the computational code prepared for 3-dimensional flutter analysis, the flutter speed is calculated as compatible with the given procedure. Flutter speeds and relative errors of each of two models are shown and compared to Bishplinghoff et. al [60] in Table 3.2.



**Table 3.1 :** Design parameters of benchmark wings.

Parameter	Wing-1	Wing-2
$\Lambda$	$30^\circ$	$45^\circ$
$m$	0.0161 slugs/ft	0.0138 slugs/ft
$m / \pi \rho_\infty b_R^2$	6.19	5.50
$I_y / mb_R^2$	0.23	0.23
$S_y / mb_R$	-0.004	-0.224
$b = b_R$	0.333	0.333
$a$	-0.02	0.20
$\omega_{w_1}$	$66\pi$	$44\pi$
$\omega_{\theta_1}$	$186\pi$	$184\pi$

**Table 3.2 :** Flutter speeds and relative errors of benchmark wings.

Wing	Reference [60]	Calculated	Error
Wing-1	277 ft/s	279 ft/s	0.8%
Wing-2	270 ft/s	268 ft/s	0.7%

### 3.3 Flutter Analysis of Goland Wing

The developed methodology is applied to calculate flutter boundaries of a well-known aeroelastic benchmark problem using Goland wing. The wing, which is treated as a cantilever beam, is first introduced in the work of Goland and Buffalo [62]. Solid model of Goland wing, whose aspect ratio is 3.3, is considered in the present work. Extensive research has been carried out to solve the flutter problem of Goland wing with various methods such as Rayleigh-Ritz analysis, Galerkin solution as analytical techniques beside computational approaches [40, 64].

In the present work, natural frequencies and the flutter speed of Goland wing are calculated by using the reference values of design parameters in Table 3.3 [61]. In Table 3.3, mass and moment of inertia of store loads are given in terms of their unit span distance. Computed results for flutter speed, flutter frequency and relative error with respect to the reference work [62] are given in Table 3.4.

The geometry of Goland wing is shown in Figure 3.2 [63] while the variation of flutter frequency with respect to damping term is shown in Figure 3.2.

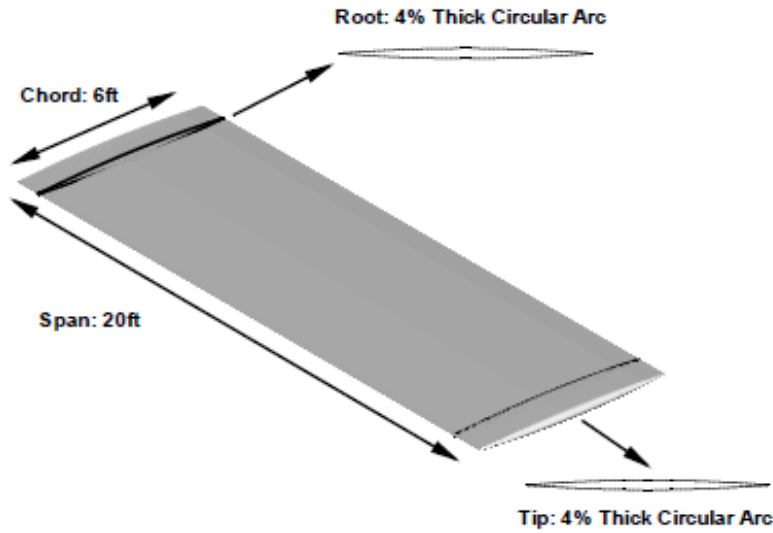


**Figure 3.2 :** Geometry of Goland wing.

**Table 3.3 :** Design parameters of Goland wing.

Parameter	Value
$L$	20 ft
$b$	3 ft
$EI / m$	$31.7 \times 10^6 \text{ lbft}^3/\text{slug}$
$GJ / I_y$	$1.23 \times 10^6 \text{ lbft}^3$
$\bar{m}$	0.746 slug / ft
$\bar{I}_y$	$1.943 \text{ slugft}^2 / \text{ft}$
$S_y$	0.447 slugft/ft
$\rho$	0.0001 slugs / ft <sup>3</sup>

**Table 3.4 :** Flutter solution results for Goland wing.

Parameter	Present Work	Goland [62]	Relative Error
$U_f$	374.7543 mph	385 mph	2.6612 %
$\omega_f$	65.5484 rad/s	67.4 rad/s	2.7471 %

The current result is satisfactory with respect to the work of Goland [62]. Both flutter speed and flutter frequency calculations agree well with the reference values. Thus, the solution methodology is again validated by a well-known aeroelastic benchmark problem and can be applied to a more realistic wing configuration as in the next part. The next section is flutter analysis of AGARD 445.6 wing. Flutter analysis of wing/store configurations in Section 6 will be also based on the presented flutter solution technique.

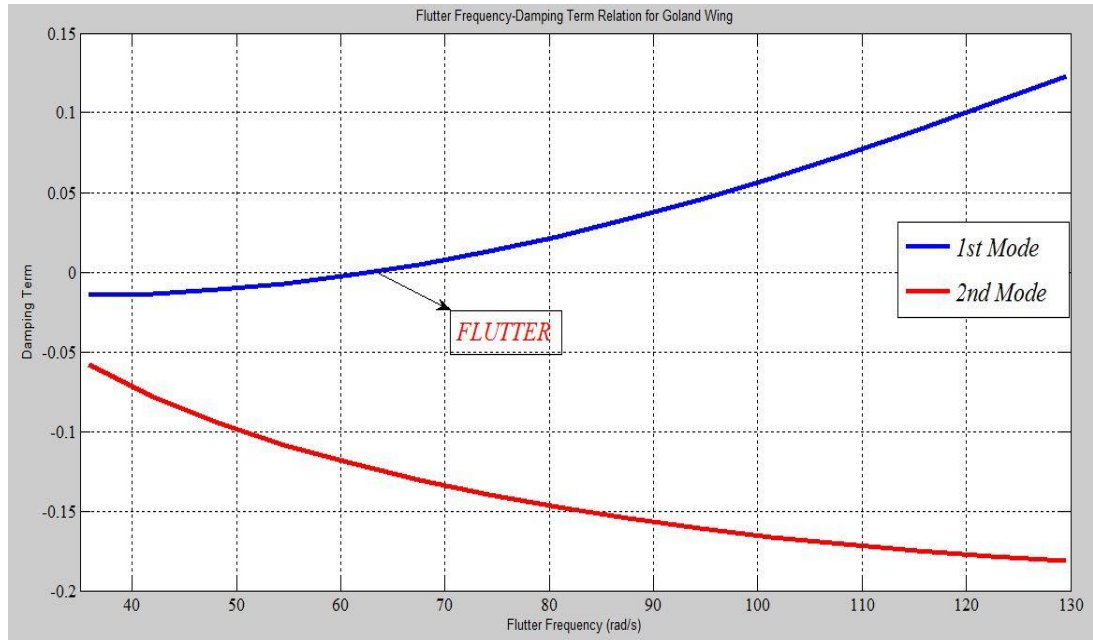


**Figure 3.3 :** Flutter frequency-damping term relation for Goland wing.

### 3.4 Flutter Analysis of AGARD 445.6 Wing

The wing structure in the next analysis is AGARD 445.6 which is the first aeroelastic configuration tested by Yates in the Transonic Dynamics Tunnel at NASA Langley Research Center [65]. AGARD 445.6, which is made of laminated mahogany, is a swept-back wing with a sweep angle of 45 degrees, taper and aspect ratios of 0.66 and 1.65 respectively. The airfoil used in this wing is symmetrical NACA65A004 profile [65]. The wing consists of two models as solid and weakened models. Wall-mounted weakened model is considered in this work.

Studies in dynamic aeroelastic analysis and flutter calculations of AGARD 445.6 wing are extensive. Several methods have been used to investigate the flutter boundaries. In the work of Beaubien [66], computational fluid dynamics is coupled with computational structural dynamics and time marching simulations are performed by using Euler and Reynolds Averaged Navier Stokes equations to calculate flutter speed. Lee-Rausch [67] performed linear stability analysis by calculating generalized aerodynamic forces for various values of reduced frequencies. Flutter characteristics are obtained by using V-g analysis which is a similar approach with the present work. Allen [68] shows that the flutter calculation of AGARD 445.6 with linear methods provides reasonable results since the design and aerodynamics of the wing are simple.

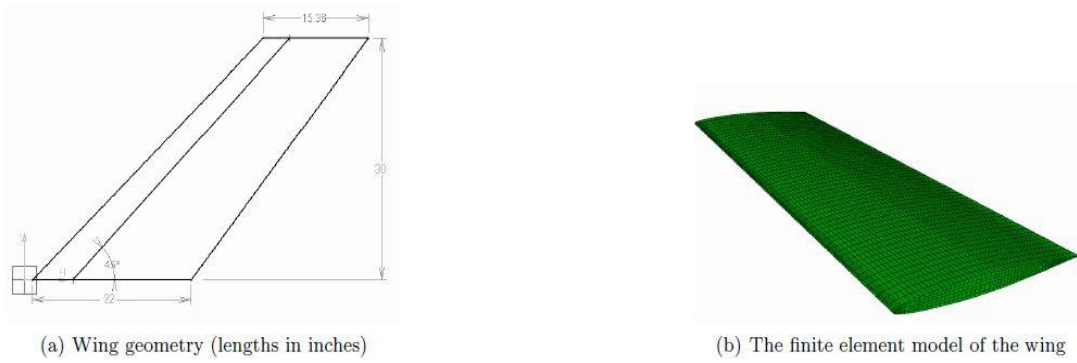


**Figure 3.4 :** Geometry and solid model of AGARD 445.6.

Flutter analysis for AGARD 445.6 wing is performed by using the pre-determined natural frequencies and flutter equations. In flutter calculation procedure, the necessary design parameters for reference station of the wing are taken from CAD model constructed in CATIA V5 by Nikbay et. al [69] and determined from the known geometrical properties of the standard configuration. The basic properties taken into account for solution are summarized in Table 3.5.

Euler-Bernoulli beam equations are considered for natural frequency determination. Euler-Bernoulli solution was previously investigated in AGARD 445.6 case by Kamakoti [70], Kamakoti and Shyy [71], Kamakoti et. al [72]. The modeling can be based on use of plate/shell elements, however bending and torsional natural frequencies calculated with beam assumption agree well with the results calculated by considering plate elements [70]. Beam elements are chosen since they provide an advantageous solution by involving a simplified procedure [71] while still providing rather accurate results. The results provided by Kamakoti [70] with 10 beam elements for the first bending and the first torsion modes are almost equivalent to the results in the work of Yates [73] which employs 120 plate elements. Therefore, Euler-Bernoulli equations are used to calculate natural frequencies of AGARD 445.6 in the present work.

Material properties of weakened model for natural frequency determination are determined from the experimental work of Yates [65].

The results of the flutter analysis for Mach number of 0.9011 are summarized in Table 3.6 and 3.7. Firstly, natural frequencies and relative errors with respect to the related experimental work are calculated.

**Table 3.5 :** Design properties of AGARD 445.6 wing .

Property	Value
$\Lambda$	$45^\circ$
$m$	1.693 kg
$\lambda$	0.66
$m / \pi \rho_\infty b_R^2$	9.4104
$I_y / mb_R^2$	0.3336
$S_y / mb_R$	0.3229
$E_y$	3671 MPa
$G_y$	409 MPa

where  $\lambda$  indicate taper ratio of the wing.  $E_y$  and  $G_y$  are elasticity and shear modulus values along spanwise direction.

**Table 3.6 :** Natural frequency solution for AGARD 445.6 wing.

Parameter	Calculated (Hz)	Experimental (Hz)	Relative Error
$\omega_{\eta_1}$	9.5409	9.5992	0.61%
$\omega_{\theta_1}$	38.4975	38.1650	0.87%

Natural frequency values well agree with experimental results [65]. Then, the next step is flutter analysis. AGARD 445.6 has a sweep angle as  $45^\circ$  that has to be considered in the related equations of motion derived before.

Solutions for flutter calculation and percentage error with respect to experimental results are in Table 3.7. Also, the flutter solutions performed by Kolonay [74] have been listed for comparison.

**Table 3.7 :** Flutter solution results for AGARD 445.6 wing.

Parameter	Calculated	Experimental [65]	Kolonay [74]	Relative Error
$U_f$	308.4513 m/s	296.7 m/s	299.97 m/s	3.96%
$\omega_f$	104.2489 rad/s	101.1 rad/s	99.0 rad/s	3.11%

Variation of flutter frequency with respect to damping term is shown in Figure 3.4. The calculated flutter boundaries for the flight regime with Mach number of 0.9011 well-agree with the experimental result.

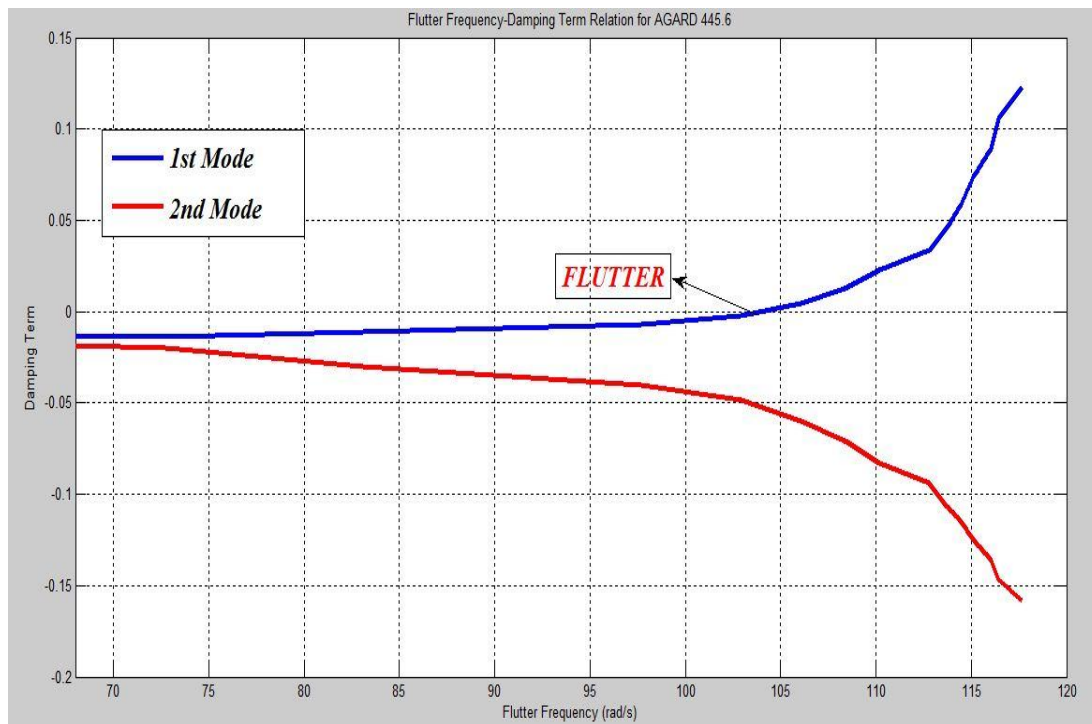


**Figure 3.5 :** Flutter frequency-damping term relation for AGARD 445.6.

## 4. AEROELASTIC DESIGN OPTIMIZATION

This section presents design optimization of 2 and 3-dimensional wing structures in order to delay aeroelastic instabilities. Firstly, a 2-dimensional airfoil model is optimized in order to maximize the speeds of aeroelastic instabilities while the second work involves flutter based design optimization of a 3-dimensional wing structure. Solution procedure is developed in MATLAB codes and then implemented into modeFRONTIER software so as to enable an automatic optimization procedure for both cases. MOGA-II and NSGA-II are used in 2-dimensional case while NSGA-II is preferred for flutter speed maximization of 3-dimensional wing structure, AGARD 445.6.

### 4.1 Multi-Objective Design Optimization of Two Dimensional Aeroelastic Systems

One of the main interests in the present work is to enhance the design quality of 2-dimensional models by maximizing the speeds of aeroelastic instabilities. Aeroelastic design optimization is applied to the first benchmark problem of Section 2 in order to achieve a more efficient design.

Design parameters of the considered benchmark problem [58] are given in Table 2.1. Optimization problem includes 3 objective functions, 5 optimization variables and 5 constraints. Objectives are maximizing the speeds of flutter, divergence and control reversal phenomena while optimization variables are defined as linear and torsional spring coefficients, static offset, moment of inertia and mass of the airfoil.

The optimization problem can be described as in (4.1) to (4.8).

$$\max_{s \in S} \{V_f\}, \quad \max_{s \in S} \{V_d\}, \quad \max_{s \in S} \{U_r\} \quad (4.1)$$

$$g_1(s) = r_\alpha - 1 < 0, \quad g_1(s) \in \Re \quad (4.2)$$

$$g_2(s) = \bar{\omega} - 1 < 0, \quad g_2(s) \in \Re \quad (4.3)$$

$$g_3(s) = 1 - \frac{U_r}{(2.3992 \times 1.15)} < 0, \quad g_3(s) \in \Re \quad (4.4)$$

$$g_4(s) = 1 - \frac{V_f}{(1.9638 \times 1.15)} < 0, \quad g_4(s) \in \Re \quad (4.5)$$

$$g_5(s) = 1 - \frac{V_d}{(2.4779 \times 1.15)} < 0, \quad g_5(s) \in \Re \quad (4.6)$$

$$S = \{s \in \Re, s_L \leq s \leq s_u\} \quad (4.7)$$

$$s = (k_h, k_\alpha, x_\alpha, I_\alpha, m) \quad (4.8)$$

where  $g_1(s)$ ,  $g_2(s)$ ,  $g_3(s)$ ,  $g_4(s)$  and  $g_5(s)$  are inequality constraints while  $V_f$ ,  $V_d$  and  $U_r$  are the speeds of flutter, divergence and control reversal respectively.  $g_1(s)$  and  $g_2(s)$  indicate the natural boundaries for reduced parameters because of physical limitations of the aeroelastic problem while  $g_3(s)$ ,  $g_4(s)$  and  $g_5(s)$  describe a level of speeds that satisfy the safety requirements for a selected safety factor as 1.15.

$s_L$  and  $s_U$  indicate the lower and upper limits of optimization variables that are chosen depending on given reference wing design values. Lower and upper limits for optimization variables are determined as stated in the Table 4.1.

**Table 4.1 :** Values of optimization variables in 2-dimensional case.

Variable	Lower Limit ( $s_L$ )	Upper Limit ( $s_U$ )	Reference Study
$k_h$	1.0 r*	5.0 r	-
$k_\alpha$	1.0 r	7.0 r	-
$x_\alpha$	0.1	0.3	0.2
$I_\alpha$	1 kgm <sup>2</sup>	3 kgm <sup>2</sup>	1.2037 kgm <sup>2</sup>
$m$	7.5 kg	12.5 kg	19.2580 kg

\* indicates that r can be an arbitrary real number since the exact value of  $k_\alpha$  and  $k_h$  cannot be determined by using reference parameters. These variables are related to the frequencies  $\omega_\alpha$  and  $\omega_h$ . The significant part for aeroelastic instability



determination is the ratio of these frequencies. Their distinct values are not used to obtain reduced speeds. Thus, the distinct values for  $k_\alpha$  and  $k_h$  are not obtained. The lower and upper limits are taken as 1.0 and 5.0 for  $k_h$  and 1.0 and 7.0 for  $k_\alpha$  in optimization software. In order to provide reasonable frequency ratios,  $g_2(s)$  constraint is defined in the optimization problem.

For optimization process, the computational code that is used to find flutter, divergence and control reversal speeds is modified is adopted to the optimization problem. In the second step, this code is coupled with the optimization software, modeFRONTIER. The optimization software provides automatic iterations with respect to design parameters. MOGA-II and NSGA-II are used as optimization algorithms. The results obtained from both of the optimization algorithms are compared to each other in order to determine the differences between them.

The optimization flow-chart for the multi-objective task is shown in Figure 4.1. The flow-chart actually contains optimization variables, constraints, optimization algorithm and objective functions.

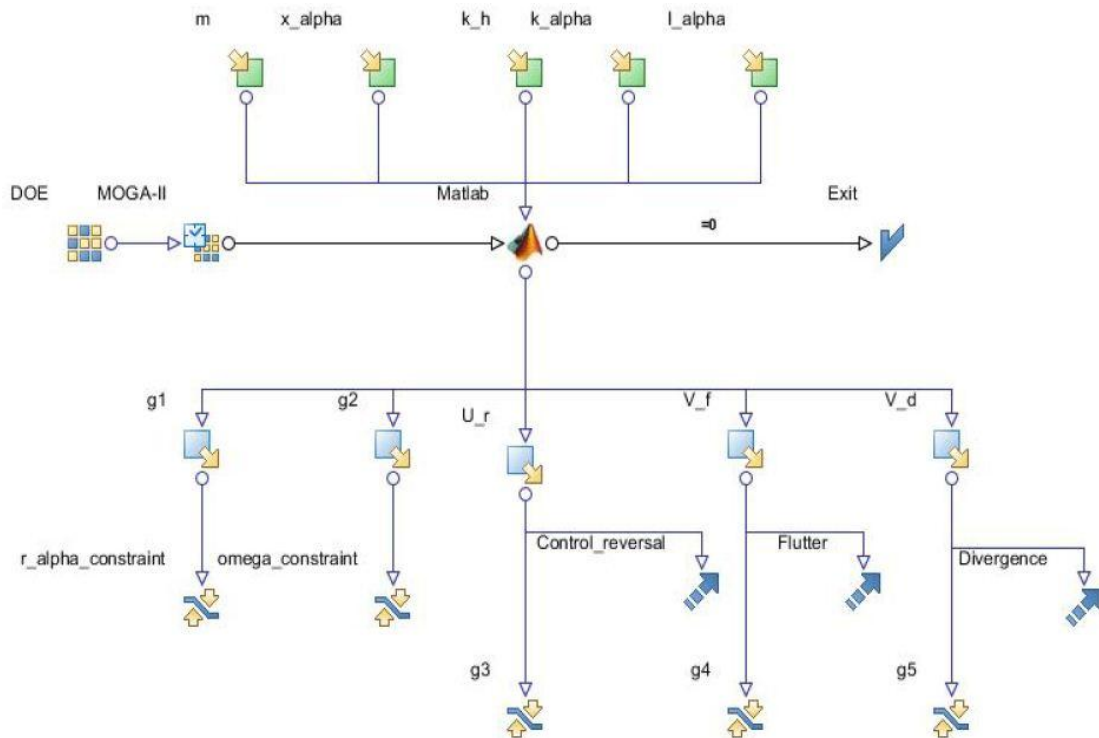


**Figure 4.1 :** Workflow of 2-dimensional aeroelastic optimization problem.

In the first optimization process, MOGA-II is used as optimization algorithm with 1000 Design of Experiments (DoE). There are 100000 total number of designs with

95483 feasible designs and 4517 infeasible designs. The solution took about 12 hours 23 minutes on a platform as Intel(R) Core(TM) 2 CPU 6400@2.13GHz processor and 2GB of RAM on Microsoft Windows 7 64-bit operating system. Set of optimum solutions is defined with respect to each objective of the problem. Designs that maximize each objective respectively are considered in the optimum solutions set. Optimum designs are included in Table 4.2.

**Table 4.2 :** Optimum designs with MOGA-II algorithm.

Design No	$V_f$	$V_d$	$U_r$	$m$
1	<b>3.5337</b>	<b>4.2603</b>	<b>3.7878</b>	<b>12.499 kg</b>
2	2.3146	4.5574	3.7878	12.494 kg
3	1.7577	2.5772	2.1869	7.50 kg

A final optimum design is selected by considering the failure point of the structure. Since flutter is seen at lowest speed values, a design that maximizes the flutter speed is desired. Thus, Design-1 is selected since it has the maximum flutter speed value. The optimum design provides gains in terms of all desired criteria as shown in Table 4.3.

**Table 4.3 :** Comparison of initial and optimum designs with MOGA-II algorithm.

	$V_f$	$V_d$	$U_r$	$m$
Initial Design	1.9638	2.4779	2.3992	19.258 kg
Optimum Design	3.5337	4.2603	3.7878	12.499 kg
Relative Change	<b>79.94%</b>	<b>71.93%</b>	<b>57.88%</b>	<b>-35.10%</b>

In the second optimization process, NSGA-II is used as optimization algorithm with 1000 DoE. There are 100000 total number of designs with 95156 feasible designs and 4844 infeasible designs. The solution took about 11 hours 15 minutes on a platform as Intel(R) Core(TM) 2 CPU 6400@2.13GHz processor and 2GB of RAM on Microsoft Windows 7 64-bit operating system. The results of selected optimum designs for the second optimization process are completely same with the first case.

Design-1 is selected since it has the maximum flutter speed value. The optimum design provides gains in terms of all desired criteria as defined in Table 4.5. After completing the optimization processes, the optimum results obtained from each of the optimization algorithms can be compared.

**Table 4.4 :** Comparison of initial and optimum designs with NSGA-II algorithm.

	$V_f$	$V_d$	$U_r$	$m$
Initial Design	1.9638	2.4779	2.3992	19.258 kg
Optimum Design	3.5337	4.2603	3.7878	12.499 kg
Relative Change	<b>79.94%</b>	<b>71.93%</b>	<b>57.88%</b>	<b>-35.10%</b>

**Table 4.5 :** Comparison of MOGA-II and NSGA-II algorithms.

Optimization Algorithm	Flutter Speed Increase (%)	Divergence Speed Increase (%)	Control Reversal Speed Increase (%)	Mass Decrease (%)
MOGA-II	79.94	71.93	57.88	35.10
NSGA-II	79.94	71.93	57.88	35.10

The only comparison criterion between two optimization algorithms is their solution times since obtained optimum results are completely same. NSGA-II reduces the computational time while producing the same optimum results. Then, it is more advantageous to use NSGA-II algorithm in further optimization applications of the present work.

The optimum design with NSGA-II has the following values in terms of optimization variables.

**Table 4.6 :** Design variables of 2-dimensional optimum model.

$k_h$	$k_\alpha$	$x_\alpha$	$I_\alpha$	$m$
1.00	7.00	0.10	3.00 kgm <sup>2</sup>	12.499 kg

## 4.2 Flutter Based Aeroelastic Design Optimization of AGARD 445.6

Flutter based aeroelastic design optimization of AGARD 445.6 wing involves the variation of taper ratio, sweep angle and material properties along the spanwise direction in order to increase the flutter boundary.

The MATLAB code developed for the flutter solution is embedded in modeFRONTIER optimization software. The objective in this optimization problem is maximizing flutter speed while the optimization variables are taper ratio, sweep angle, elasticity and shear modulus of the wing. Natural frequencies are also calculated with respect to optimization parameters since modal analysis is a part of flutter solution. The optimization problem is defined in (4.15) to (4.21).

$$\max_{s \in S} U_f(s) \quad (4.15)$$

$$S = \{s \in \mathfrak{R}, s_L \leq s \leq s_U\} \quad (4.16)$$

$$s = \{\lambda, \Lambda, E_y, G_y\} \quad (4.17)$$

$$0.65 \leq \lambda \leq 1.0 \quad (4.18)$$

$$0^\circ \leq \Lambda \leq 60^\circ \quad (4.19)$$

$$2000\text{MPa} \leq E_y \leq 3000\text{MPa} \quad (4.20)$$

$$200\text{MPa} \leq G_y \leq 300\text{MPa} \quad (4.21)$$

NSGA-II is chosen as optimization algorithm with 1000 DoE. The optimization took about 50 minutes 43 seconds on a platform as Intel(R) Core(TM) 2 CPU 6400@2.13GHz processor and 2GB of RAM on Microsoft Windows 7 64-bit operating system.

A design with maximum flutter speed of 361.8843 m/s is given as optimum solution among 100000 feasible solutions. Design parameters in optimum structure and initial configuration and optimization workflow in modeFRONTIER are shown in Figure 4.2 and Table 4.7.

**Table 4.7 :** Design variables of initial and optimum AGARD 445.6 models.

Design	$\lambda$	$\Lambda$	$E_y$	$G_y$
Initial [63]	0.66	45°	3671 MPa	409 MPa
Optimum	0.65	59.65°	2020.85 MPa	299.02 MPa

Optimum design provides considerable improvement in flutter boundary of AGARD 445.6 wing. Since flutter is a catastrophic aeroelastic phenomenon, any increase in its boundary provides a more reliable flight. The optimum flutter speed and improvement with respect to analytical solution are expressed in Table 4.9. The optimum result provides a more reliable design by producing approximately 17% of increase in flutter boundary.

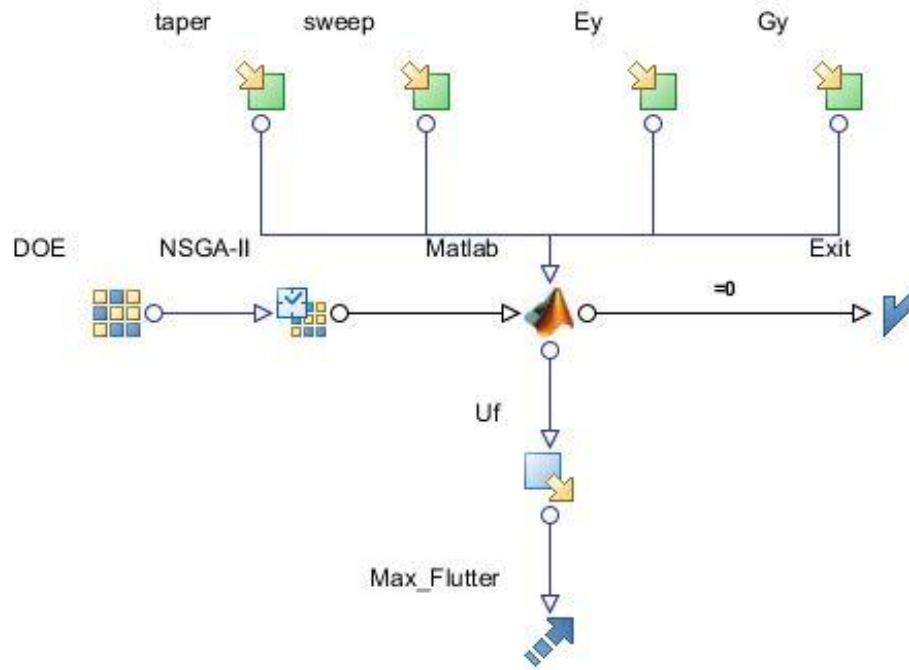


**Figure 4.2 :** Optimization workflow for AGARD 445.6.

**Table 4.8 :** Flutter results of initial and optimum AGARD 445.6 models.

Design	Calculated	Optimized
Flutter Speed (m/s)	308.4513	361.8843
Improvement (%)	-	17.3230%



## 5. UNCERTAINTY BASED AEROELASTIC ANALYSIS

In this section, aeroelastic analyses are performed by considering uncertainties in structural, geometric and aerodynamic parameters for 2 and 3-dimensional wing structures. The first part includes 2-dimensional aeroelastic analyses with uncertainties in structural parameters and aerodynamics. 3-dimensional flutter analysis by considering the effects of structural and geometric uncertainties forms the second part. All random parameters are distributed with Gaussian distribution and modeled with  $10^5$  samples by using MCS method.

Traditional uncertainty quantification methods in aeroelastic analysis is based on choosing the best design among the model set by introducing the best distribution for random parameters. Sources of uncertainties are various [75].

- Initial and boundary conditions
- Geometric features
- Parametric variations in physical parameters
- Modeling errors

Deterministic methods can be adequate for small variations while increased amount of uncertainties must require probabilistic methods. Safety factor approach used in deterministic methods can cause design of heavy aircraft structures. Design requirements in a deterministic model are defined strictly and any variation in parameters can probably violate the constraints, however system reliability can be increased with probabilistic analyses.

Many types of probability distributions can be used to model the random parameters. Gaussian distribution is preferred in this work within the context of MCS. Gaussian distribution is used when small variations in random parameters are considered [75].

A random variable with Gaussian distribution is given in (5.1) [75] where  $f_X(x)$  is the probability density function of the random variable,  $x$ .  $\sigma_x$  and  $\mu_x$  are mean value

and standard deviation of  $x$ . Gaussian distribution, also known as normal distribution, of  $x$  is shown as  $N(\mu_x, \sigma_x)$ .

$$f_x(x) = \frac{1}{\sigma_x \sqrt{2\pi}} \exp \left[ -\frac{1}{2} \left( \frac{x - \mu_x}{\sigma_x} \right)^2 \right], \quad -\infty < x < +\infty \quad (5.1)$$

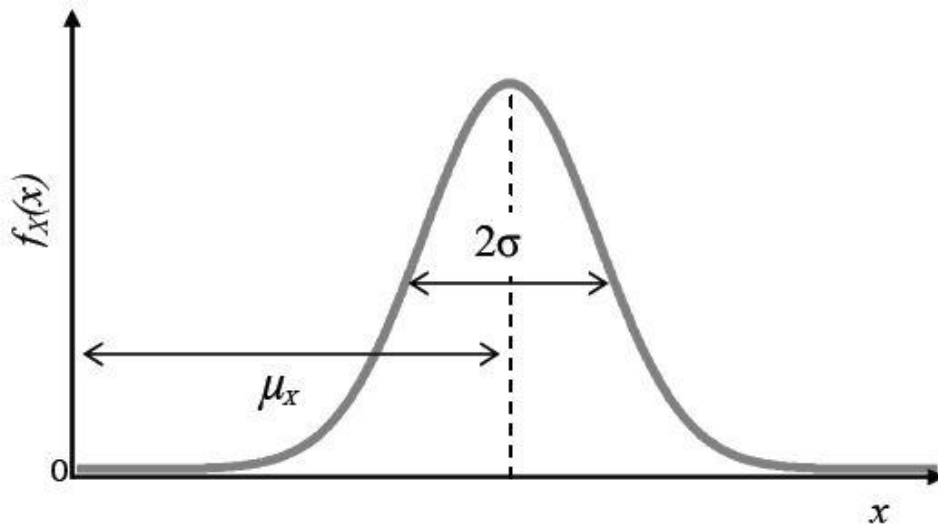


**Figure 5.1 :** Properties of Gaussian distribution.

MC methods make use of repeated random sampling for probabilistic variables to reach the random results. They basically contain simulation of a physical system while randomly changing the parameters [75]. Computational process of MC methods can be summarized as:

- A distribution type for random variables is selected.
- A sampling set is created from the distribution.
- Simulations are generated by using the sampling set.

The accuracy of MCS is directly related to number of samples as defined in (5.2) [75].

$$MCS \text{ Accuracy} = \frac{1}{\sqrt{n}} \quad (5.2)$$

In order to represent more accurate aeroelastic systems in the present work,  $10^5$  samples are used for each random variable in probabilistic analyses. The accuracy of



MCS is 0.3162% under these conditions. Variations are considered with respect to *COV* approach where:

$$COV = \frac{\sigma_x}{\mu_x} \% \quad (5.3)$$

In this thesis, *COV* is taken as either 1% or 5% in all uncertainty based aeroelastic analyses. The first uncertainty problem is applied for 2-dimensional aeroelastic case while initial design of AGARD 445.6 wing is the topic of 3-dimensional flutter analysis with uncertainties.

## 5.1 Uncertainty Based 2-Dimensional Aeroelastic Analysis

2-dimensional aeroelastic analysis with uncertainties in structural and aerodynamic parameters is carried out in order to obtain the robust speeds of flutter, divergence and control reversal phenomena. Random variables are defined as mass of the airfoil, moment of inertia and aerodynamic parameters. *COV* = 1% and *COV* = 5% approaches are used to model uncertainties. Minimum, maximum and mean speed values are obtained while minimum speeds are taken into account by considering robustness. The robust speed values are compared to the deterministic values. The uncertainty analyses are applied to the first initial airfoil model of Section 2.

### 5.1.1 *COV*=1% case

**Table 5.1** : Statistical information about 2-dimensional case with *COV* = 1% .

Parameter	Det. Value	Min. Value	Mean Value	Max. Value
$c_{L_\alpha}$	6.2832	6.0022	6.2834	6.5683
$c_{L_\beta}$	2.4870	2.3871	2.4868	2.5859
$c_{M_\alpha}$	1.8850	1.8031	1.8850	1.9628
$c_{M_\beta}$	-0.3340	-0.3488	-0.3340	-0.3201
$\rho$	1.2260 kg/m <sup>3</sup>	1.1754 kg/m <sup>3</sup>	1.2260 kg/m <sup>3</sup>	1.2854 kg/m <sup>3</sup>
$I_\alpha$	1.2037 kgm <sup>2</sup>	1.1530 kgm <sup>2</sup>	1.2037 kgm <sup>2</sup>	1.2590 kgm <sup>2</sup>
m	19.2580 kg	18.3229 kg	19.2584 kg	20.2208 kg
$V_f$	1.9638	<b>1.9008</b>	1.9639	2.0278
$V_d$	2.4780	<b>2.3819</b>	2.4781	2.5697
$U_r$	2.3993	<b>2.3109</b>	2.3993	2.4835

The minimum, mean and maximum values of random parameters as a result of  $10^5$  samples and deterministic results are summarized in Table 5.1.

### 5.1.2 $COV=5\%$ case

In the second case,  $COV$  is taken as 0.05 in order to model the random parameters. The minimum, mean and maximum values of random variables and deterministic values are summarized in Table 5.2.

**Table 5.2 :** Statistical information about 2-dimensional case with  $COV = 5\%$  .

Parameter	Det. Value	Min. Value	Mean Value	Max. Value
$c_{L_\alpha}$	6.2832	4.7878	6.2845	7.6069
$c_{L_\beta}$	2.4870	1.9414	2.4873	3.0367
$c_{M_\alpha}$	1.8850	1.4806	1.8851	2.3126
$c_{M_\beta}$	-0.3340	-0.4071	-0.3340	-0.2519
$\rho$	1.2260 kg/m <sup>3</sup>	0.9155 kg/m <sup>3</sup>	1.2258 kg/m <sup>3</sup>	1.4841 kg/m <sup>3</sup>
$I_\alpha$	1.2037 kgm <sup>2</sup>	0.9593 kgm <sup>2</sup>	1.2037 kgm <sup>2</sup>	1.5004 kgm <sup>2</sup>
m	19.2580 kg	15.0782 kg	19.2584 kg	24.0024 kg
$V_f$	1.9638	<b>1.7035</b>	1.9656	2.4249
$V_d$	2.4780	<b>2.0526</b>	2.4810	3.0895
$U_r$	2.3993	<b>1.9894</b>	2.4016	2.9743

The resulting distributions for aeroelastic instabilities are shown in Figure 5.2, 5.3 and 5.4 with comparisons of  $COV=1\%$  and  $COV=5\%$  cases.

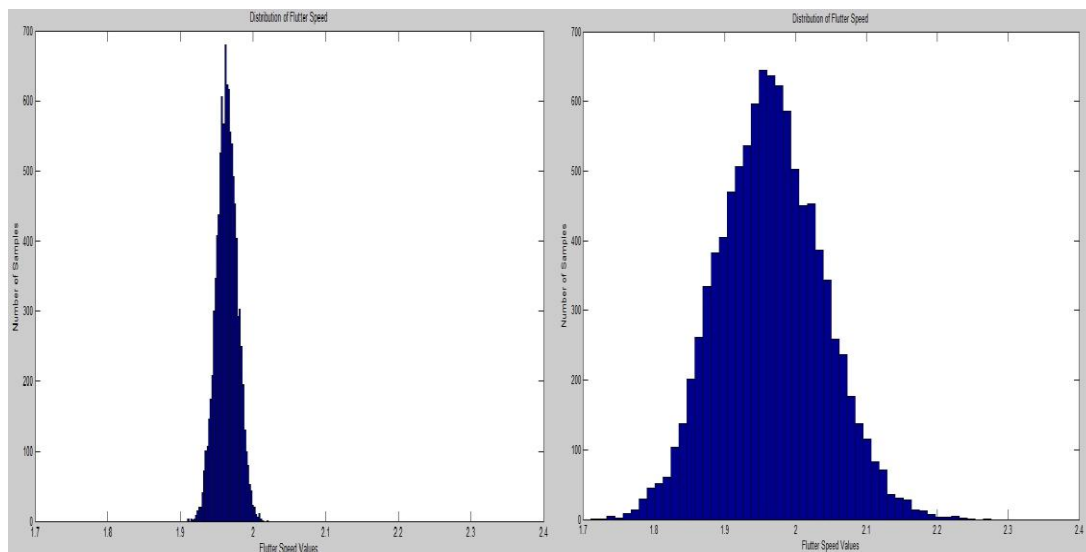


**Figure 5.2 :** Flutter speed histograms with  $COV=1\%$  and  $COV=5\%$ .

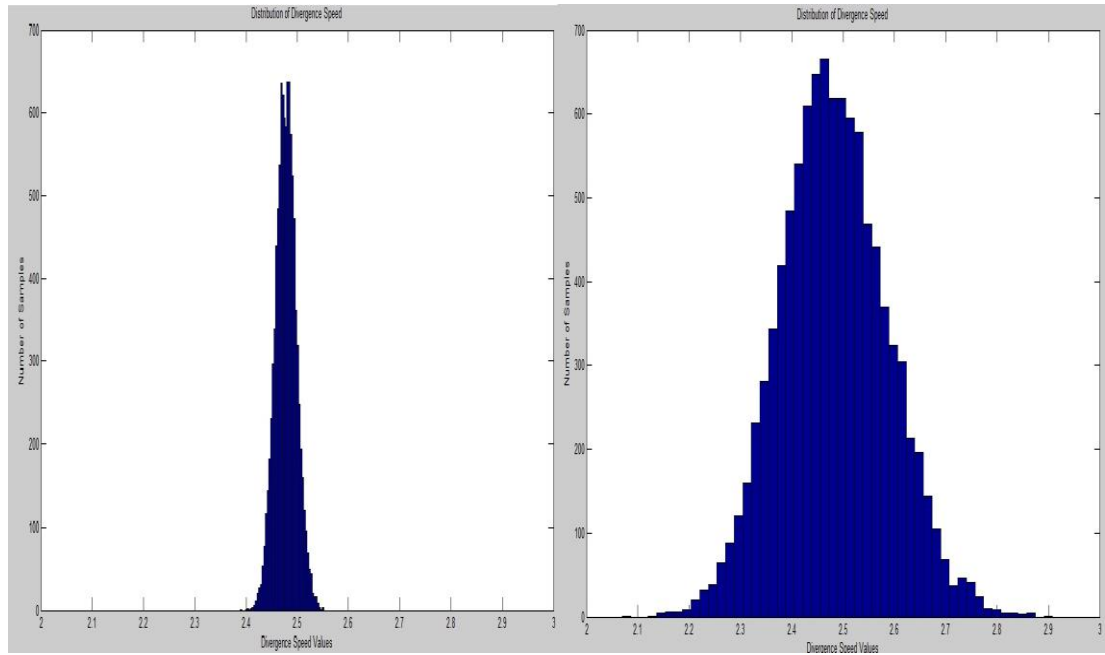


**Figure 5.3 :** Divergence speed histograms with  $COV=1\%$  and  $COV=5\%$ .

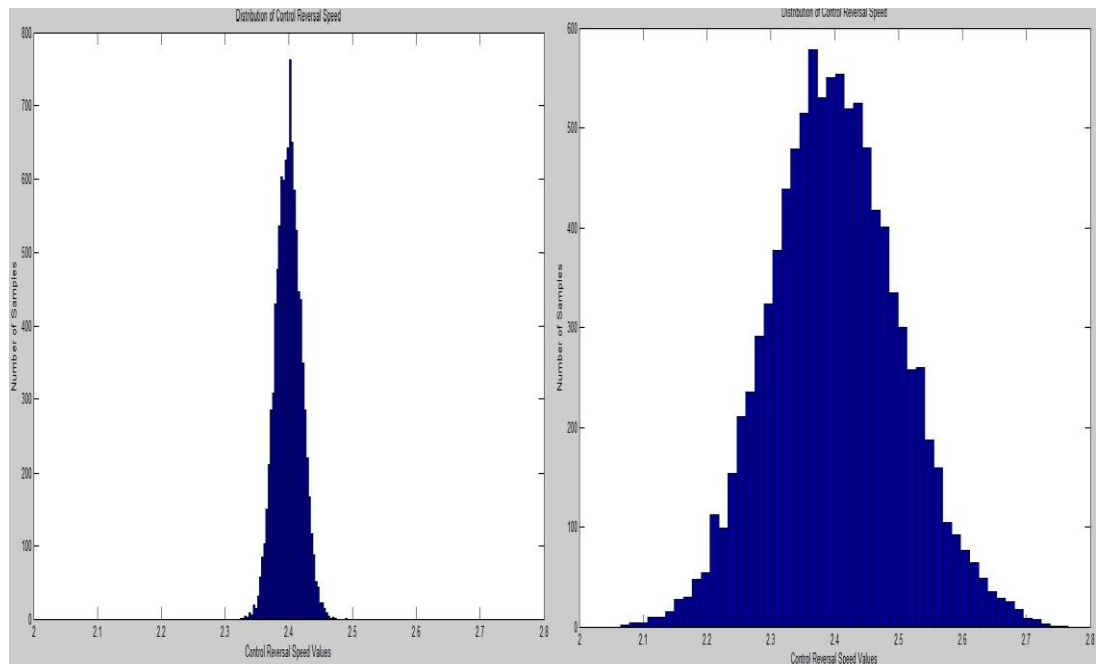


**Figure 5.4 :** Control reversal speed histograms with  $COV=1\%$  and  $COV=5\%$ .

The deterministic solutions do not seem to be reliable when compared to the results of uncertainty based aeroelastic analyses. The minimum speed values must be considered for reliability. The decreases in speeds of aeroelastic instabilities are shown in Table 5.3 for  $COV=1\%$  and  $COV=5\%$  cases.  $COV=1\%$  approach is a more likely case since the variations of uncertainties are relatively small and appropriate to

the design of such a 2-dimensional simple aeroelastic configuration however  $COV=5\%$  approach can represent a very uncertain case.

**Table 5.3 :** Comparison of uncertainty based aeroelastic analyses.

Case	$V_f$	$V_d$	$U_r$
Deterministic	1.9638	2.4779	2.3992
$COV=1\%$	1.9008	2.3819	2.3109
$COV=5\%$	1.6535	2.0526	1.9894

## 5.2 Uncertainty Based 3-Dimensional Flutter Analysis

This section addresses flutter analysis of a 3-dimensional wing structure by considering uncertainties in structural properties. Random parameters are defined as elasticity and shear modulus along spanwise direction.  $COV = 1\%$  and  $COV = 5\%$  approaches are again used to model random variables. The robust flutter analysis is applied to initial reference design of AGARD 445.6 wing. As the principle of robust analysis, the minimum flutter speed is taken into consideration for the worst-case scenario. Robust flutter speed is compared to deterministic value.

### 5.2.1 $COV=1\%$ case

Uncertainties are included by using  $COV = 1\%$ . Minimum, mean and maximum values of random parameters and deterministic result are summarized in Table 5.4.

**Table 5.4 :** Statistical information about AGARD 445.6 case with  $COV = 1\%$ .

Parameter	Det. Value	Min. Value	Mean Value	Max. Value
$E_y$	3671 MPa	3520.20 MPa	3671 MPa	3834.0 MPa
$G_y$	409 MPa	390.98 MPa	409.01 MPa	428.46 MPa
$U_f$	308.4513 m/s	<b>296.7518 m/s</b>	308.4606 m/s	319.9008 m/s

The distribution of flutter speed is so close to the normal distribution since small variations are considered in random parameters.

### 5.2.2 $COV=5\%$ case

$COV=0.05$  is used to generate random samples for uncertainty based flutter analysis. Minimum, mean and maximum values of random parameters and deterministic result are summarized in Table 5.5.

The distribution of flutter speeds for  $COV=1\%$  and  $COV=5\%$  cases is shown in Figure 5.5.

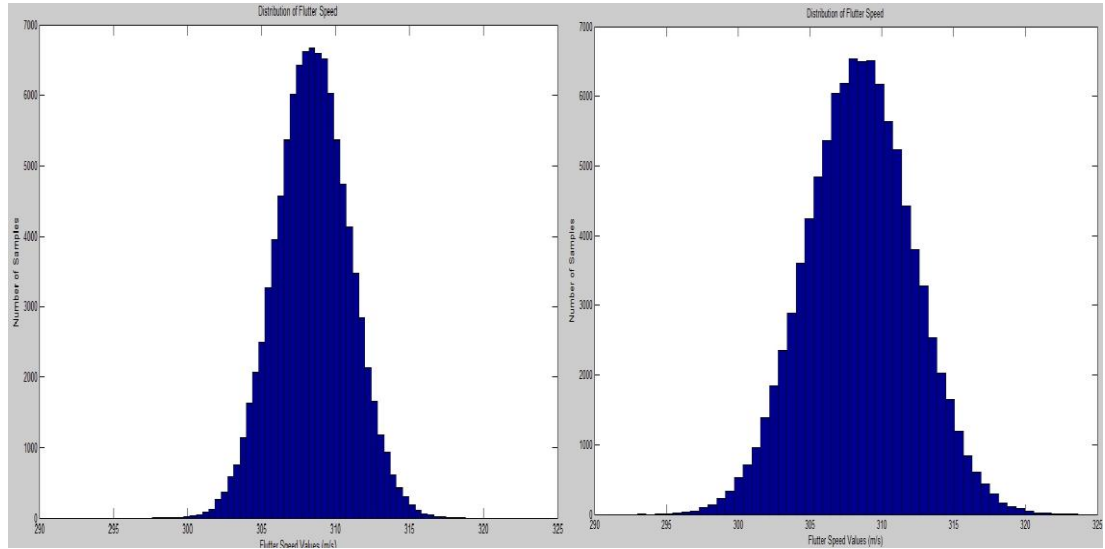


**Figure 5.5 :** AGARD 445.6 flutter speed histograms.

**Table 5.5 :** Statistical information about AGARD 445.6 case with  $COV = 5\%$  .

Parameter	Det. Value	Min. Value	Mean Value	Max. Value
$E_y$	3671 MPa	2871.80 MPa	3671 MPa	4512.80 MPa
$G_y$	409 MPa	315.24 MPa	408.99 MPa	504.80 MPa
$U_f$	308.4513 m/s	<b>290.6844 m/s</b>	308.4763 m/s	324.0019 m/s

The deterministic flutter solution again does not seem to be reliable due to the results of uncertainty based analyses. The results of  $COV=1\%$  approach as a more probable case and  $COV=5\%$  approach as an extraordinary case due to possibilities of high quality manufacturing techniques of today's world are considered and compared to deterministic result in Table 5.6. Flutter speed in  $COV=5\%$  approach can be considered for high level of safety in structural design of AGARD 445.6 wing.

**Table 5.6 :** Comparison of uncertainty based flutter analyses.

Case	$U_f$
Deterministic	308.4513 m/s
$COV=1\%$	296.7518 m/s
$COV=5\%$	290.6844 m/s

Producing a reliable design for both 2 and 3-dimensional wing structures subjected to structural, geometric and aerodynamic uncertainties requires robustness based analysis.

Deterministic aeroelastic analyses and optimization applications can form a mathematical basis for further studies but they are not sufficient for a realistic and reliable design. Besides robust aeroelastic analysis, optimization studies must even be based on robustness criterion. Robust aeroelastic optimization is accomplished by considering 2 and 3-dimensional clean wing structures in Section 7.

## 6. FLUTTER BASED OPTIMIZATION AND UNCERTAINTY BASED FLUTTER ANALYSIS OF WING/STORE CONFIGURATIONS

The present work involves deterministic and probabilistic flutter analysis and flutter based design optimization of wing/store configurations with external loads placed in various stations along the wing span. One of the main purposes of the present section is to define a general solution methodology for the flutter analysis of wing/store configurations where the store loads can be as missiles, launchers or fuel tanks. The parametric solution is expected to provide a guideline for further analyses and optimization studies in various types of wing/store configurations ranging from simplest models to designs with high complexity levels including fighter aircraft wings. Aeroelastic design optimization aims to reach the best configuration with optimum placement of stores along wing span while the aim of robust analysis is demonstration of the worst condition for the current design. An example representation of a wing/store configuration is given in Figure 6.1 [76].

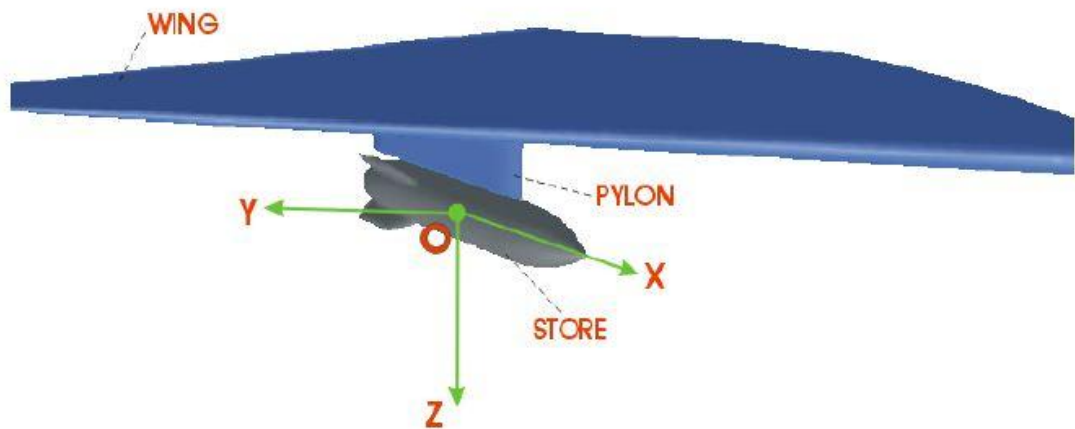


**Figure 6.1 :** General representation of a wing/store configuration.

The flutter solution involves structural effects as masses and inertias of store loads to determine the critical speed. The effects of pylon structure and store aerodynamics are neglected. The solution procedure is firstly validated by using Goland wing and an external store which is placed in different stations along wing span as in the work

of Fazelzadeh [77]. The validated solution is then used to analyze flutter for AGARD 445.6 wing/store configurations. Analyses are applied to two different models composed of standard and previously optimized AGARD 445.6 clean wings with store loads. The objectives are to determine the best locations for the store loads in order to maximize the flutter speed of the wing. In flutter analysis of AGARD 445.6 wing/store models, the store loads are modeled as point masses and their inertias are neglected due to lack of technical information. Structural effects of external stores are taken into account as point masses. The loading configurations are divided into three categories as 3, 4 and 5-stations cases. Total masses of store loads are kept the same in each configuration. Since the main purpose is to obtain the best wing/store configuration for a “given” clean wing model, initial and optimum designs of clean AGARD 445.6 wing are compared to each other in order to investigate if the optimum clean wing model is still the best design even with store loads. The best configuration based on flutter criterion with optimum station number and the type of wing are selected.

Finally, an uncertainty based flutter analysis is performed for the best design in order to examine the available worst case scenerio by considering robustness. Uncertainties in locations and masses of store loads, material properties as elasticity and shear modulus values of the wing structure are considered before performing the flutter analyses. Analyses are performed for  $COV = 1\%$  and  $COV = 5\%$  cases respectively for variations in material properties and store masses and  $COV = 0.25\%$  for variations in locations with  $10^5$  generated samples by MCS. Location parameters are given a different  $COV$  due to the physical properties of the AGARD 445.6 wing. A greater  $COV$  value as in other parameters causes infeasible designs such that the store locations exceed the wing span. Minimum available flutter speeds are taken into account for both cases due to the basic principle of robust design. Deterministic and probabilistic flutter speeds are compared to each other in order to examine the effects of structural and geometric uncertainties.

## **6.1 Solution and Validation of Flutter Analysis of Wing/Store Configurations**

The flutter solution technique for 3-dimensional wings is extended so that the structural effects of store loads along the wing span could be examined. Structural properties of external loads such as the masses and inertias are considered as store



effects in the flutter methodology. The additional effects of store masses are added through mass density values and the location where the related masses place while inertia moments of the store loads are included by considering the span positions. The updated flutter coefficients of the solution determinant with store loads effects are summarized in (6.1) to (6.4).

$$A = \frac{1}{\pi \rho_{\infty} b_R^2} (1 - \omega^2 Z) \int_0^1 (m_w + m_s) \phi^2 d\tilde{y} + \cos \Lambda \int_0^1 \left( \frac{b}{b_R} \right)^2 L_h \phi^2 d\tilde{y} \quad (6.1)$$

where  $m_w$  and  $m_s$  indicate total mass of wing and store load.

$$B = -\frac{1}{\pi \rho_{\infty} b_R^3} \int_0^1 S_y \phi \varphi d\tilde{y} + \cos \Lambda \int_0^1 \left( \frac{b}{b_R} \right)^3 \left( L_{\theta} - L_h \left( \frac{1}{2} + a \right) \right) \phi \varphi d\tilde{y} \quad (6.2)$$

$$C = -\frac{1}{\pi \rho_{\infty} b_R^3} \int_0^1 S_y \phi \varphi d\tilde{y} + \cos \Lambda \int_0^1 \left( \frac{b}{b_R} \right)^3 \left( M_h - L_h \left( \frac{1}{2} + a \right) \right) \phi \varphi d\tilde{y} \quad (6.3)$$

$$D = \frac{1}{\pi \rho_{\infty} b_R^4} (1 - Z) \int_0^1 (I_{wy} + I_{sy}) \phi^2 d\tilde{y} + \cos \Lambda \int_0^1 \left( \frac{b}{b_R} \right)^4 \left( M_{\theta} - (M_h + L_{\theta}) \left( \frac{1}{2} + a \right) + L_h \left( \frac{1}{2} + a \right)^2 \right) \phi^2 d\tilde{y} \quad (6.4)$$

where  $I_{wy}$  and  $I_{sy}$  are total moment of inertias of the wing and store load respectively. By using the definition for span distance of store load,  $L_s$ , (6.5) and (6.6) are obtained.

$$m_s = \bar{m}_s \times L_s \quad (6.5)$$

$$I_{sy} = \bar{I}_{sy} \times L_s \quad (6.6)$$

$\bar{m}_s$  and  $\bar{I}_{sy}$  are mass and moment of inertia of store loads per their unit spans.

The remaining solution is the same with the presented procedure for flutter calculation of 3-dimensional clean wing models.

The extended flutter solution methodology including the effects of external stores is applied to the aeroelastic benchmark problem of Goland wing. The work of

Fazelzadeh [77] including external store effects in flutter boundary of Goland wing is chosen as comparative study to validate the methodology.

Reference values of the example model are shown in Table 6.1 while the locations of external stores and the experimental [78] and numerical flutter speed results [77] are shown and compared with the calculated results in Table 6.2.

**Table 6.1 :** Reference values of example Goland wing/store model.

Parameter	Value
$L$	1.2192 m
$b$	0.1016 m
$EI_{wy}$	403.76 Nm <sup>2</sup>
$GJ / I_{wy}$	198.58 Nm <sup>2</sup>
$\bar{m}_w$	1.2942 kgm <sup>-1</sup>
$\bar{I}_{wy}$	0.0036 kgm
$e.a.$	43.7%
$c.g.$	45.4%
$\rho$	1.224 kgm <sup>-3</sup>
$m_s$	1.578 kg
$I_{sy}$	0.0185 kgm <sup>2</sup>

Flutter speed-damping term plots are shown in Figure 6.2 to 6.5.

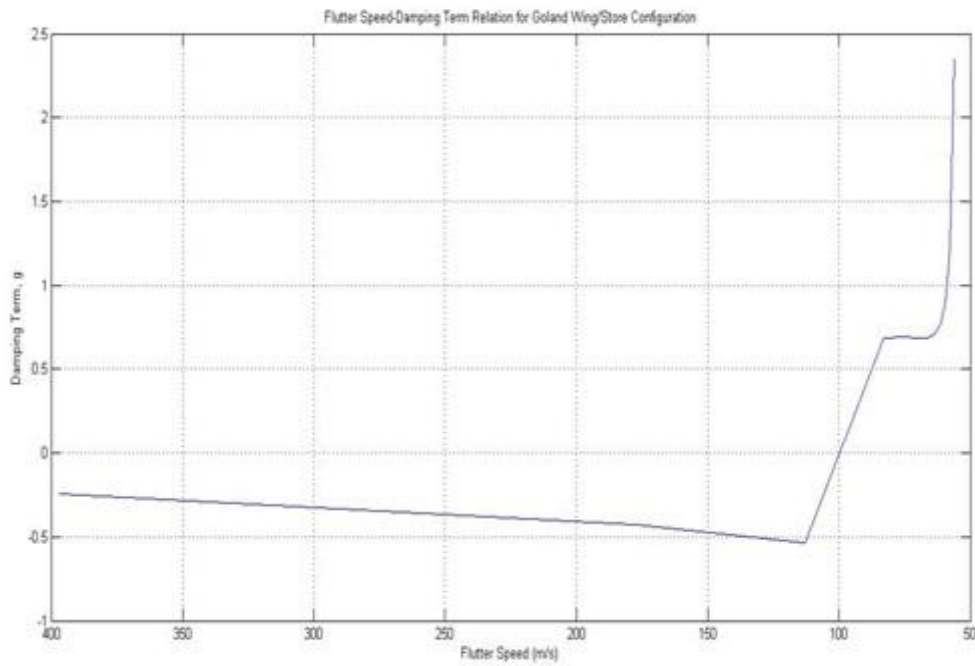


**Figure 6.2 :** Flutter speed-damping term relation for  $y_s=0.2794$  m.

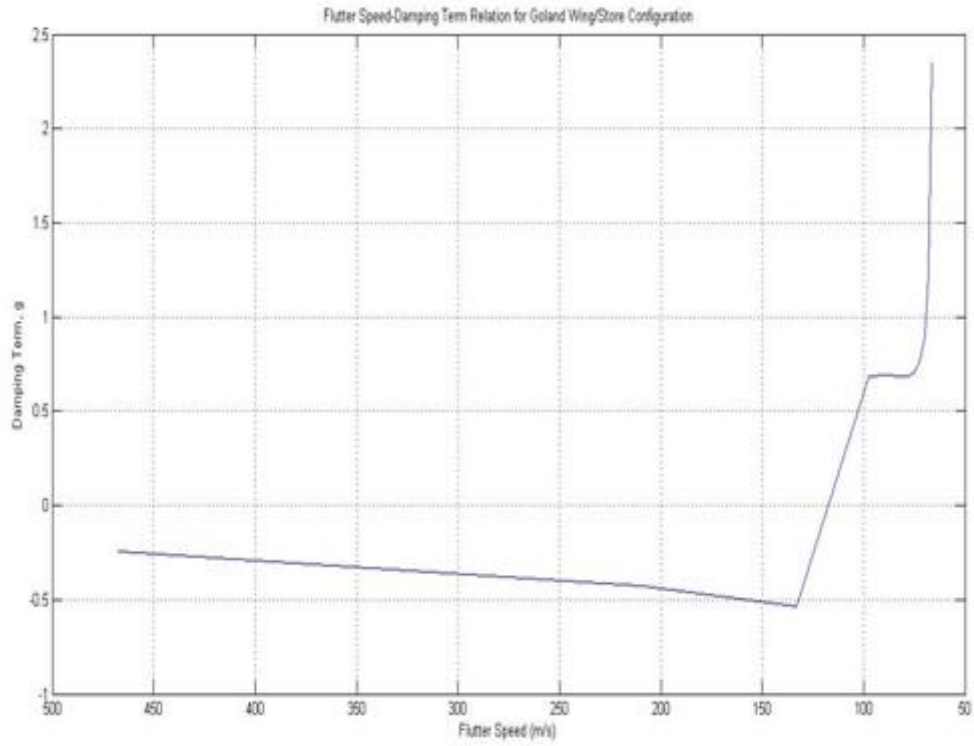


**Figure 6.3 :** Flutter speed-damping term relation for  $y_s=0.4318$  m.

The obtained results are satisfactory with respect to relative error values for each configuration when compared to both numerical [77] and experimental [78] solutions.

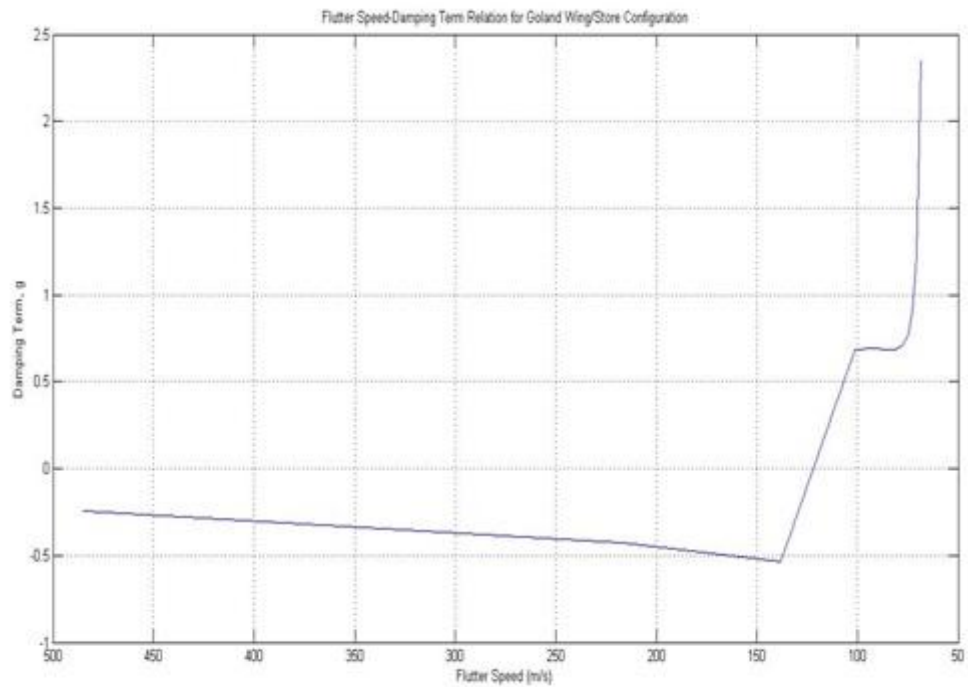


**Figure 6.4 :** Flutter speed-damping term relation for  $y_s=1.1684$  m.

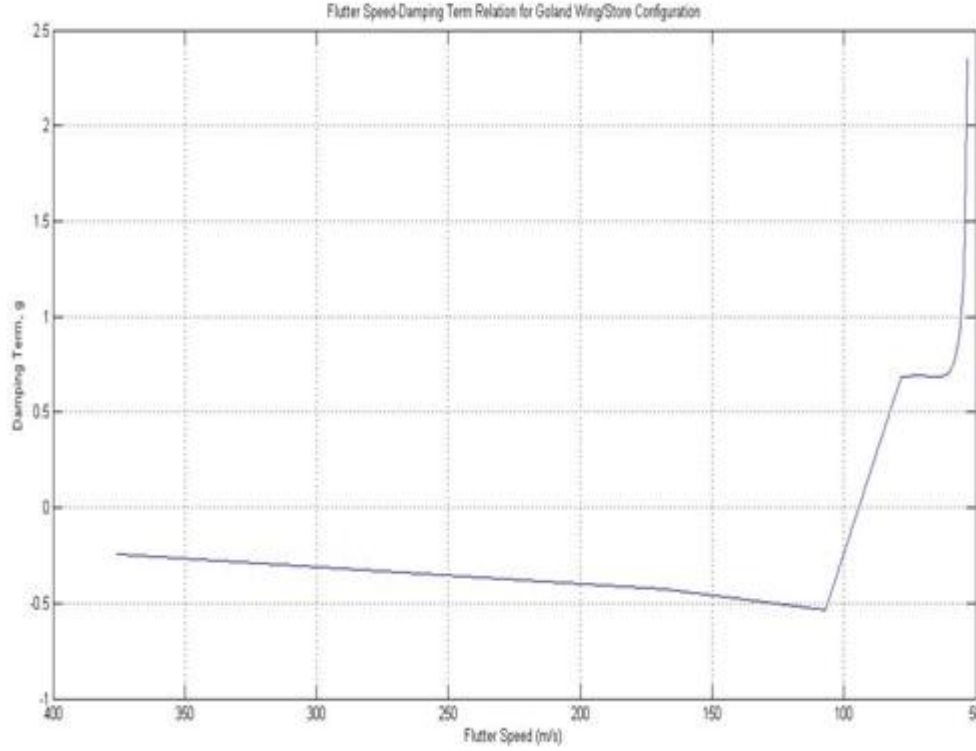


**Figure 6.5 :** Flutter speed-damping term relation for  $y_s=1.2192$  m.

**Table 6.2 :** Flutter results for example wing/store configuration.

Store Location	Numerical Result [77]	Experimental Result [78]	Calculated Solution	Relative Error wrt Experiment
0.2794 m	100.89 m/s	98.75 m/s	96.0679 m/s	2.7160 %
0.4318 m	124.05 m/s	116.43 m/s	113.1926 m/s	2.7806 %
1.1684 m	112.17 m/s	112.17 m/s	121.7199 m/s	8.5138 %
1.2192 m	91.44 m/s	97.54 m/s	94.3449 m/s	3.2757 %

## 6.2 Flutter Based Optimization of Initial AGARD 445.6 Wing/Store Configuration

Three flutter based design optimization works are performed by considering 3, 4 and 5 stations respectively along the wing span. The objectives are both to maximize the flutter speeds while the distances along span measured from the root of the wing for each station are defined as optimization variables. Optimum distances of the stations that maximize the flutter speed of the wing are obtained by considering equal mass for each of them.

The design parameters for AGARD 445.6 initial wing model are given in Table 3.5.

### 6.2.1 Flutter based optimization for 3-stations case

An optimization problem is constructed by considering 3-stations carrying equal masses. The total store mass is 1.25 kg (1.25 kg / 3 for each station) while the mass of the wing is 1.693 kg.

The optimization objective is maximizing the flutter speed while design parameters are selected as the distances of the stations from the root of the wing for 3 stations. Although the masses are considered as point masses for a preliminary application, this approach is not realistic. Constraints are determined for distances between stations in order to place the related masses in a more realistic manner.

$$\max_{s \in S} U_f(s) \quad (6.7)$$

$$S = \{s \in \mathbb{R}, s_L \leq s \leq s_U\} \quad (6.8)$$

$$s = \{y_1, y_2, y_3\} \quad (6.9)$$

$$0 \leq y_1 \leq 0.762 \text{ m} \quad (6.10)$$

$$0 \leq y_2 \leq 0.762 \text{ m} \quad (6.11)$$

$$0 \leq y_3 \leq 0.762 \text{ m} \quad (6.12)$$

$$x_1 = y_1 - y_2 \leq -0.04 \quad (6.13)$$

$$x_2 = y_2 - y_3 \leq -0.04 \quad (6.14)$$

where  $y_1, y_2, y_3$  are the distances for each station measured from the root of the wing while  $x_1, x_2$  are the constraints for the locations of stations. The optimization workflow is shown in Figure 6.6.

NSGA-II is used as optimization algorithm with 1000 DoE in order to obtain considerable amount of feasible designs since the constraints of the problem are rather strict. 100000 total designs are generated with 70451 feasible and 29549 infeasible designs. The solution took about 10 hours 58 minutes on a platform which has Intel(R) Core(TM) 2 CPU 6400@2.13GHz processor and 2GB of RAM on Microsoft Windows 7 64-bit operating system.

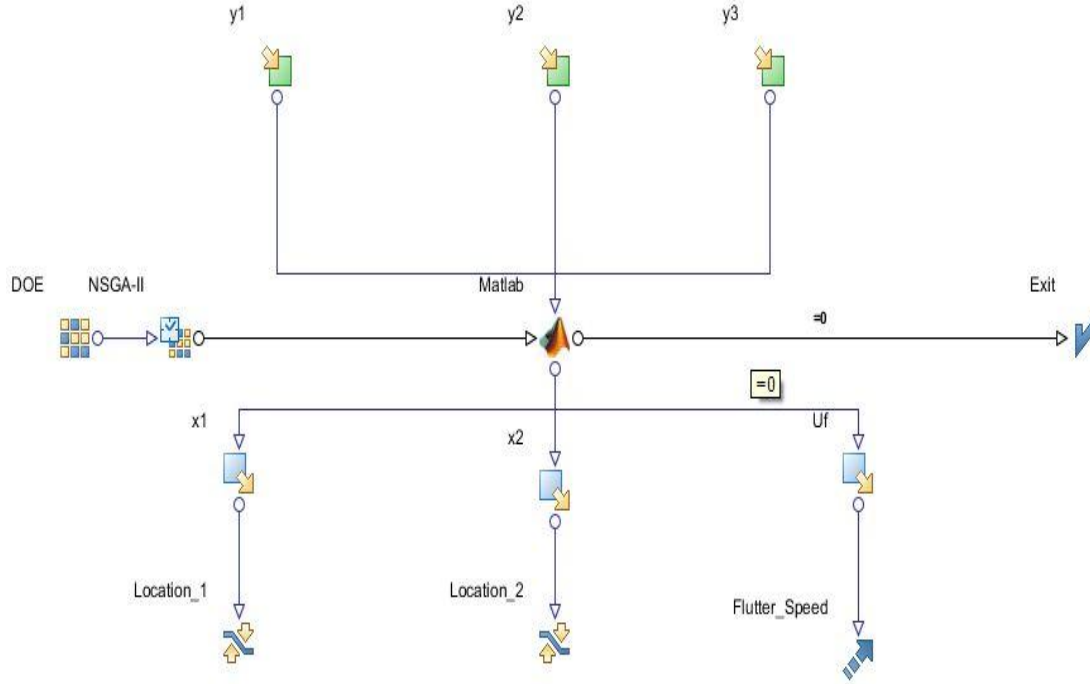


**Figure 6.6 :** Optimization workflow for 3-stations case.

Optimum design with maximum flutter speed is given in Table 6.3.

**Table 6.3 :** Optimum design parameters for 3-stations case.

Parameter	Value
$y_1$	0.68113 m
$y_2$	0.72122 m
$y_3$	0.76196 m
$U_f$	232.04 m/s

### 6.2.2 Flutter based optimization for 4-stations case

Firstly, an optimization problem is constructed by considering 4-stations carrying equal masses. The total store mass is 1.25 kg (1.25 kg / 4 for each station).

Optimization is performed by considering the same objective while constraints and variables are considered for 4-stations case as follows.

$$\max_{s \in S} U_f(s) \quad (6.15)$$

$$S = \{s \in \mathfrak{R}, s_L \leq s \leq s_U\} \quad (6.16)$$

$$s = \{y_1, y_2, y_3, y_4\} \quad (6.17)$$

$$0 \leq y_1 \leq 0.762 \text{ m} \quad (6.18)$$

$$0 \leq y_2 \leq 0.762 \text{ m} \quad (6.19)$$

$$0 \leq y_3 \leq 0.762 \text{ m} \quad (6.20)$$

$$0 \leq y_4 \leq 0.762 \text{ m} \quad (6.21)$$

$$x_1 = y_1 - y_2 \leq -0.04 \quad (6.22)$$

$$x_2 = y_2 - y_3 \leq -0.04 \quad (6.23)$$

$$x_3 = y_3 - y_4 \leq -0.04 \quad (6.24)$$

where  $y_1, y_2, y_3, y_4$  are the distances for each station measured from the root of the wing while  $x_1, x_2, x_3$  are the constraints for the locations of stations.

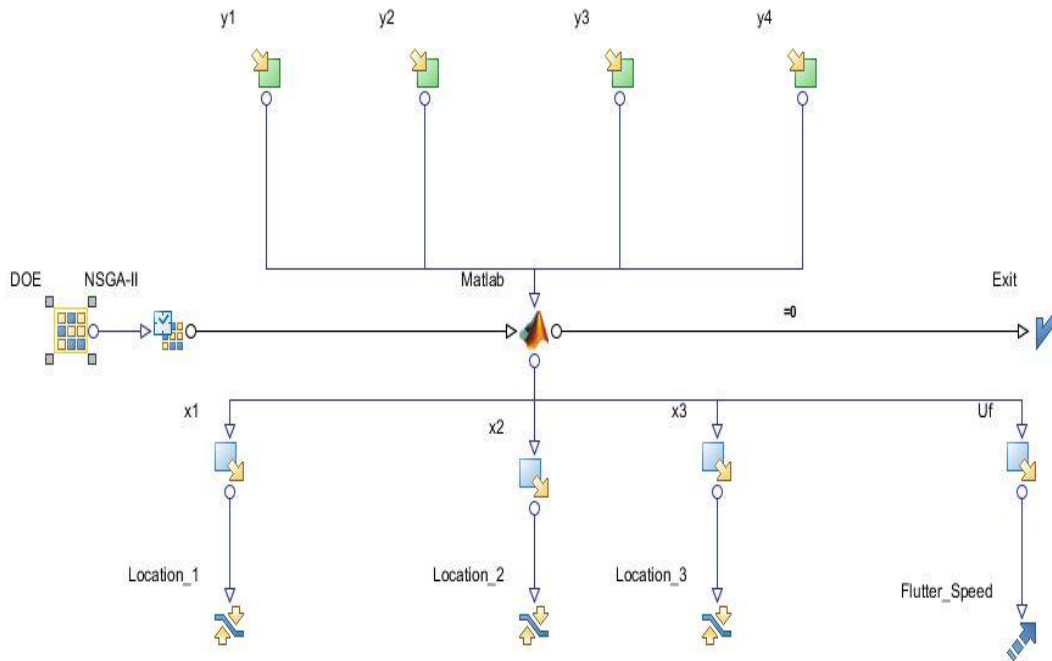


**Figure 6.7 :** Optimization workflow for 4-stations case.

NSGA-II is used as optimization algorithm with 1000 DoE. 100000 total designs are produced with 64189 feasible and 35811 infeasible designs. The solution took about 10 hours 56 minutes on a platform as Intel(R) Core(TM) 2 CPU 6400@2.13GHz processor and 2GB of RAM on Microsoft Windows 7 64-bit operating system. Optimum design with maximum flutter speed is given in Table 6.4.

**Table 6.4 :** Optimum design parameters for 4-stations case.

Parameter	Value
$y_1$	0.63283 m
$y_2$	0.67948 m
$y_3$	0.72057 m
$y_4$	0.76200 m
$U_f$	221.43 m/s

### 6.2.3 Flutter based optimization for 5-stations case

An optimization problem is constructed by considering 5-stations with equal masses.

The store total mass is 1.25 kg (1.25 kg / 5 for each station).

Optimization is performed by considering the same objective while constraints and variables are considered for 5-stations case.

$$\max_{s \in S} U_f(s) \quad (6.25)$$

$$S = \{s \in \Re, s_L \leq s \leq s_U\} \quad (6.26)$$

$$s = \{y_1, y_2, y_3, y_4, y_5\} \quad (6.27)$$

$$0 \leq y_1 \leq 0.762 \text{ m} \quad (6.28)$$

$$0 \leq y_2 \leq 0.762 \text{ m} \quad (6.29)$$

$$0 \leq y_3 \leq 0.762 \text{ m} \quad (6.30)$$

$$0 \leq y_4 \leq 0.762 \text{ m} \quad (6.31)$$

$$0 \leq y_5 \leq 0.762 \text{ m} \quad (6.32)$$

$$x_1 = y_1 - y_2 \leq -0.04 \quad (6.33)$$

$$x_2 = y_2 - y_3 \leq -0.04 \quad (6.34)$$

$$x_3 = y_3 - y_4 \leq -0.04 \quad (6.35)$$



$$x_4 = y_4 - y_5 \leq -0.04 \quad (6.36)$$

where  $y_1, y_2, y_3, y_4, y_5$  are the distances for each station measured from the root of the wing while  $x_1, x_2, x_3, x_4$  are the constraints for the locations of stations.

The optimization workflow is shown in Figure 6.8.

NSGA-II is again used as optimization algorithm with 1000 DoE. 100000 total designs are obtained with 59587 feasible and 40413 infeasible designs. The solution took about 11 hours 20 minutes on a platform as Intel(R) Core(TM) 2 CPU 6400@2.13GHz processor and 2GB of RAM on Microsoft Windows 7 64-bit operating system.

Optimum design with maximum flutter speed is given in Table 6.5.

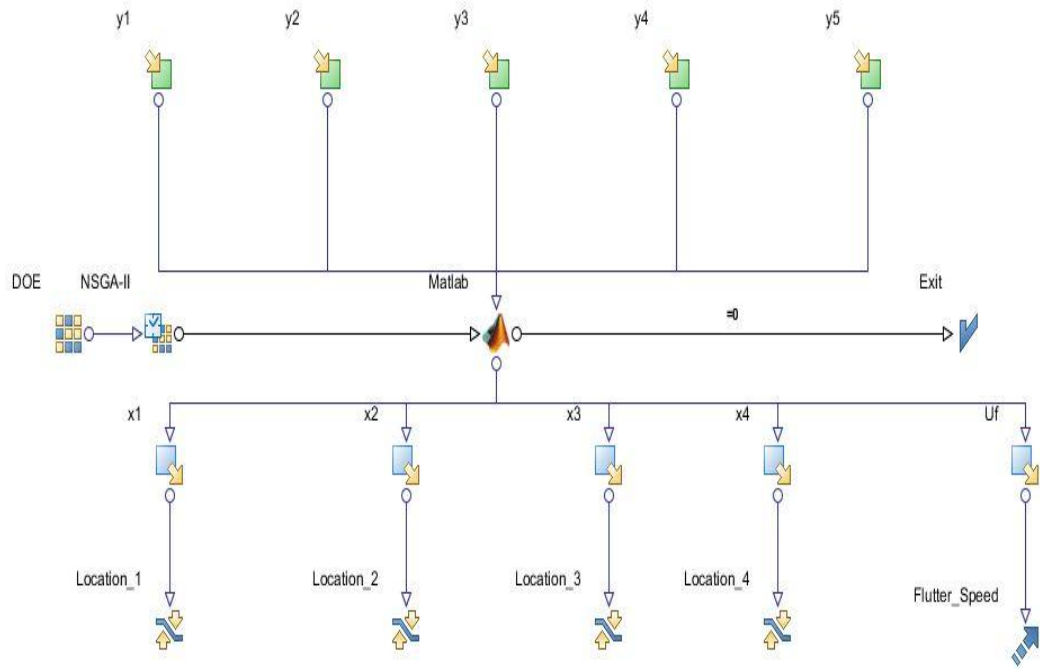


**Figure 6.8 :** Optimization workflow for 5-stations case.

**Table 6.5 :** Optimum design parameters for 5-stations case.

Parameter	Value
$y_1$	0.5771 m
$y_2$	0.61801 m
$y_3$	0.65928 m
$y_4$	0.71182 m
$y_5$	0.76200 m
$U_f$	212.32 m/s

#### 6.2.4 Comparison of flutter results for different configurations of stations

Flutter speeds of AGARD 445.6 initial configurations with respect to the number of stations along the wing span are compared in Table 6.6.

**Table 6.6 :** Comparison of flutter speeds with respect to station numbers.

Number of Stations	$U_f$ (m/s)	Decrease (%)
3	232.04	24.77
4	221.43	28.21
5	212.32	31.17
Clean Wing	308.4513	-

The results indicate that the flutter speed increases as the total number of stations decreases for the initial AGARD 445.6 wing/store configurations.

Comparison of optimum locations for related stations along the wing span of the initial wing configuration is shown in Table 6.7.

**Table 6.7 :** Optimum locations with respect to station numbers.

Number of Stations	1 <sup>st</sup> Station (m)	2 <sup>nd</sup> Station (m)	3 <sup>rd</sup> Station (m)	4 <sup>th</sup> Station (m)	5 <sup>th</sup> Station (m)
3	0.68113	0.72122	0.76196	-	-
4	0.63283	0.67948	0.72057	0.76200	-
5	0.57710	0.61801	0.65928	0.71182	0.76200

#### 6.3 Flutter Based Optimization of Optimum AGARD 445.6 Wing/Store Configuration

Three flutter based design optimization works are performed by considering 3, 4 and 5 stations respectively along the span of optimum AGARD 445.6 wing/store configurations. The objectives are both to maximize the flutter speed while the distances from the root of the wing for each station are defined as optimization variables. Optimum distances of the stations that maximize the flutter speed of the wing are obtained by considering equal mass effects for each of them.

The design parameters for optimum AGARD 445.6 wing model are given in Table 6.8.

**Table 6.8 :** Initial design parameters of optimum AGARD 445.6.

Parameter	Value
$E_y$	2020.85 MPa
$G_y$	299.02 MPa
$\lambda$	0.65
$\Lambda$	59.65°

**6.3.1 Flutter based optimization for 3-stations case**

The same optimization problem in Section 6.2.1 is considered. As in the initial configuration case, the optimization problem is consisted of an objective as maximizing the flutter speed while design parameters are selected as the distances of the stations from the root of the wing. Constraints are determined for distances between stations in order to place the related masses in a more realistic manner.

NSGA-II is used as optimization algorithm with 1000 DoE. 100000 total designs are produced with 70451 feasible and 29549 infeasible designs. The solution took about 10 hours 58 minutes on a platform as Intel(R) Core(TM) 2 CPU 6400@2.13GHz processor and 2GB of RAM on Microsoft Windows 7 64-bit operating system.

**Table 6.9 :** Optimum design parameters for 3-stations case.

Parameter	Value
$y_1$	0.68113 m
$y_2$	0.72122 m
$y_3$	0.76196 m
$U_f$	314.46 m/s

**6.3.2 Flutter based optimization for 4-stations case**

Optimization is performed by considering the same objective while constraints and variables are considered for 4-stations case.

NSGA-II is used as optimization algorithm with 1000 DoE. 100000 total designs are generated with 64189 feasible and 35811 infeasible designs. The solution took about 10 hours 56 minutes on a platform which has Intel(R) Core(TM) 2 CPU 6400@2.13GHz processor and 2GB of RAM on Microsoft Windows 7 64-bit operating system.

Optimum design with maximum flutter speed is given in Table 6.10 with optimum store locations.

**Table 6.10 :** Optimum design parameters for 4-stations case.

Parameter	Value
$y_1$	0.63283 m
$y_2$	0.67948 m
$y_3$	0.72057 m
$y_4$	0.76200 m
$U_f$	288.89 m/s

### 6.3.3 Flutter based optimization for 5-stations case

Optimization is performed for 5-stations case by considering the same design optimization problem.

NSGA-II is again used as optimization algorithm with 1000 DoE. 100000 total designs are produced with 59587 feasible and 40413 infeasible designs. The solution took about 9 hours 24 minutes 43 seconds on a platform as Intel(R) Core(TM) 2 CPU 6400@2.13GHz processor and 2GB of RAM on Microsoft Windows 7 64-bit operating system.

Optimum design with maximum flutter speed is given in Table 6.11.

**Table 6.11 :** Optimum design parameters for 5-stations case.

Parameter	Value
$y_1$	0.57710 m
$y_2$	0.61801 m
$y_3$	0.65928 m
$y_4$	0.71182 m
$y_5$	0.76200 m
$U_f$	265.11 m/s

### 6.3.4 Comparison of flutter results for different configurations of stations

The flutter speeds of optimum AGARD 445.6 configurations with respect to the number of stations along the wing span are compared in Table 6.12.

It is seen that distributing the external stores into more stations decreases the flutter boundary, even though the total mass of stores is kept constant.

Comparison of optimum locations of the stations along the wing span is given in Table 6.13.

**Table 6.12 :** Comparison of flutter speeds with respect to station numbers.

Number of Stations	$U_f$ (m/s)	Decrease (%)
3	314.46	13.10
4	288.89	20.17
5	265.11	26.74
Clean Wing	361.8843	-

The results again indicate that the flutter speed increases with decreasing number of stations.

**Table 6.13 :** Optimum locations with respect to station numbers.

Number of Stations	1 <sup>st</sup> Station (m)	2 <sup>nd</sup> Station (m)	3 <sup>rd</sup> Station (m)	4 <sup>th</sup> Station (m)	5 <sup>th</sup> Station (m)
3	0.68113	0.72122	0.76196	-	-
4	0.63283	0.67948	0.72057	0.76200	-
5	0.57710	0.61801	0.65928	0.71182	0.76200

#### 6.4 Comparison of Flutter Results for Initial and Optimum AGARD 445.6 Wing/Store Configuration

Flutter based optimizations are further performed by considering 3,4 and 5 store locations for both initial and previously optimized designs of AGARD 445.6 wing/store configurations. The flutter speed is greater when the number of stations decreases, as seen previously.

Flutter speed variations of initial and optimum wing structures with respect to various numbers of stations is shown in Figure 6.9.

Optimum wing is more sensitive to the variations with respect to increasing number of store locations, however in all considered cases, optimum models have greater flutter speeds. Figure 6.9 indicates that optimum wing with store masses in 3 stations case provides the most efficient design. Despite carrying 1.25 kg additional masses as store loads, the flutter boundary of the best design is even greater than the flutter speed value of initial clean wing model. After specifying the best wing/store configuration involving optimized clean wing model with store loads in 3 stations, the flutter boundaries now have to be determined in the presence of uncertainties in

structural and geometric parameters. Then, the final robust design is provided by the robust design optimization application in Section 7.

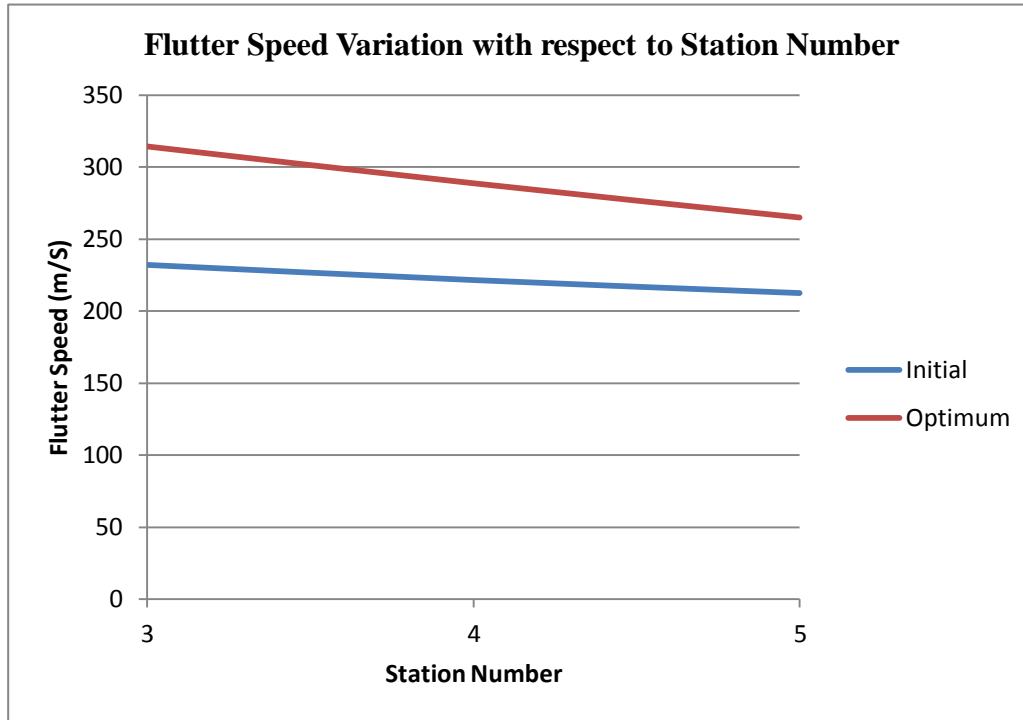


**Figure 6.9 :** Flutter speed variation with respect to station number.

### 6.5 Uncertainty Based Flutter Analysis of AGARD 445.6 Wing/Store Configuration

This section involves uncertainty based flutter analysis of the best AGARD 445.6 wing/store configuration determined in previous section. The considered design is optimum AGARD 445.6 clean wing with external stores placing in 3 stations.

**Table 6.14 :** Deterministic values of random variables in wing/store model.

Variable	Value
$y_1$	0.68113 m
$y_2$	0.72122 m
$y_3$	0.76196 m
$m_1$	0.4167 kg
$m_2$	0.4167 kg
$m_3$	0.4167 kg
$E_y$	2020.85 MPa
$G_y$	299.02 MPa

Structural and geometric uncertainties are assumed to affect the wing/store model. Structural uncertainties involve the store masses and material properties while positions of store loads along wing span form the geometric uncertainties.

Random parameters are defined as masses and locations of store loads, elasticity and shear modulus with  $COV=1\%$  and  $COV=5\%$  and locations of store loads with  $COV=0.25\%$  approach. In Table 6.14,  $m_1$ ,  $m_2$  and  $m_3$  are masses of store loads.

### 6.5.1 $COV=1\%$ case

Masses of store loads, elasticity and shear modulus are distributed with respect to  $COV=1\%$  approach while  $COV$  is taken as 0.0025 for the distances of stations. The maximum value for the distance of the 3<sup>rd</sup> station can not exceed the total span distance.

The difference between theoretical and minimum flutter speeds is calculated as 1.7224% by considering reliability.

**Table 6.15 :** Statistical results of 3-stations case with  $COV=1\%$ .

Parameter	Det. Value	Min. Value	Mean Value	Max. Value
$y_1$	0.68113 m	0.6742 m	0.6811 m	0.6890 m
$y_2$	0.72122 m	0.7125 m	0.7212 m	0.7291 m
$y_3$	0.76196 m	0.7618 m	0.7619 m	0.7620 m
$m_1$	0.4167 kg	0.3982 kg	0.4167 kg	0.4342 kg
$m_2$	0.4167 kg	0.3994 kg	0.4167 kg	0.4338 kg
$m_3$	0.4167 kg	0.3990 kg	0.4166 kg	0.4339 kg
$E_y$	2020.85 MPa	1926.1 MPa	2020.8 MPa	2105.1 MPa
$G_y$	299.02 MPa	286.59 MPa	299.01 MPa	314.41 MPa
$U_f$	314.46 m/s	<b>309.0437 m/s</b>	314.4534 m/s	319.7874 m/s

### 6.5.2 $COV=5\%$ case

Masses of store loads, elasticity and shear modulus are distributed with respect to  $COV=5\%$  approach while  $COV$  is taken as 0.0025 for the distances of stations. The statistical results are shown in Table 6.16 while flutter speed histograms for  $COV=1\%$  and  $COV=5\%$  cases are shown in Figure 6.10.

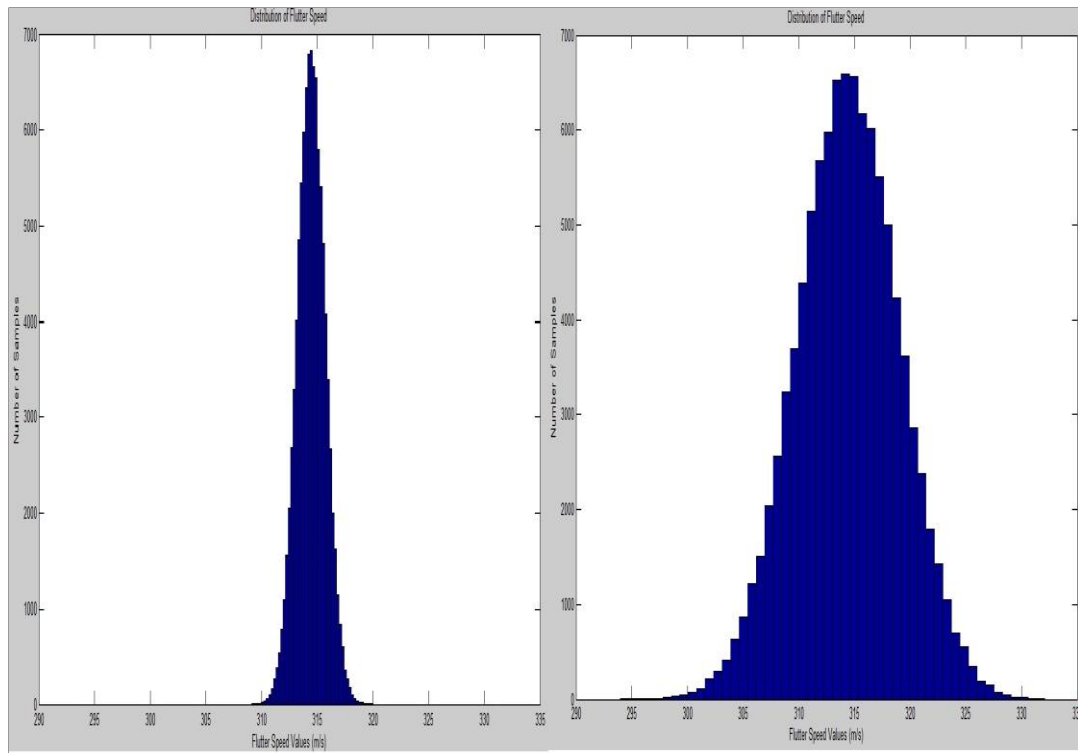


**Figure 6.10 :** Flutter speed histograms for  $COV=1\%$  and  $COV=5\%$ .

**Table 6.16 :** Statistical results of 3-stations case with  $COV=5\%$ .

Parameter	Det. Value	Min. Value	Mean Value	Max. Value
$y_1$	0.68113 m	0.6734 m	0.6811 m	0.6888 m
$y_2$	0.72122 m	0.7135 m	0.7212 m	0.7293 m
$y_3$	0.76196 m	0.7618 m	0.7619 m	0.7620 m
$m_1$	0.4167 kg	0.3301 kg	0.4166 kg	0.5091 kg
$m_2$	0.4167 kg	0.3310 kg	0.4167 kg	0.5016 kg
$m_3$	0.4167 kg	0.3125 kg	0.4166 kg	0.5053 kg
$E_y$	2020.85 MPa	1535.9 MPa	2021.2 MPa	2427.5 MPa
$G_y$	299.02 MPa	237.48 MPa	298.95 MPa	362.40 MPa
$U_f$	314.46 m/s	<b>300.4018 m/s</b>	314.4313 m/s	328.8310 m/s

The difference between theoretical and minimum flutter speeds is calculated as 4.4706% by considering for reliability.

The design properties of final optimum robust wing/store configuration with deterministic and minimum flutter speed values are given in Table 6.17.

By considering the technological possibilities of today's world conditions, it is more likely to distribute the uncertainties with  $COV=1\%$ , however the aim of the present work is to determine strictly reliable wing configurations. Thus,  $COV=5\%$  case is



determined as the comparative study for deterministic analyses and deterministic and robust design optimization works while uncertainty based analyses with  $COV=1\%$  approach even provides realistic flutter results.

**Table 6.17:** Design properties and flutter results of optimum wing/store model.

Variable	Value
$\lambda$	0.65
$\Lambda$	59.65°
$E_y$	2020.85 MPa
$G_y$	299.02 MPa
$y_1$	0.68113 m
$y_2$	0.72122 m
$y_3$	0.75404 m
$m_s$	0.76196 kg
$U_f^{\text{det}}$	314.46 m/s
$U_f^{\text{min}}$	<b>300.4018 m/s</b>



## 7. ROBUST AEROELASTIC DESIGN OPTIMIZATION OF WING/STORE CONFIGURATIONS BASED ON FLUTTER CRITERIA

The present work finally involves robust optimization of wing/store configurations based on flutter criteria in order to design the most efficient and reliable structures in terms of aeroelastic instabilities.

Results in a deterministic model can differ from the real world conditions since uncertainties in input parameters such as material, geometric properties and operating conditions can severely affect the system outputs. Deterministic methods can provide high performance designs however the randomness in uncertain parameters can cause reduction in the expected performance of the real system. In order to achieve both an efficient and a reliable design even under the worst case conditions of the design parameters, it is necessary to make use of robust optimization strategies. Robust optimization improves the given design in a way that it satisfies all scenerios about uncertain parameters by determining an expected minimum level for output variables. General formulation of a robust optimization problem is given in [79].

$$\min F(\nu) \quad (7.1)$$

$$\text{subject to } g_F(\nu) = \frac{F_1(\nu)}{F(\nu)} \leq \varepsilon \quad (7.2)$$

$$g_j(\nu) + \sum_{i=1}^{n_d} \left| \frac{\partial g_j(\nu)}{\partial \nu_i} \right| |\Delta \nu_i| \leq 0; \quad j=1, \dots, n_c \quad (7.3)$$

$$(\nu_i)_{lower} + \Delta \nu_i \leq \nu_i \leq (\nu_i)_{upper} - \Delta \nu_i; \quad i=1, \dots, n_d \quad (7.4)$$

$$F_1(\nu) = \sqrt{\sum_{i=1}^{n_d} \left[ \left( \frac{\partial F(\nu)}{\partial \nu_i} \right)^2 (\Delta \nu_i)^2 \right]} \quad (7.5)$$

where  $\nu$  specifies the design variables.  $F_1(\nu)$  points out the relative change of objective function due to variations and (7.2) behaves like an additional constraint that limits the relative change with a specified magnitude,  $\varepsilon$ . (7.3) is related to the robust constraints and involves magnitude of changes and sensitivity of  $j$ th constraint with respect to  $i$ th design variable. Total number of constraints are denoted by  $n_c$  and  $n_d$  shows total number of design variables. Upper and lower limits of optimization variables are specified in (7.4) while (7.5) shows the change of objective function by making use of Taylor expansion method.

In the present work, robust optimization studies are considered to provide more reliable designs even under the worst case scenarios of the real world. The robust results are adequately satisfying under declared levels of uncertainty. Robust aeroelastic optimization work is divided into three categories by considering 2-dimensional airfoil, 3-dimensional AGARD 445.6 clean wing and 3-dimensional AGARD 445.6 wing/store configuration. The objective is to maximize flutter speed in the presence of both deterministic and probabilistic optimization variables. Constraints are defined with the same manner in the previous optimization studies. Random variables in uncertainty based analyses are defined as probabilistic parameters while the other deterministic parameters of the previous aeroelastic optimization studies remain as deterministic optimization variables.  $COV=5\%$  case is considered as the worst case uncertainty scenario in today's world possibilities. The deterministic solution codes of previous sections are coupled with the optimization software. Random parameters are varied with given distributions via modeFRONTIER. The statistical properties as mean values and standard deviations of random variables are also defined in modeFRONTIER by considering  $COV=5\%$ . MORDO (Multi-Objective Robust Design Optimization) module of modeFRONTIER is used to obtain robust results since MORDO searches for the optima of the mean and standard deviation of a stochastic response rather than the optima of the deterministic response [80]. MORDO can find the robust design under a given or assumed variation of design parameters [81].

MCS method distributes the random optimization variables by using of 1000 DoE and 100 generations for each of DoE. The applied settings point out  $10^5$  total design samples. The considered amount of samples increases the computational time

however the fast NSGA-II algorithm [82] and the 2<sup>nd</sup> order PCE in MORDO are preferred in all robust optimization studies to reduce the computational time.

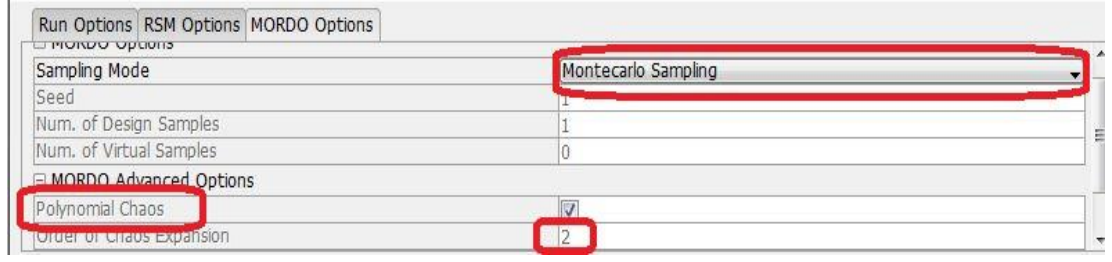


**Figure 7.1** : MORDO settings in modeFRONTIER.

PCE has successfully been used in uncertainty analysis [69] since introduction of the homogeneous chaos by Wiener [83]. A 2<sup>nd</sup> order PCE, which is used within the context of robust optimization studies of the present work, is given in (7.6) [69].

$$u(\theta) = b_0 + b_1\xi_1(\theta) + b_2\xi_2(\theta) + b_3(\xi_1^2(\theta) - 1) + b_4\xi_1(\theta)\xi_2(\theta) + b_5(\xi_2^2(\theta) - 1) \quad (7.6)$$

where  $u(\theta)$  is Gaussian random response,  $b_i$  ( $i=1$  to 5) is generalized Fourier coefficient,  $\xi_1$  and  $\xi_2$  are two independent standard Gaussian random variables defined in (7.7).

$$\xi = \frac{x - \mu_x}{\sigma_x} \quad (7.7)$$

The definition of generalized Fourier coefficients is given in (7.8) [69].

$$b_i = \frac{E[u(\theta)\psi_i(\vec{\xi}(\theta))]}{E[\psi_i(\vec{\xi}(\theta))\psi_i(\vec{\xi}(\theta))]} \quad (7.8)$$

where  $E[.]$  and  $\psi$  denote expected value operation and orthogonal polynomials. They have to satisfy the condition defined in (7.9).

$$\begin{aligned} \psi_0 &= 1, E[\psi_i] = 0 \text{ and } E[\psi_i\psi_j] = E[\psi_i^2]\delta_{ij} \text{ for } \forall i, j \\ E[\xi^0] &= 1, E[\xi^k] = 0 \text{ for } \forall k \text{ odd} \end{aligned} \quad (7.9)$$

## 7.1 Robust Aeroelastic Optimization of 2-Dimensional Airfoil

Firstly, an optimization work is carried out so as to achieve a robust aeroelastic design for the first 2-dimensional airfoil model of Section 2. Random variables in uncertainty based analysis are assigned as probabilistic optimization variables while

the others in deterministic optimization case remain the same. The robust design is mainly based on flutter speed. The objectives are defined as maximizing flutter, divergence and control reversal speeds. Optimization problem can be defined as follows.

$$\max_{s \in S} \{V_f^{prob}\}, \quad \max_{s \in S} \{V_d^{prob}\}, \quad \max_{s \in S} \{U_r^{prob}\} \quad (7.10)$$

$$g_1^{prob}(X_R, s) = r_\alpha - 1 < 0, \quad g_1^{prob}(s) \in \mathfrak{R} \quad (7.11)$$

$$g_2^{prob}(X_R, s) = \bar{\omega} - 1 < 0, \quad g_2^{prob}(s) \in \mathfrak{R} \quad (7.12)$$

$$S = \{s \in \mathfrak{R}, s_L \leq s \leq s_u\} \quad (7.13)$$

$$s = \{s^{det}, s^{prob}\} \quad (7.14)$$

$$s^{det} = (k_h, k_\alpha, x_\alpha) \quad \text{and} \quad s^{prob} = (m, I_\alpha) \quad (7.15)$$

$$X_R = (m, I_\alpha, \rho, c_{L_\alpha}, c_{L_\beta}, c_{M_\alpha}, c_{M_\beta}) \quad (7.16)$$

where  $s^{det}$  and  $s^{prob}$  indicate deterministic and probabilistic optimization variables respectively and  $X_R$  denotes set of random parameters. Similarly,  $g_1^{prob}$  and  $g_2^{prob}$  are probabilistic constraint functions. The lower and upper bounds of optimization variables are specified in Table 4.1.

The objectives and constraints are also probabilistic since they can be defined in terms of mass and moment of inertia as probabilistic variables. All probabilistic parameters have statistical features such as standard deviation, minimum, mean and maximum values, etc. Robust analysis and optimization require investigations of available minimum values as the worst case conditions. Thus, the minimum values of maximized objectives have to be considered and optimum design has to be selected among them. The minimum of maximized values is the desired objective for the robust optimization problem. Since flutter occurs before divergence and control reversal phenomena, the optimum design can be obtained by only considering flutter. The minimum of maximum flutter speeds among robust designs provides the optimum robust design based on aeroelastic instability criteria.

100000 total designs with 78325 feasible designs and 10000 robust designs with 9241 feasible designs are obtained while the solution took about 40 hours 39 minutes on a platform as AMD Athlon (TM) 64 X2 Dual Core 4600+2.41GHz processor and 2GB of RAM on Microsoft Windows XP operating system.

The optimization workflow is shown in Figure 7.2.

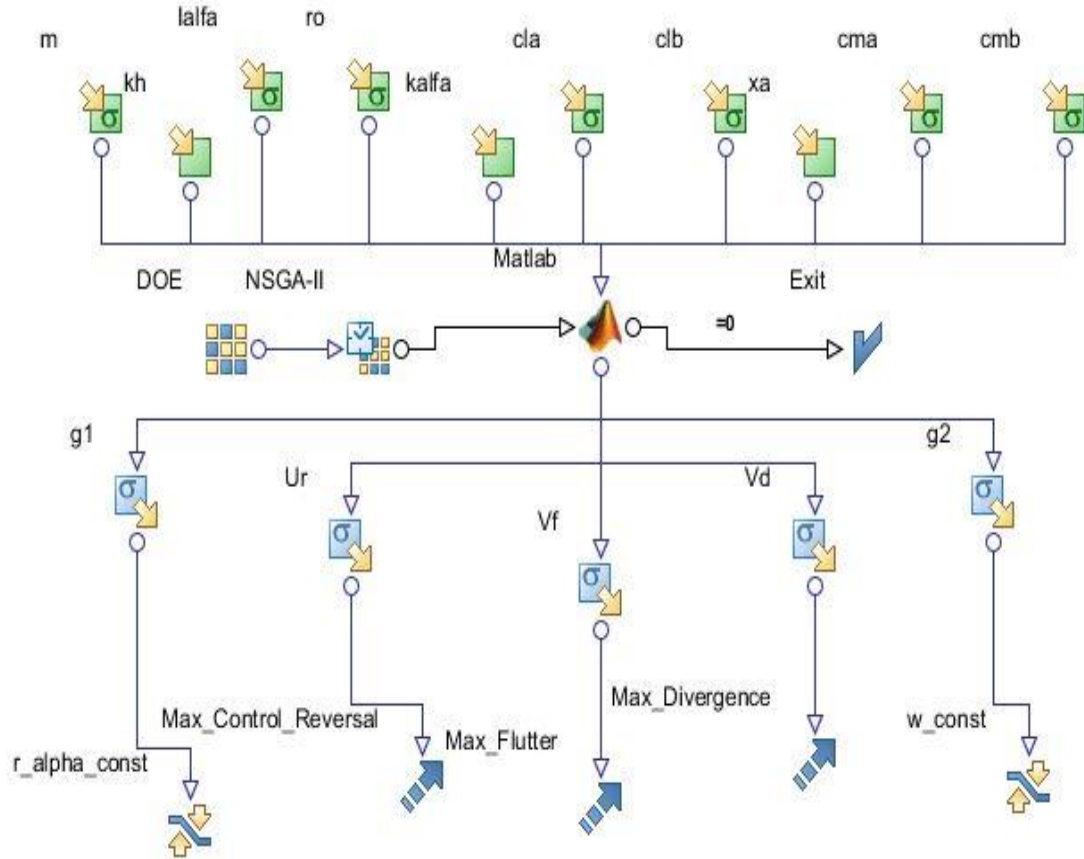


**Figure 7.2 :** Workflow of 2-dimensional robust aeroelastic optimization.

The probability density distributions of the objective functions are given in Figure 7.3, 7.4 and 7.5.

The design variables of robust aeroelastic optimization work are summarized in Table 7.1 with optimum robust speeds of aeroelastic instabilities. The superscript “robust” indicates the parameters in optimum robust design while superscript “det” points out the deterministic design.

The boundaries of aeroelastic instabilities in optimum robust design are lower than the values in optimum deterministic design since the robust design points out the worst case conditions.

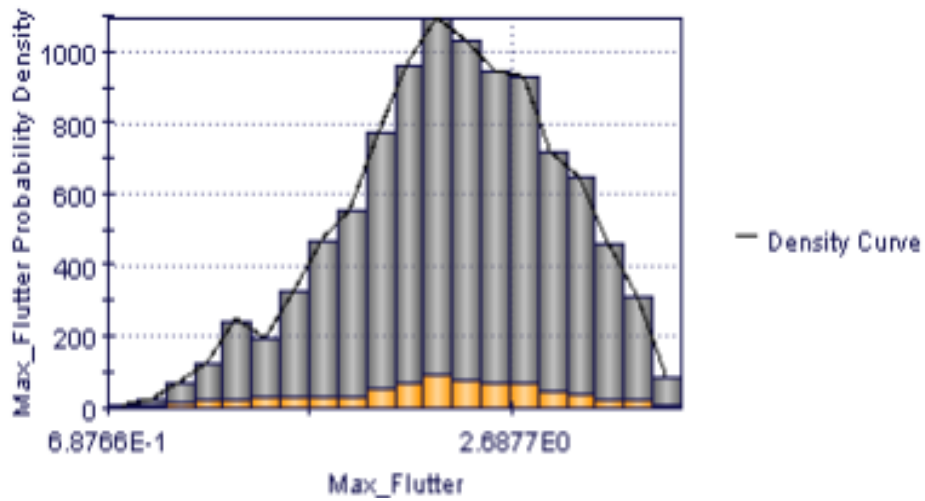


**Figure 7.3 :** Probability density distribution of maximum flutter speed.

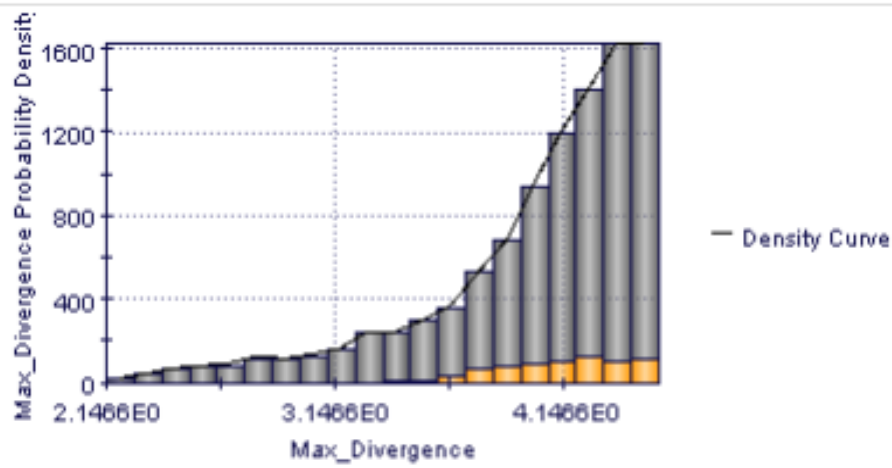


**Figure 7.4 :** Probability density distribution of maximum divergence speed.

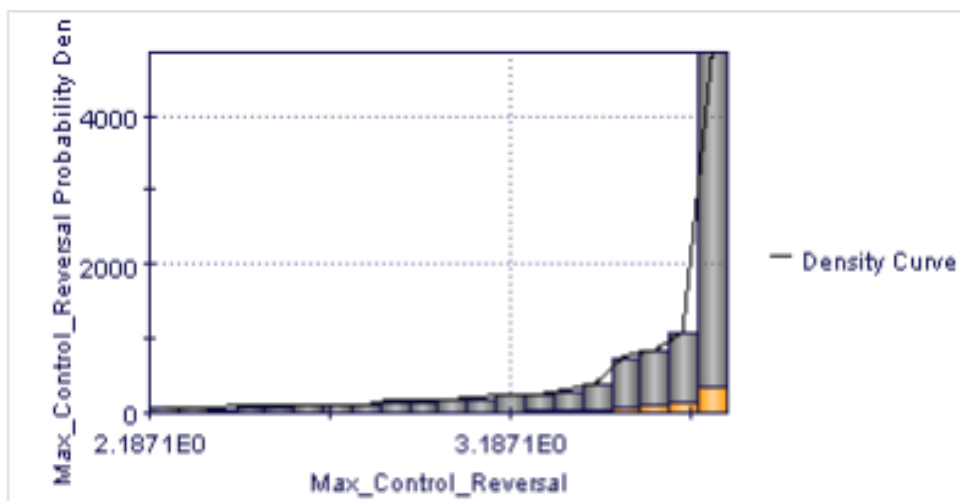


**Figure 7.5 :** Probability density distribution of maximum control reversal speed.



**Table 7.1:** Optimum robust design properties of 2-dimensional airfoil model.

Design Variable	Optimum Value
$k_h$	1.0107
$k_\alpha$	6.6962
$x_\alpha$	0.10031
$m$	12.330 kg
$I_\alpha$	2.9919 kgm <sup>2</sup>
$V_f^{robust}$	<b>3.3967</b>
$V_f^{det}$	<b>3.5337</b>
$V_d^{robust}$	<b>4.0766</b>
$V_d^{det}$	<b>4.2603</b>
$U_r^{robust}$	<b>3.6369</b>
$U_r^{det}$	<b>3.7878</b>

Table 7.2 involves the comparison of design parameters in deterministic and robust aeroelastic models.

**Table 7.2:** Comparison of deterministic and robust design parameters.

Case	$k_h$	$k_\alpha$	$x_\alpha$	$m$	$I_\alpha$
Deterministic	1.00	7.00	0.10	12.499 kg	3.00 kgm <sup>2</sup>
Robust	1.0107	6.6962	0.10031	12.330 kg	2.9919 kgm <sup>2</sup>

## 7.2 Robust Optimization of AGARD 445.6 Clean Wing

This section involves robust optimization of AGARD 445.6 clean wing based on flutter criteria. Random parameters (elasticity and shear modulus along spanwise direction) in uncertainty based flutter analysis are defined as probabilistic optimization variables in robust optimization while taper ratio and sweep angle are again deterministic parameters. Optimization problem can be determined as follows.

$$\max_{s \in S} U_f^{prob}(s) \quad (7.17)$$

$$S = \{s \in \mathfrak{R}, s_L \leq s \leq s_U\} \quad (7.18)$$

$$s = \{s^{det}, s^{prob}\} \quad (7.19)$$

$$s^{\text{det}} = (\lambda, \Lambda) \quad \text{and} \quad s^{\text{prob}} = (E_y, G_y) \quad (7.20)$$

$$X_R = (E_y, G_y) \quad (7.21)$$

$$0^\circ \leq \Lambda \leq 60^\circ \quad (7.22)$$

$$2000\text{MPa} \leq E_y \leq 3000\text{MPa} \quad (7.23)$$

$$200\text{MPa} \leq G_y \leq 300\text{MPa} \quad (7.24)$$

The robust optimization study is performed in modeFRONTIER coupled with the computational code for the deterministic solution. 100000 total designs and 10000 robust designs are obtained while the solution took about 9 hours 18 minutes 10 seconds on a platform as Intel(R) Core(TM) 2 CPU 6400@2.13GHz processor and 2GB of RAM on Microsoft Windows 7 64-bit operating system. The workflow of the optimization problem is given in Figure 7.6.

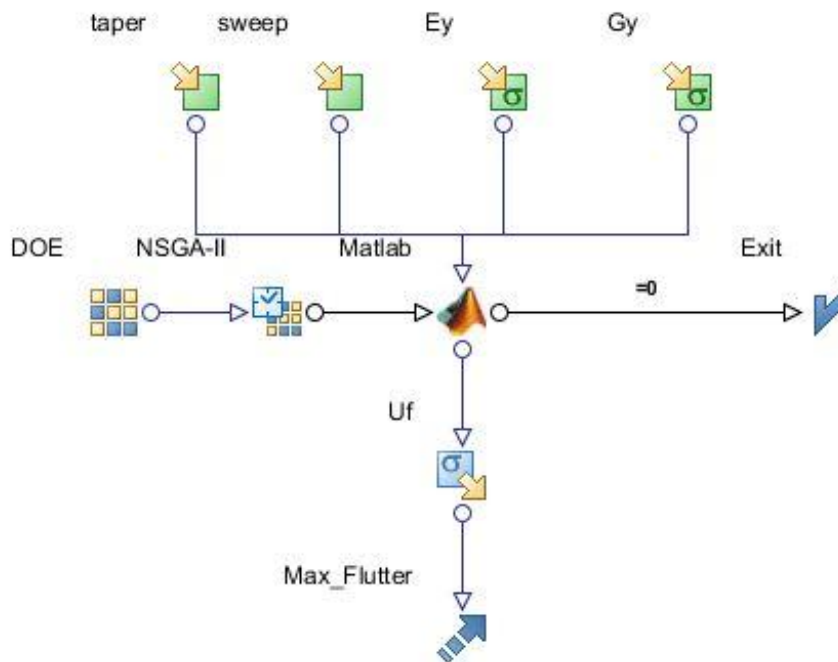


**Figure 7.6 :** Robust optimization workflow of clean AGARD 445.6 wing.

The probability density distribution of the objective function is given in Figure 7.7. The optimum robust design is obtained by considering the maximum of minimum probabilistic flutter speeds among robust designs. The design properties of optimum robust design is shown in Table 7.3. Optimum robust and deterministic flutter speeds

are also given in Table 7.3 while comparison of deterministic and robust design variables are given in Table 7.4.

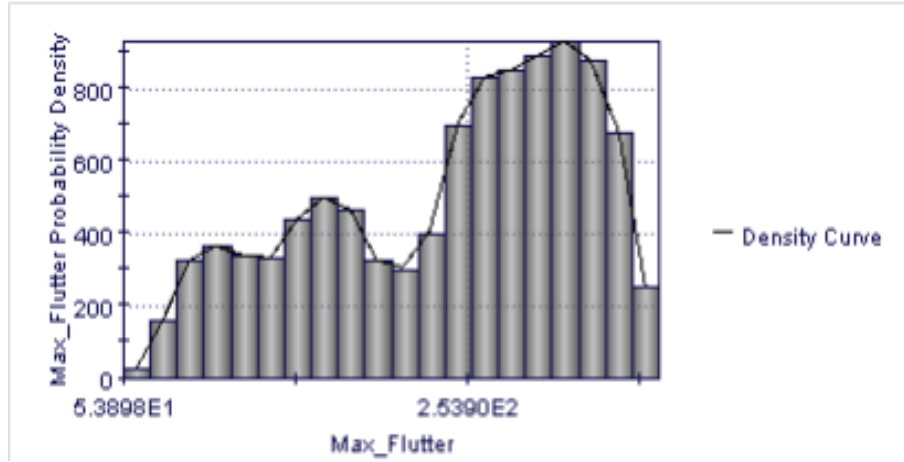


**Figure 7.7 :** Probability density distribution of maximum flutter speed.

**Table 7.3:** Optimum robust design properties of AGARD 445.6 clean wing.

Design Variable	Optimum Value
$\lambda$	0.65
$\Lambda$	$59^\circ$
$E_y$	2001.96 MPa
$G_y$	298.34 MPa
$U_f^{robust}$	<b>356.9322 m/s</b>
$U_f^{det}$	<b>361.8843 m/s</b>

**Table 7.4:** Comparison of deterministic and robust design parameters.

Case	$\lambda$	$\Lambda$	$E_y$	$G_y$
Deterministic	0.65	$59.65^\circ$	2020.85 MPa	299.02 MPa
Robust	0.65	$59^\circ$	2001.96 MPa	298.34 MPa

The designs obtained by deterministic and robust optimization studies are similar with close flutter speed values. The robust design which represents the worst case conditions is in the vicinity of deterministic design since no constraints are defined for the optimization.

### 7.3 Robust Optimization of AGARD 445.6 Wing/Store Configuration

Final robust optimization work involves AGARD 445.6 wing/store configuration in which stores are placed 3-stations since this case is identified as the most efficient

way to distribute the external loads in flutter analysis in the previous scenario. Random parameters (locations of stations, masses of stores, elasticity and shear modulus along spanwise direction) in uncertainty based analysis are determined as probabilistic optimization parameters while taper ratio and sweep angle are again deterministic variables. Masses of stores were not design variables in deterministic optimization work. Thus, they are defined as probabilistic variables with constant mean values in robust optimization. Optimization problem can be set up as follows.

$$\max_{s \in S} U_f^{prob}(s) \quad (7.25)$$

$$S = \{s \in \mathfrak{R}, s_L \leq s \leq s_U\} \quad (7.26)$$

$$s = \{s^{\det}, s^{prob}\} \quad (7.27)$$

$$s^{\det} = (\lambda, \Lambda) \quad \text{and} \quad s^{prob} = (E_y, G_y, y_1, y_2, y_3) \quad (7.27)$$

$$X_R = (m_1, m_2, m_3, E_y, G_y, y_1, y_2, y_3) \quad (7.28)$$

$$0.65 \leq \lambda \leq 1.0 \quad (7.29)$$

$$0^\circ \leq \Lambda \leq 60^\circ \quad (7.30)$$

$$2000\text{MPa} \leq E_y \leq 3000\text{MPa} \quad (7.31)$$

$$200\text{MPa} \leq G_y \leq 300\text{MPa} \quad (7.32)$$

$$0 \leq y_1 \leq 0.762 \text{ m} \quad (7.33)$$

$$0 \leq y_2 \leq 0.762 \text{ m} \quad (7.34)$$

$$0 \leq y_3 \leq 0.762 \text{ m} \quad (7.35)$$

$$x_1^{prob} = y_1 - y_2 \leq -0.04 \quad (7.36)$$

$$x_2^{prob} = y_2 - y_3 \leq -0.04 \quad (7.37)$$

The robust optimization study is performed in modeFRONTIER by coupling it with the computational code developed for the deterministic solution of wing/store configuration. Uncertainties are distributed with MCS and  $COV=5\%$  estimation is used for each random parameter except for distance of stations where store loads place. Due to physical limitations for the placement,  $COV=0.25\%$  estimation is used for  $y_1$ ,  $y_2$  and  $y_3$ . The constraints also become probabilistic since they are related to random parameters. 100000 total designs and 10000 robust designs are obtained while the number of feasible designs are 70917 in total designs and 7094 in robust designs. The solution took about 9 hours 14 minutes 55 seconds on a platform as Intel(R) Core(TM) 2 CPU 6400@2.13GHz processor and 2GB of RAM on Microsoft Windows 7 64-bit operating system. The workflow of the optimization problem is given in Figure 7.8.

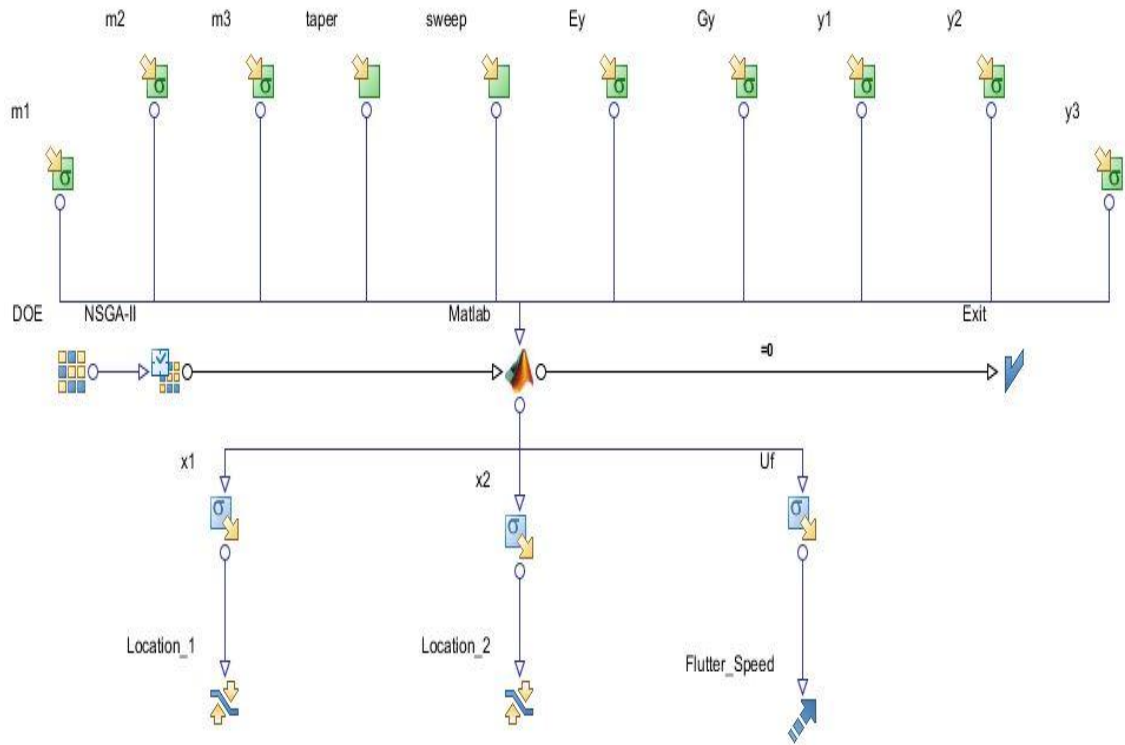


**Figure 7.8 :** Robust optimization workflow of AGARD 445.6 wing/store model.

The probability density distribution of the objective function is given in Figure 7.9. The yellow samples in probability distribution of maximum flutter speed indicate the infeasible designs.

The optimum robust design is obtained by considering the maximum of minimum probabilistic flutter speeds among robust designs.

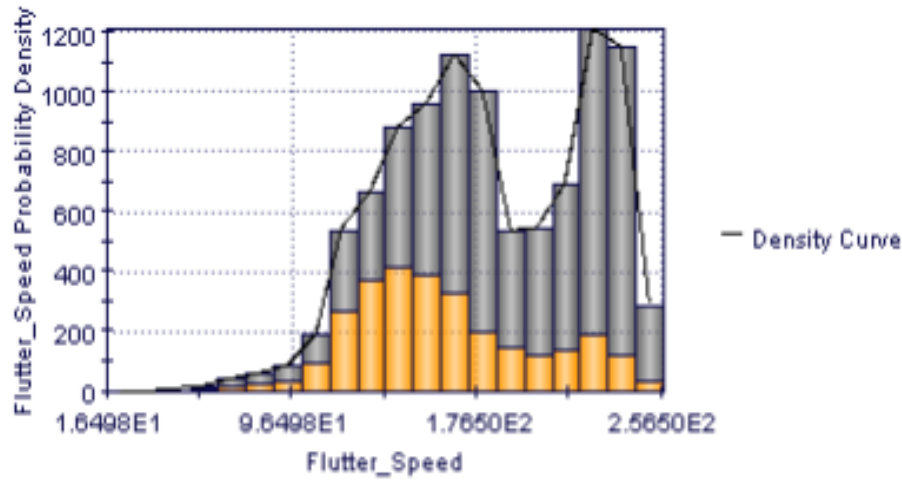


**Figure 7.9 :** Probability density distribution of maximum flutter speed.

The design properties of optimum robust design is shown in Table 7.5 with optimum robust and deterministic flutter speeds while comparison of deterministic and robust optimization studies are given in Table 7.6.

**Table 7.5:** Optimum robust design of AGARD 445.6 wing/store model.

Design Variable	Optimum Value
$\lambda$	0.96
$\Lambda$	59.83°
$E_y$	2387.92 MPa
$G_y$	294.65 MPa
$y_1$	0.2392 m
$y_2$	0.4516 m
$y_3$	0.7286 m
$U_f^{robust}$	<b>253.56 m/s</b>
$U_f^{det}$	<b>314.46 m/s</b>

**Table 7.6:** Comparison of deterministic and robust design parameters.

Case	$\lambda$	$\Lambda$	$E_y$	$G_y$	$y_1$	$y_2$	$y_3$
Det	0.65	59.65°	2020.85 MPa	299.02 MPa	0.6811 m	0.7212 m	0.7620 m
Robust	0.96	59.83°	2387.92 MPa	294.65 MPa	0.2392 m	0.4516 m	0.7286 m

The designs obtained by deterministic and robust optimization studies are rather different from each other. The robust design which represents the worst case conditions point out a quite different design of wing/store configuration especially in

terms of store locations and taper ratio. Since the optimum design variables of robust and deterministic optimization studies are almost the same in clean wing case, the difference in wing/store model is coming from the store loads and constraints defined for their locations. In the presence of strict constraints, robust designs can not be as flexible as deterministic models since they have to satisfy the worst case conditions under the effects of uncertainties. By considering uncertain parameters, robust design optimization is prerequisite for real and reliable designs of such wing/store configurations.





## 8. CONCLUSIONS AND RECOMMENDATIONS

In the present work, flutter analysis methods for 2 and 3-dimensional wings and wing/store models are developed while the designs are optimized based on aeroelastic instability criteria. The first and the basic approach involves the use of open loop dynamics and stability analysis procedure for a 2-dimensional airfoil model in order to obtain the critical speed values of flutter, divergence and control reversal as aeroelastic instabilities. The solution method is implemented in a MATLAB code and validated by using a benchmark problem from literature. A multi-objective optimization process using modeFRONTIER as an optimization software is applied to the benchmark airfoil model to delay the speeds of related instabilities by changing the design and model parameters.

An analytical flutter analysis method for 3-dimensional wing structures using assumed mode technique is developed for the purpose of enabling aeroelastic optimization based on flutter criterion efficiently. The flutter solution employs Lagrange equations with energy terms and also Theodorsen function for aerodynamic load calculation. Free vibration analysis of aircraft wing is performed analytically since flutter solution requires determination of bending and torsional natural frequencies. Proposed flutter solution is validated by two benchmark problems from literature, and then applied to Goland and AGARD 445.6 models which are 3-dimensional aircraft wing structures. Flutter frequency and flutter speed computed for Goland and AGARD 445.6 wings agree well with the experimental results. The flutter solution code developed in MATLAB is fully automatic with input parameters of taper ratio, sweep angle, elasticity and shear modulus and is used to examine the sensitivity of flutter speed on these parameters. Next, flutter code is coupled with an optimization framework to perform flutter based aeroelastic optimization. The objective of the optimization problem is maximization of flutter speed while introducing taper ratio, sweep angle, elasticity and shear modulus as optimization variables.

The flutter solution methodology for 3-dimensional wing structures is extended to include wing/store configurations via revised MATLAB code. The new solution is validated by using a benchmark problem that involves a store mass placed at different positions along span of Goland wing. Then, the solution is applied to AGARD 445.6 wing/store configurations which consist of 3, 4 and 5-stations cases along the span. These cases indicate that the store loads are placed in 3, 4 and 5 stations respectively while the total mass of external loads are kept constant for each configuration. The optimum distances of stations for each case are obtained by flutter based aeroelastic optimization studies. The optimum placement configuration in terms of flutter speed is found as 3-stations case.

Uncertainty based aeroelastic analyses are applied to initial and optimized 2 and 3-dimensional wing models and wing/store configuration in order to obtain minimum speeds. The uncertainties are modeled by using MCS with  $10^5$  samples.  $COV=1\%$  and  $COV=5\%$  are used to include the effects of randomness. The available minimum speeds of aeroelastic instabilities are considered for reliability. Deterministic and probabilistic flutter results are compared to each other for both initial and optimum wing models.

The final part of the present work involves robust optimization of 2 and 3-dimensional clean wing models and 3-dimensional optimum wing/store configuration with external loads in 3 stations. Robust optimization provides the most realistic optimum case for the wing structures since the uncertainties are taken into consideration simultaneously during optimization process. MATLAB codes for deterministic flutter solutions of each case are coupled with the optimization software which provides random distributions with respect to MCS for probabilistic variables by using  $10^5$  samples. Optimum flutter speeds are obtained through the minimum of maximized flutter speeds in optimum robust designs.

As a consequence, the present work provides deterministic and probabilistic flutter solution methodology for wing structures ranging from simple designs to more complicated 3-dimensional models and wing/store configurations as well as applications of deterministic and robust aeroelastic optimization work. Developed flutter strategies form a basis for the flutter analysis and flutter based optimization of more complex structures and can be extended to the use of military and civilian purposes and requirements. Structural and aerodynamic nonlinearities must be considered for a more realistic application such as a fighter aircraft wing. In addition,

all structural and aerodynamic effects of store loads must be included in calculations. Nonlinear aerodynamic effects for wing/store configurations in transonic flow regime is critical in the design of fighter aircrafts.



## REFERENCES

- [1] **Wright, J. R., and Cooper, J. E.** (2007). Introduction to Aircraft Aeroelasticity and Loads. John Wiley & Sons Ltd.
- [2] **Shubov, M. A.** (2004). Mathematical Modeling and Analysis of Flutter in Bending-Torsion Coupled Beams, Rotating Blades and Hard Disc Drives. *Journal of Aerospace Engineering*, Vol.17, No.56, pp. 256-269.
- [3] **Matsushita, H., Miyata, T., Christiansen, L. E., Lehn-Schiøler, T., Mosekilde, E.** (2002). Nonlinear Dynamics Approach of Modeling the Bifurcation for Aircraft Wing Flutter in Transonic Speed. *The Society of Instrument and Control Engineers (SICE) Annual Conference*, Osaka, Japan.
- [4] **Goura, G.** (2001). Time Marching Analysis of Flutter Using Computational Fluid Dynamics. *PhD Thesis*, University of Glasgow Department of Aerospace Engineering.
- [5] **Lee, B. H. K.** (1984). A Study of Transonic Flutter of a Two-Dimensional Airfoil Using the U-g and p-k Methods. Canada National Research Council Aeronautical Report.
- [6] **Ju, Q., and Qin, S.** (2009). New Improved g Method for Flutter Solution. *Journal of Aircraft*, Vol. 46, No.6, pp. 1284-1286.
- [7] **Lind, R.** (2002). Match-Point Solutions for Robust Flutter Analysis. *Journal of Aircraft*, Vol. 39, No. 1, pp. 91-99.
- [8] **Nissim, E., and Gilyard, G. B.** (1989). Method for Experimental Determination of Flutter Speed by Parameter Identification. NASA Technical Paper.
- [9] **Borglund, R.** (2007). Robust Aeroelastic Analysis in the Laplace Domain: The  $\mu$ -p Method. *International Forum on Aeroelasticity and Structural Dynamics*, Stockholm, Sweden.
- [10] **Pitt, D. M.** (2000). A Complex Velocity Solution of the Flutter Equations. *41<sup>st</sup> Structures, Structural Dynamics and Materials Conference and Exhibit*, Atlanta, USA.
- [11] **Dorf, R.C.** (2008). Modern Control Systems. Prentice Hall.
- [12] **Brooking, B. M.** (1998). Flutter Analysis of a Two Dimensional Airfoil Containing Structural Hysteresis Nonlinearities. *MSc Thesis*, Carleton University Ottawa-Carleton Institute for Aerospace & Mechanical Engineering.

- [13] **Murty, H. S.** (1995). Aeroelastic Stability Analysis of an Airfoil with Structural Nonlinearities Using a State Space Unsteady Aerodynamics Model. *36<sup>th</sup> AIAA/ASME/ASCE/AHS/ASC Structures, Structural Dynamics, and Materials Conference*, New Orleans, USA.
- [14] **Eller, D.** (2009). Aeroelasticity and Flight Mechanics: Stability Analysis Using Laplace-Domain Aerodynamics. *International Forum on Aeroelasticity and Structural Dynamics*, Seattle, USA.
- [15] **Rheinfurth, M. H., Swift, F. W., Marshall, G. C.** (1966). A New Approach to the Explanation of the Flutter Mechanism. NASA Technical Note.
- [16] **Jeffrey, A.** (1991). Flutter Evaluation and Control of an Airfoil Solved in the Laplace Domain. *MSc Thesis*, McGill University Department of Mechanical Engineering.
- [17] **Heeg, J.** (1993). Analytical and Experimental Investigation of Flutter Suppression by Piezoelectric Actuation. NASA Technical Paper-3241.
- [18] **Walker, M.** (2009). Unsteady Aerodynamics of Deformable Thin Airfoils. *MSc Thesis*, Virginia Polytechnic Institute and State University.
- [19] **Wagner, H.** (1925). Über die Entstehung des dynamischen Auftriebes von Tragflügeln. *Journal of Applied Mathematics and Mechanics*, pp: 17-35.
- [20] **Garrick, I. E.** (1938). On Some Reciprocal Relations in the Theory of Nonstationary Flows. NACA Report No: 629.
- [21] **Marzocca, P., and Librescu, L.** (2001). Aeroelastic Response of Swept Aircraft Wings in a Compressible Flow Field. *39<sup>th</sup> Aerospace Sciences Meeting and Exhibit*, Reno, USA.
- [22] **Kargarnovin, M. H., and Mamandi, A.** (2007). Aeroelastic Response for Pure Plunging Motion of a Typical Section Due to Sharp Edged Gust, Using Jones Approximations Aerodynamics. *World Academy of Science, Engineering and Technology*, Vol.36, pp. 154-161.
- [23] **Zouari, R.** (2008). Détection Précoce d'Instabilité Aéroélastique des Structures Aéronautiques. *Doctorat Thèse*, L'Université de Rennes.
- [24] **Marzocca P., Librescu, L., Kim, D-H., Schober S.** (2007). Development of an Indicial Function Approach for the Two-Dimensional Incompressible/Compressible Aerodynamic Load Modelling. *Journal of Aerospace Engineering*, Vol. 221, No. 3, pp. 453-463.
- [25] **Lind, R.** (1997). A Presentation on Robust Flutter Margin Analysis and a Flutterometer. NASA/TM-97-206220.
- [26] **Danowski, B. P., Chrstos, J. F., Klyde, D. H., Farhat, C., Brenner, M.** (2010). Evaluation of Aeroelastic Uncertainty Methods. *Journal of Aircraft*, Vol.47, No.4, pp.1266-1273.
- [27] **Heinze, S., Ringertz, U., Borglund, D.** (2009). Assessment of Uncertain External Store Aerodynamics Using  $\mu$ -p Flutter Analysis. *Journal of Aircraft*, Vol.46, No.3, pp.1062-1067.

- [28] **Borglund, D., Ringertz, U.** (2006). Efficient Computation of Robust Flutter Boundaries Using  $\mu$ -k Method. *Journal of Aircraft*, Vol.43, No.6, pp.1763-1769.
- [29] **Potter, S., and Lind, R.** (2001). Developing Uncertainty Models for Robust Flutter Analysis Using Ground Vibration Test Data. NASA/TM-2001-210392.
- [30] **Poirion, F.** (2005). Chaos Polynomial Representation of Parametric Uncertainties in Aeroelasticity. *International Forum on Structural Dynamics and Aeroelasticity*, Munich, Germany.
- [31] **Heinze, S., and Borglund, D.** (2008). Robust Flutter Analysis Considering Mode Shape Variations. *Journal of Aircraft*, Vol.45, No.3, pp.1070-1074.
- [32] **Desai, A., and Sarkar, S.** (2010). Analysis of a Nonlinear Aeroelastic System with Parametric Uncertainties Using Polynomial Chaos Expansion. *Mathematical Problems in Engineering*, Vol.2010, Article ID: 379472.
- [33] **Borglund, D., and Ringertz, U.** (2009). Solution of the Uncertain Flutter Eigenvalue Problem Using  $\mu$ -p Analysis. *International Forum on Structural Dynamics and Aeroelasticity*, Seattle, USA.
- [34] **Borglund, D.** (2008). Robust Eigenvalue Analysis Using the Structured Singular Value: The  $\mu$ -p Flutter Method. *AIAA Journal*, .46, No.11, pp.2806-2813.
- [35] **Carlsson, M., and Karlsson A.** (2007). Robust Aeroelastic Analysis of the Gripen Fighter Including Flight Test Model Validation. *International Forum on Structural Dynamics and Aeroelasticity* Stockholm, Sweden.
- [36] **Prazenica, R.J., Lind, R., Kurdila, A. J.** (2003). Uncertainty Estimation from Volterra Kernels for Robust Flutter Analysis. *Journal of Guidance, Control, and Dynamics*, Vol.26, No.2, pp.331-339.
- [37] **Beran, P. S., Lindsley N.J., Camberos, J., Kurdi, M.** (2009). Stochastic Nonlinear Aeroelasticity. AFRL-RB-WP-TR-2009-3057.
- [38] **Poirion, F.** (1998). Aeroelastic Stability of Aircraft with Uncertain Parameters. *7<sup>th</sup> International Conference on Structural Safety and Reliability*, Kyoto, Balkema.
- [39] **Marques, S., Badcock, K. J., Khodaparast, H. H., Mottershead, J. E.** (2010). Transonic Aeroelastic Stability Predictions Under the Influence of Structural Variability. *Journal of Aircraft*, Vol.47, No.4, pp.1229-1239.
- [40] **Kurdi, M., Lindsley, N., Beran, P.** (2007). Uncertainty Quantification of the Golan<sup>+</sup> Wing's Flutter Boundary. *AIAA Atmospheric Flight Mechanics Conference and Exhibit*, Hilton Head, South Carolina.
- [41] **Abbas, L. K., Chen, Q., Marzocca, P., Milanese, A.** (2008). Non-linear Investigations of Store(s) Induced Limit Cycle Oscillations. *Journal of Aerospace Engineering*, Vol. 222, No.1, pp:63-80.

- [42] **Byreddy, C., Grandhi, R. V., Beran, P.** (2005). Dynamic Aeroelastic Instabilities of an Aircraft Wing with Underwing Store in Transonic Regime. *Journal of Aerospace Engineering*, Vol. 18, No.4, pp: 206-214.
- [43] **Kim, D. H., Park, Y. M., Lee, I., Kuon, O. J.** (2005). Non-linear Aeroelastic Computations of a Wing/Pylon/Finned-Store Using Parallel Computing. *AIAA Journal*, Vol. 43, No.1, pp:53-62.
- [44] **Chen, P. C., Sulaeman, E., Liu, D. D., Denegri, C. M.** (2002). Influence of External Store Aerodynamics on Flutter/LCO of a Fighter Aircraft. *43<sup>th</sup> AIAA/ASME/ASCE/AHS/ASC Structures, Structural Dynamics, and Materials Conference*, Denver, CO.
- [45] **Beran, P. S., Khot, N. S., Eastep, F. E., Snyder, R. D., Zweber, J. V.** (2004). Numerical Analysis of Store Induced Limit-Cycle Oscillation. *Journal of Aircraft*, Vol. 41, No. 6, pp: 1315-1326.
- [46] **Khot, N. S., Beran, P. S., Zweber, J. V., Eastep, F. E.** (2003). Influence of Tip Store Mass Location on Wing Limit Cycle Oscillation. *44<sup>th</sup> AIAA/ASME/ASCE/AHS/ASC Structures, Structural Dynamics, and Materials Conference*, Norfolk, VA.
- [47] **Beran, P. S., Khot, N. S., Eastep, F. E., Snyder, R. D., Zweber, J. V., Huttshell, L. J., Scott, J. N.** (2002). The Dependence of Store-Induced Limit-Cycle Oscillation Predictions on Modeling Fidelity. *NATO-RTO Applied Vehicle Technology Panel Symposium*.
- [48] **Byreddy, C., Grandhi, R. M., Beran, P.** (2005). Dynamic Aeroelastic Instabilities of an Aircraft Wing with Underwing Store in Transonic Regime. *Journal of Aerospace Engineering*, Vol. 18, No. 4, pp: 206-214.
- [49] **Graham, M. R., Oliveira, M. C., Callafon, R. A.** (2007). Analysis and Design Methodologies for Robust Aeroservoelastic Structures. *AIAA Atmospheric Flight Mechanics Conference and Exhibit*, Hilton Head, South Carolina.
- [50] **Borglund, D.** (2004). The  $\mu$ -k Method for Robust Flutter Solutions. *Journal of Aircraft*, Vol.41, No.5, pp: 1209-1216.
- [51] **Borglund, D., and Nilsson, U.** (2004). Robust Wing Flutter Suppression Considering Aerodynamic Uncertainty. *Journal of Aircraft*, Vol.41, No.2, pp: 331-334.
- [52] **Zink, P. S., Raveh, D. E., Mavris, D. N.** (2004). Robust Structural Design of an Active Aeroelastic Wing with Maneuver Load Inaccuracies. *Journal of Aircraft*, Vol.41, No.3, pp: 585-593.
- [53] **Dodson, M., and Parks, G. T.** (2009). Robust Aerodynamic Design Optimization Using Polynomial Chaos. *Journal of Aircraft*, Vol.46, No.2, pp: 635-646.
- [54] **Karpel, M., Moulin, B., Idan, M.** (2003). Robust Aeroservoelastic Design with Structural Variations and Modeling Uncertainties. *Journal of Aircraft*, Vol.40, No.5, pp: 946-954.



- [55] **Wan, Z., Xiao, Z., Chao, Y.** (2011). Robust Design Optimization of Flexible Backswept Wings with Structural Uncertainties. *Journal of Aircraft*, Vol.48, No.5, pp: 1806-1809.
- [56] **Kim, J., Bates, D. G., Postlethwaite.** (2005). Nonlinear Robust Performance Analysis Using Gradient-Based Optimisation – An Aeroelastic Case-Study. *Proceedings of the 44<sup>th</sup> IEEE Conference on Decision and Control, and the European Control Conference 2005*, Seville, Spain.
- [57] **Witteveen, J. A. S., and Iaccarino, G.** (2010). Simplex Elements Stochastic Collocation for Uncertainty Propagation in Robust Design Optimization. *48th AIAA Aerospace Sciences Meeting Including The New Horizons Forum and Aerospace Exposition*, Orlando, Florida.
- [58] **Dowell, E. H., Crawley, E. F., Curtiss, Jr. H. C., Peters, D. A., Scanlan, R. H., Sisto, F.** (1995). A Modern Course in Aeroelasticity. Kluwer Academic Publishers.
- [59] **Ursu, I., Stoia-Djeska, M., Ursu, F.** (2004). Active Control Laws for Flutter Suppression. *Annals of University of Craiova*, No.27.
- [60] **Bisplinghoff, R. L., Ashley, H., Halfman, R.L.** (1955). Aeroelasticity. Addison-Wesley.
- [61] **Cunningham, H. J., Batina, J. T., Bennett, R. M.** (1988). Modern Wing Flutter Analysis by Computational Fluid Dynamics Methods. *Journal of Aircraft*, Vol.25, No.10, pp: 962-968.
- [62] **Goland, M., and Buffalo, N. Y.** (1945). The Flutter of a Uniform Cantilever Beam. *Journal of Applied Mechanics*, 12, pp: 197-208.
- [63] **Khodaparast, H. H.** (2010). Stochastic Finite Element Model Updating and its Application in Aeroelasticity. *PhD Thesis*, University of Liverpool.
- [64] **Qiangjun, Z.** (2010). Modeling the Effect of Taper Ratio on Wing Flutter. *International Conference on Computer Application and System Modeling*, Shanxi, Taiyuan.
- [65] **Yates, E.** (1985). Standard Aeroelastic Configurations for Dynamic Response I-Wing 445.6. AGARD Report No.765.
- [66] **Beaubien, R. J., Nitzsche, F., Feszty, D.** (2005). Time and Frequency Domain Flutter Solutions for the AGARD 445.6 Wing. *International Forum on Aeroelasticity and Structural Dynamics*, Munich, Germany.
- [67] **Lee-Rausch, E. M., and Batina, J. T.** (1993). Calculation of AGARD Wing 445.6 Flutter Using Navier-Stokes Aerodynamics. *AIAA 11th Applied Aerodynamics Conference*, Monterey, California.
- [68] **Allen, C. B., Jones, D., Taylor, N. V., Badcock, K. J., Woodgate, M. A., Rampurawala, A. M., Cooper, J. E., Vio, G. A.** (2004). A Comparison of Linear and Non-Linear Flutter Prediction Methods: A Summary of PUMA DARP Aeroelastic Results. *Royal Aeronautical Society Aerodynamics Conference*, London.
- [69] **Nikbay, M., Fakkusoglu, N., Kuru, M. N.** (2010). Reliability Based Multidisciplinary Optimization of Aeroelastic Systems with Structural and Aerodynamic Uncertainties. *13<sup>th</sup> AIAA/ISSMO Multidisciplinary*

*Analysis and Optimization (MAO) Conference*, Fort Worth, Texas, USA.

- [70] **Kamakoti, R.** (2004). Computational Aeroelasticity Using a Pressure-Based Solver. *PhD Thesis*, University of Florida.
- [71] **Kamakoti, R., Shyy, W.** (2004). Fluid-Structure Interaction for Aeroelastic Applications. *Progress in Aerospace Sciences*, Vol.40, No.8, pp: 535-558.
- [72] **Kamakoti, R., Lian, Y., Regisford, S., Kurdila, A., Shyy, W.** (2002). Computational Aeroelasticity Using a Pressure-Based Solver. *AIAA 40<sup>th</sup> Aerospace Sciences Meeting & Exhibit*, Reno, NV, USA.
- [73] **Yates, E.** (1987). AGARD Standard Aeroelastic Configurations for Dynamic Response, Candidate Configuration I.-Wing 445.6. NASA TM 100492.
- [74] **Kolonay, R. M.** (2002). Computational Aeroelasticity, Presented in Technical Course Organized by *The Applied Vehicle Technology Panel (AVT) on Application of Adaptive Structures in Active Aeroelastic Control*, METU, Ankara, Turkey.
- [75] **Choi, S. K., Grandhi, R. V., Canfield, R. A.** (2006). Reliability-based Structural Design. Springer.
- [76] **Panagiotopoulos, E. E., and Kyparissis S. D.** (2010). CFD Transonic Store Separation Trajectory Predictions with Comparison to Wind Tunnel Investigations. *International Journal of Engineering*, Vol.3, No.6, pp: 538-553.
- [77] **Fazelzadeh, S. A., Mazidi, A., Kalantari, H.** (2009). Bending-Torsional Flutter of Wings with an Attached Mass subjected to a Follower Force. *Journal of Sound and Vibration*, Vol.323, No.1, pp:148-162.
- [78] **Runyan, H. L., and Watkins, C.E.** (1949). Flutter of a uniform wing with an arbitrarily placed mass according to a differential equation analysis and a comparison with experiment. NASA Technical Report, NACA TN 1848.
- [79] **McAllister, C. D., and Simpson, T.W.** (2003). Multidisciplinary Robust Optimization of an Internal Combustion Engine. *Journal of Mechanical Design*, Vol.125, No.1, pp:124-130.
- [80] **Clarich, A., and Pediroda, T.W.** (2009). Robust Design Applications with modeFRONTIER, applying NODESIM-CFD Tools. *NODE-SIM CFD Workshop on Quantification of CFD Uncertainties*, Brussels, Belgium.
- [81] **Parashar, S., Clarich, A., Geremia, P., Otani, A.** (2010). Reverse Multi-Objective Robust Design Optimization (R-MORDO) Using Chaos Collocation Based Robustness Quantification for Engine Calibration. *10th AIAA Aviation Technology, Integration, and Operations (ATIO)Conference*, Fort Worth, Texas, USA.
- [82] **Deb, K., Pratap, A., Agarwal, S., Meyarivan, T.** (2002). A Fast and Elitist Multi-Objective Genetic Algorithm. *IEEE Transactions on Evolutionary Computation*, Vol.6, No.2, pp: 182-197.

- [83] **Wiener, N.**, (1938). The Homogenous Chaos. *American Journal of Mathematics*, Vol.60, pp: 897-936.



## CURRICULUM VITAE



**Name Surname:** Pınar Acar

**Place and Date of Birth:** Şişli / 06.01.1988

**E-Mail:** acarpin@itu.edu.tr

**B.Sc.:** ITU Astronautical Engineering (2010)

### Professional Experience and Rewards:

- Research Assistant in ITU Faculty of Aeronautics and Astronautics (Started in November 2010)
- Scholarship from The Scientific and Technological Research Council of Turkey (TUBITAK) (Started in October 2010)
- Member of TURKSAT 3USAT Satellite Project in ITU
- Honor student in ITU Astronautical Engineering Department (2010) and Nişantaşı Anadolu Lisesi (2006)

### List of Publications and Patents:

- Nikbay M., Kuru M. N., Acar P., 2011: A CFD Based Multidisciplinary Optimization of Aeroelastic Systems with Coupled Reliability Constraints. *ECCOMAS CFD and Optimization Conference*, Antalya, Turkey.
- Acar P., Nikbay M., 2010: İki Boyutlu Bir Kanadın Flutter Probleminin Laplace Dönüşümüyle Çözülmesi. *III. Ulusal Havacılık ve Uzay Konferansı*, Eskişehir, Türkiye.
- Nikbay M., Acar P., Kılıç Ç., 2012: Istanbul Technical University Contribution to AePW-1. *Aeroelastic Prediction Workshop-1 (AePW-1)*, Honolulu, USA (Abstract submitted).
- Acar P., Nikbay M., Aslan A. R., 2012: Design Optimization of a 3-Unit Satellite De-Orbiting Mechanism. *Small Satellites Systems and Services the 4S Symposium*, Portoroz, Slovenia (Abstract submitted).
- Umit E., Acar P., Nikbay M., Aslan A. R., 2012: Magnetorquer Coil Design Optimization for Small Satellites. *Small Satellites Systems and Services the 4S*

*Symposium*, Portoroz, Slovenia (Abstract submitted).

▪ Nikbay M., Acar P., Aslan A. R., 2012: Reliability Based Design Optimization of a CubeSat De-Orbiting Mechanism. *14<sup>th</sup> AIAA/ISSMO Multidisciplinary Analysis and Optimization (MAO) Conference*, Indianapolis, USA (Abstract submitted).

## **PUBLICATIONS/PRESENTATIONS ON THE THESIS**

▪ Nikbay M., Acar P., 2011: Integrating Analytical Aeroelastic Instability Analysis into Design Optimization of Aircraft Wing Structures. *TWMS Journal of Applied and Engineering Mathematics*, Vol.1, No.2, pp: 237-253.

▪ Nikbay M., Acar P., 2012: Flutter Based Design Optimization of Aircraft Wings with Analytical Approaches, *53<sup>rd</sup> AIAA/ASME/ASCE/AHS/ASC Structures, Structural Dynamics, and Materials Conference*, Honolulu, USA (Accepted for presentation).

▪ Nikbay M., Acar P., 2012: Robust Aeroelastic Design Optimization of Wing/Store Configurations Based on Flutter Criteria. *14<sup>th</sup> AIAA/ISSMO Multidisciplinary Analysis and Optimization (MAO) Conference*, Indianapolis, USA (Abstract submitted).